Terms and Conditions of Use of Digitised Theses from Trinity College Library Dublin

Copyright statement

All material supplied by Trinity College Library is protected by copyright (under the Copyright and Related Rights Act, 2000 as amended) and other relevant Intellectual Property Rights. By accessing and using a Digitised Thesis from Trinity College Library you acknowledge that all Intellectual Property Rights in any Works supplied are the sole and exclusive property of the copyright and/or other IPR holder. Specific copyright holders may not be explicitly identified. Use of materials from other sources within a thesis should not be construed as a claim over them.

A non-exclusive, non-transferable licence is hereby granted to those using or reproducing, in whole or in part, the material for valid purposes, providing the copyright owners are acknowledged using the normal conventions. Where specific permission to use material is required, this is identified and such permission must be sought from the copyright holder or agency cited.

Liability statement

By using a Digitised Thesis, I accept that Trinity College Dublin bears no legal responsibility for the accuracy, legality or comprehensiveness of materials contained within the thesis, and that Trinity College Dublin accepts no liability for indirect, consequential, or incidental, damages or losses arising from use of the thesis for whatever reason. Information located in a thesis may be subject to specific use constraints, details of which may not be explicitly described. It is the responsibility of potential and actual users to be aware of such constraints and to abide by them. By making use of material from a digitised thesis, you accept these copyright and disclaimer provisions. Where it is brought to the attention of Trinity College Library that there may be a breach of copyright or other restraint, it is the policy to withdraw or take down access to a thesis while the issue is being resolved.

Access Agreement

By using a Digitised Thesis from Trinity College Library you are bound by the following Terms & Conditions. Please read them carefully.

I have read and I understand the following statement: All material supplied via a Digitised Thesis from Trinity College Library is protected by copyright and other intellectual property rights, and duplication or sale of all or part of any of a thesis is not permitted, except that material may be duplicated by you for your research use or for educational purposes in electronic or print form providing the copyright owners are acknowledged using the normal conventions. You must obtain permission for any other use. Electronic or print copies may not be offered, whether for sale or otherwise to anyone. This copy has been supplied on the understanding that it is copyright material and that no quotation from the thesis may be published without proper acknowledgement.

A STUDY OF THE ROLE OF OIL ADDITIVES IN THE FAILURE OF BALL BEARINGS

A thesis submitted to the
University of Dublin
in accordance with the
requirements of the degree of
Doctor of Philosophy
in the
Faculty of Engineering
Department of Mechanical and
Manufacturing Engineering

October 1999

Niall Brennan

SUMMARY

This thesis examines the influence that extreme pressure oil additives have in the failure of ball bearings. Additives are commonly used in lubricating oils to improve their properties. In recent years some sections of research and industry have suggested that additives are responsible for causing premature failures in rolling bearings. The resultant costs involved in replacing bearings, even in simple applications, through losses in production and maintenance can be high. This study investigates rolling contact fatigue in ball bearings in the presence of sulphur/phosphorus additives. Additive reactivity on metal surfaces is also examined using a static hot-wire method.

Rolling contact fatigue testing was carried using a series of oils to assess how bearing life is effected by additives. The majority of fatigue testing was carried out using novel test rigs at the University of Bristol. Four oils were used in the Bristol rigs, a base oil used as a reference, and three other oils containing various percentages of sulphur and phosphorus elements. Comparative fatigue testing was also carried out at the SKF research facility in The Netherlands.

The hot-wire technique traditionally was used to measure the corrosion of metals surfaces at very high temperatures. In this test a wire surface is corroded by a chemical attack. Sensitive resistance measurements are used to calculate the small changes in diameter of the wire caused by the corrosion. This study concentrates on reactions that take place at more moderate temperatures < 450 °C.

This research found that the presence of additives can either increase or decrease bearing life depending on the operating conditions. The reactivity of oils on metal surfaces was shown to be more than a function of temperature. Passivation of the corrosive reactions was found to be caused by product film formation.

DECLARATION

The accompanying dissertation entitled "A study of the role of oil additives in the failure of ball bearings" is submitted in support of an application for the degree of Doctor of Philosophy in Engineering at the University of Dublin.

The dissertation is based on independent work by the candidate, except where clearly referenced. No portion of the work referred to in this dissertation has been submitted in support of an application for another degree or qualification in this, or any other university or other institute of learning.

The views and opinions expressed in this thesis are solely those of the author and not the University of Dublin. The Library of Trinity College is granted discretionary powers to lend or copy the thesis upon request.

I declare that the above statements are true,

Niall Brennan

Niall Brennan

October 1999.

ACKNOWLEDGEMENTS

This work has only been possible through the co-operation and support of a large number of people. In particular, I wish to express my sincere thanks to my supervisor, Professor Andrew Torrance, from Trinity College Dublin. I would like to thank Dr. John Morgan for his guidance at the University of Bristol.

I am grateful to Mr. Des Neale his technical assistance, and to SKF (bearing manufacturers) for providing the funding to make this study possible.

Finally, I cannot thank my family enough for their patience and encouragement.

CONTENTS

LIST OF FIGURES

LIST OF TABLES

NOMENCLATURE

a	semi-major axis
a_1	life adjustment factor for reliability
a_2	life adjustment factor for material
a_3	life adjustment factor for operating conditions
a_{SKF}	SKF life adjustment factor
(add)	concentration of additive
A	area of wire
b	semi-minor axis
cla.	centre line average (roughness)
C	dynamic load rating
E	activation energy
E_Y	Young's modulus
E'	reduced Young's modulus
f_t	loss of hardness adjustment factor
F	total normal load
(Fe)	number of iron atoms on the wire surface
FeS	iron sulphide
k	constant in rate of reaction equation
h_c	central film thickness
h_o	minimum film thickness
H_c	dimensionless film thickness
l	length of wire
L	predicted bearing life
L_{LP}	Lundberg - Palmgren life
L_{LP10}	Lundberg - Palmgren L_{10} life

L_{SKF}	SKF adjusted life
L_x	FAG adjusted life
L_{05}	life rating 95% survival
L_{10}	basic life rating 90% survival
p	exponent of the life equation
P	equivalent dynamic bearing load
r_o	original radius of wire
Δr	thickness of corroded wire
R	resistance of wire
R_1	initial resistance of reaction wire
R_2	initial resistance of dummy wire
R_3	resistance of reaction wire after reaction
R_4	resistance of dummy wire after reaction
R_{11}	ball radius 1
R_{12}	ball radius 2
R_{21}	track radius 1
R_{22}	track radius 2
R_G	gas constant
R_o	initial resistance of wire
R_x	reduced radius x-direction
R_y	reduced radius y-direction
$\Delta R, \Delta R_o$	change of resistance due to corrosion
ΔR_T	resistance change due to temperature
ΔR_D	resistance change due to corrosion
S	survival probability
t	time to failure
T	time when 63.2% have failed

T	absolute temperature
u	surface velocity in x-direction
U	dimensionless speed parameter
V_1	voltage drop across channel 1
V_2	voltage drop across channel 2
V_{wire}	voltage drop across the wire
W	dimensionless load parameter
z	depth beneath contact surface

Greek Symbols

α	pressure-viscosity parameter
β	Weibull life dispersion parameter
η	dynamic viscosity
Λ	roughness parameter (lambda ratio)
μ	dynamic viscosity
ρ	electrical resistivity
σ_{max}	maximum Hertzian stress
τ_{max}	maximum shear stress
τ_{oct}	maximum octahedral shear stress
ν	Poisson's ratio
ν_1	Poisson's ratio of ball
ν_2	Poisson's ratio of raceway

Mathematical functions

F(t)	failure probability

Acronyms

A/D	analogue-to-digital
AW	anti-wear
DC	direct current
DPP	diphenyl phosphate
EDAX	electron dispersive x-ray analysis
EHD	elasto-hydrodynamic
EP	extreme pressure
ERC	engineering research centre
FTIR	Fourier transform infra-red analysis
HVI	high viscosity index
IC	internal combustion
ISO	international standards organisation
LM	light microscopy
OM	optical microscopy
PE	petroleum ether
PID	proportional integral derivative
rpm	revolutions per minute
RCF	rolling contact fatigue
SAM	scanning Auger microscopy
SEM	scanning electron microscopy
S/P	sulphur/phosphorus
SKF	Svenska Kullagerfabriken (Swedish bearing manufacturers)
TCP	tricresyl phosphonate
VB	visual basic
ZDDP	zinc dialkyldithiophosphate

CHAPTER 1

1 INTRODUCTION

1.1 PROJECT BACKGROUND

A bearing can fail for many reasons such as excessive loading, poor metal quality and rough handling during installation. If the bearing avoids such abuse it will eventually wear out and fail. The type of fatigue which covers bearing components is called rolling contact fatigue (RCF). To help bearings roll smoothly during operation lubricants are added between the surfaces of contact. In most engineering applications, grease and oil account for the bulk of lubrication. In special applications, solid lubricants or even water can be used. Increased demands due to higher operating temperatures, since the development of the combustion engine, has seen the need to use oil additives in lubricants.

Many papers have been written on the benefits of additives in bearings. Life improvement promises are a major selling strategy for most new products. However, in the last twenty years some studies have cast a shadow of doubt over the widespread use of additives. Summers-Smith [1] draws a good analogy between drugs and additives, "Lubricating oils are like drugs: proving the beneficial effects is comparatively easy; ensuring that there will be no harmful effects is a much more difficult proposition". The difficulty in identifying the harmful effects, is caused by the complexity of the reaction mechanisms involved in bearing/lubricant systems. The effects of temperature on reactivity, and the nature of the reaction films that are formed and transported in the contact zone, are not fully understood.

This research project was started after an investigation by Torrance et al. [2] into an additive's influence on the pitting and wear of a ball bearing steel. Two oils, one base

oil and one containing S/P additive, were used to test the fatigue life of a ball-on-cylinder contact. When the additive was present a more polished surface was observed on the cylinder's surface, but the L_{10} life of the material was reduced. This result highlighted that additives do not always have a positive effect in stressed contacts. Prior to this study, Torrance [3] had observed the presence of an additive element in cracks formed by rolling contact fatigue. Corrosion enhanced fatigue was suspected to be part of the failure mechanism. Wan [4] had also published results concerning the detrimental effects of an organic phosphate on bearing fatigue.

This current study will look at two related subjects: fatigue testing and oil/metal reactivity. Rolling contact fatigue tests were carried out in two laboratories, the first series at the University of Bristol over a period of three years, with supplemental tests used for comparison carried out at the SKF ERC research facility near Utrecht in The Netherlands. The tests at Bristol compared the effects of four oils, under conditions of mild stress and low Lambda ratio. Higher stresses and a higher lambda ratio were used for the ERC tests.

The second major part of this study was the development of a new hot-wire rig to test the reactivity of lubricants on metals. A modern version of the "Barcroft" hot-wire rig was developed, and a test plan was devised to test the oils used in the Bristol fatigue tests. In the original work by Barcroft [5] and Sakurai [6], oil/metal reactions were examined at high temperatures between 450-700 °C. In this study lower temperatures of reaction were investigated, which are more representative of the flash temperatures experienced in metal-to-metal contacts. The majority of hot-wire tests were carried out between 300-450 °C.

1.2 THE USE OF MINERAL OILS

The use of hydrocarbon mineral oils is a fairly recent development in the history of tribology. Traditional lubricants such as animal fats and vegetable oils were commonly used until the 19th Century. Demands for increased performance and the increases in lubricant costs around that time started a search for suitable alternatives. Prior to 1850, scientists had concentrated their research efforts on the physical nature of friction rather than lubrication. Discoveries of mineral oil, and the development of machinery, sparked a new era in lubrication understanding. After a number of reports documented the suitability of hydrocarbon mineral oils in a range of applications, the popularity of the new lubricant flourished.

Hydrocarbon base oils, even after refining, are complex mixtures of aliphatic or saturated ring hydrocarbons which are chosen to give particular viscosity properties. Base oils can also contain small concentrations of nitrogen and sulphur. These impurities make it difficult to standardize lubricant behaviour.

1.3 WHY USE ADDITIVES ? - LUBRICATING REGIMES

When moving surfaces are brought together, even if they are polished, rubbing inevitably leads to friction. The material at the contacting points can seize and tear which can produce high local temperatures. Adding a fluid film to separate the surfaces, which is thicker that the combined roughnesses of surfaces, is one way to reduce friction. The metal seizures are eliminated as the lubricant is sheared while separating the surfaces. This regime is known as hydrodynamic lubrication.

If the loads are high between surfaces of high elastic moduli, oil viscosity increases with pressure. Increasing the speed of the oil into the contact can cause a force to build up which separates the surfaces. This is called elasto-hydrodynamic lubrication. If this film breaks down, and metal-to-metal contact occurs, this regime is called boundary lubrication. Even when bearings are properly chosen for an application, boundary conditions will still exist at start up and shutdown. It is for this reason that additives are mixed in lubricating oils in practice.

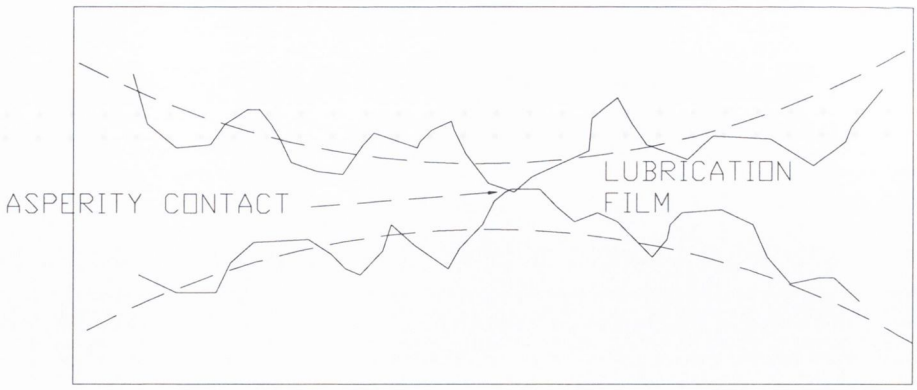

Figure 1.1 Asperity contact through lubricant

Since the banning of lead from oil additives, due to environmental considerations, sulphur has emerged as its main replacement. The most common forms of sulphur additives are sulphurized fats, olefins and terpenes. The reactivity of sulphur has been documented by Manteuffel et al. [7]. They measured the quantity of sulphur in the load wear track and found that its concentration was 100 times greater than that of the unworn region.

1.4 OVERVIEW OF ROLLING CONTACT FATIGUE TESTING

1.4.1 Fatigue testing at the University of Bristol

The rolling contact fatigue machines at the University of Bristol were used to test the influence of additives on the life of bearings. The machines were originally designed to investigate the influence of grinding processes on the fatigue life of bearing materials. The original cylindrical specimens have been replaced by 6305 deep groove ball bearings. The ensuing decrease in contact stress (caused by the geometrical changes at the contact) is compensated by increasing the combined roughness at the surface. This measure was taken to ensure that failure times did not become excessive. The oils tested on the Bristol rigs were:

- Shell Vitrea M100 (a base oil without additive)
- Shell Vitrea M100 + 2% Lubrizol 5034a (sulphur/phosphorus additive package)
- Shell Vitrea M100 + 5% Lubrizol 5034a (sulphur/phosphorus additive package)
- Shell Spirax AX 80W/90 (EP multipurpose gear oil containing S/P)

Twelve tests were carried out for each oil, with each test lasting for a maximum period of four weeks. The Vitrea neat oil acted as a base line to compare the oils containing additives against. The failure modes were examined using optical microscopy (OM) and scanning electron microscopy (SEM).

1.4.2 Fatigue testing at SKF engineering and research centre

A series of independent tests were carried out by SKF at the ERC. The test specimens used were 6206 DGBB bearings in the R2F rigs. The stresses were higher in these tests, with maximum Hertzian stresses of 4.2 (GPa). The tests were run at 80 °C and at speeds of 2,500 rpm. The oils tested using the R2F rigs were:

- TT 68 base oil containing no additives
- Volvo 97305 containing unknown additives
- Volvo 97037 containing unknown additives
- Shell Spirax AX 80W-90 (EP multipurpose gear oil containing S/P)

1.5 OVERVIEW OF HOT-WIRE METHOD OF REACTIVITY MEASUREMENT

Oil additives are blended with base oils to change their chemical and physical properties. Extreme pressure (EP) additives are used to improve life where a high degree of metal-to-metal contact is expected. The additives are thought to react with the metal surfaces producing a film of low shear strength. The result of this is that the effective lambda ratio is increased and hence the life increases.

As the oil reacts with the metal surface it would be useful to quantify the rate of corrosion. The hot-wire method has been used successfully by Barcroft [5], Sakurai et al. [6], and Han and Li [8] to test the reactivity between metals and additives. The test consists of calculating the change in the radius of a wire, when heated and corroded, by means of resistance measurements. From equation (1.1) it is seen that a decrease of wire diameter causes the wire resistance to increase.

$$R = \frac{\rho l}{A} \tag{1.1}$$

In previous hot-wire research test temperatures exceeded 400 °C and have been carried out above 700 °C. In this study tests were carried out at a lower temperature range of 140-450 °C. Below 300 °C corrosion reactions were not detectable by this method, but reaction films were seen to form at lower temperatures. To date reaction films at lower temperatures have been investigated using the EP immersion test. This test, described later in this thesis, has shown that dark films form on the metal surfaces at 160 °C.

1.6 OBJECTIVES OF WORK

The objectives of the work in this thesis may be summarised as follows:

a) To compare differences in rolling contact fatigue life data for bearings lubricated with base oils against ones containing concentrations of S/P additives.

b) To analyse the failure modes of the bearings and identify characteristic modes caused by the presence of additives in the oil.

c) To construct a modern hot-wire rig in the style used by Barcroft to test corrosion.

d) To quantify the reactivity of EP additives on metal surfaces, and to calculate activation energies of the reactions.

e) To identify factors caused by EP additives leading to early failures in bearings.

f) To identify lubricants which are appropriate for use in Hertzian contacts at elevated temperatures.

1.7 STRUCTURE OF THESIS

A survey of the literature describing the effects of additives in rolling contact is given in Chapter 2. Bearing life, endurance testing and failure prediction models are examined. Literature on the subjects of bearing steel and typical failure modes are then reviewed. The review then focuses on the chemistry of the extreme pressure additives used in Hertzian contacts. An extensive review of film formation and additive mechanisms forms the next part of the chapter. Parameters affecting bearing testing and failure are summarised. Finally papers concerning the Barcroft hot-wire method for measuring oil/metal reactivity are examined.

A description of the rolling contact fatigue rigs used at the University of Bristol is given in Chapter 3. The machines use a novel method of loading and lubricating the specimen by hydrostatic loading. The rolling contact fatigue rigs have been modified for this study to allow the temperature of the lubricants to be elevated to 70 °C. The testing conditions are presented, with full calculations of Hertzian stress calculations and lubricant film thickness given in Appendix (A). The test conditions and properties of the lubricants used are then presented. Finally, the test conditions of a series of fatigue tests carried out by SKF using their R2F rigs at their research facility in Holland are outlined. The stress and film calculations for these tests are given in Appendix (B).

The design and construction of a new hot-wire rig used to quantify the reactivity of EP additives is given in Chapter 4. The rig is made up of two main components, a heating circuit to initiate reactions and a measuring circuit to quantify the extent of corrosion on the metal surface. Some changes have been made to the original Barcroft design and all major sections of the rig are discussed in detail. Experimental procedures for the new two wire system are outlined. Methods of estimating reaction temperatures by using temperature/resistance characteristic graphs are outlined. Finally experimental details of a validation test are described.

Chapter 5 focuses on the rolling contact fatigue results. Results from the Bristol rigs and the R2F rigs used by SKF are plotted using Weibull analysis. Failure modes are investigated with the use of optical and SEM micro-graphs. Changes in bearing surface roughness of tested raceways are measured using a Zygo interferometer. FTIR analysis of oils samples is used to monitor oxidation changes in the lubricants.

Results of the hot-wire tests are presented in Chapter 6. Lubricant reactivity on two metals, iron and stainless steel, is measured for a series of lubricants. In some cases the Arrhenius equation can be applied to the results in order to calculate the activation energy for the system. An elemental analysis of a typical film produced by an EP additive is given. A mounted wire section was inspected using EDAX and the distribution of elements were given.

Finally, in Chapter 7, conclusions are drawn as to the merits and performance of the rolling contact fatigue testing program, and the limits and usefulness of the hot-wire technique are discussed. Final conclusions are made, and areas of future work identified.

CHAPTER 2

2 REVIEW OF LITERATURE

2.1 INTRODUCTION

As seen in Chapter 1, bearings fail for reasons such as poor machine design, inappropriate loading and inadequate lubrication. If these modes of failure are avoided a bearing will fail eventually by rolling contact fatigue. It is estimated [9] that 10% of all bearing failures are caused by such fatigue. The following sections will review literature published on the subjects of bearing life and failure, fatigue testing methods, the influence of additives on life and additive reactivity.

Section two of this chapter looks at bearing life theories and life endurance testing. Improved metal cleanliness [10] has meant that fewer bearings fail due to the classic subsurface mode, caused by non-metallic inclusions. As a result of this, lubricants have now become a more important factor influencing life. The test methods used to quantify influences on rolling contact fatigue life are discussed. From the information obtained from years of testing, the bearing industry has tried to predict using equations when bearings are likely to fail. Failure models are reviewed and the statistical nature of failure distribution is discussed.

The properties of bearing steels and types of failure modes commonly experienced in bearings are reviewed in section three. The main features involved in failure: pitting, wear and cracking are investigated. Crack formation and propagation are discussed, and the advances made in failure analysis through scanning electron microscopy are highlighted. Hydrogen embrittlement is reviewed at the end of this section, the detrimental effects of water content and contamination are also noted.

Section four deals with research that has been carried out on oil additives. Early papers are generally in favour of the use of additive, citing the benefits of increased life. Recently however, papers have been written challenging the widespread use of additives in lubrication applications. The chemistry of additives and the study of their decomposition are investigated. The factors affecting tribological situations are also reviewed. The complexities of reaction products and their analysis are also noted.

The final section of this chapter reviews papers dealing with the hot-wire technique for measuring additive reactivity. Barcroft [5] pioneered the test technique in 1960 working for Shell research. Since then the hot-wire method has been used by several researchers to investigate reactions at high temperatures. The test method, assumptions and analysis methods are discussed in detail, as this test method forms a substantial amount of the work carried out in this thesis.

2.1.1 Tribology

All of the subjects to be reviewed in this chapter can be classified under one heading - tribology. The term tribology was introduced in the 1966 in a British Department of Education and Science Report on the lubrication needs in industry commonly known as the Jost report. In this report, the potential financial benefits to industry resulting from sound friction management were realised. Hutchings [11] described tribology as the science and technology of interacting surfaces in relative motion, it includes the study of friction, wear, bearings and lubrication. Czichos [12] describes how most major countries founded committees for tribology, as they realised that through better tribological practises large financial benefits could be achieved.

2.1.2 Lubrication

The role of a lubricant is to reduce friction and wear in machinery, they protect metals against rust and corrosion, and act as heat transfer agents. Without lubrication at a mating surface damage will occur. For many years it was thought that no oil film could exist at the point of highest pressure in the contact area. Now it is generally accepted that not only is a film present but the nature of the lubricant is an important factor influencing life. The properties of a lubricating oil can be customised by adding chemical compounds called additives. Types of additives include anti-wear agents

(AW), anti-foamers, emulsifiers, extreme pressure (EP), antioxidants, viscosity improvers, rust inhibitors and friction modifiers.

The shift from using vegetable and animal oils (many of which were unstable) to mineral oils caused a major upheaval in the lubrication industry. Increased demand from industry caused the price of these unstable lubricants to increase. Soon studies had shown that mineral oils were suitable for many lubrication applications. The switch to using mineral oil came in the middle of the 19th Century. The additive industry first became important when the internal combustion engine was developed. Additives were introduced to reduce friction, control sludge formation and inhibit rust. The engineer turned to the chemist for help when sound engineering might have yielded better results. Additives today allow machinery to operate under harsh conditions which would have been unthinkable at the start of the century.

2.2 FATIGUE LIFE PREDICTION

2.2.1 The life of a ball bearing

The life of a bearing is expressed as the number of revolutions that it is capable of enduring before the first sign of fatigue. A large batch of bearings tested under identical conditions will have lives that will vary widely. For this reason, life is usually expressed in terms of a basic life rating, the L_{10} Life. The L_{10} life is the number of cycles that 90% of bearings can be expected to survive under similar operating conditions. This standard rating, is calculated from information obtained from testing a large sample of bearings to failure. Since life is strongly influenced by the load applied, a basic dynamic load rating, C, is defined. The load rating of a bearing is the load for which the L_{10} equals 1,000,000 revolutions. The basic ISO life prediction equation, seen later, simply relates load and life [13].

In 1977 the ISO introduced a revised life equation, which included three life adjustment factors to allow for reliability, material and operating conditions. The a_1 factor is used when a life greater than the L_{10} life is needed, for example, when the L_{05} life is required the a_1 factor drops from 1.0 to 0.62. The second factor, a_2, makes adjustments for steel quality. The third factor, a_3, makes adjustments for operating

conditions. A further development is the SKF "New Life Theory", this theory is an extension of the of the work of Lundberg and Palmgren. This theory takes into account the fatigue load limit and factors related to lubrication and contamination.

2.2.2 Methods of endurance testing

Endurance testing of bearings has been conducted within the bearing industry since 1910. The purpose of endurance testing is to, audit the standard of bearings, to compare quality against competitors, to confirm catalogue commitments, to monitor the influence of lubricants and to add support for theories. Endurance testing comes at a high cost; running large batches of bearing to failure is expensive. Results of testing between 1930-50 were used to support Lundberg and Palmgren [14][15] theory. As full scale testing is costly, there have been many efforts to accelerate endurance testing. Goss and Ioannides [16] describe how important factors such as load, speed, temperatures and contamination are tested in modern research facilities.

Leenders [17] describes how bearing tests are accelerated to minimise testing time. Conditions are severe compared to normal testing, factors such as load, oil operating temperatures and film thickness are optimised. Care must be taken that the conditions are not unrealistic. When Cameron [18] reviewed boundary and EP lubrication since 1937, he pointed out that if fatigue test conditions are not realistic then the results would not be reliable for comparison. Wang et al. [19] is a classic example of this, where the 4-ball machine is used to produce Hertzian stresses of up to 9 (GPa). At such high stresses the heat transfer properties of the oil is sometimes the primary parameter influencing performance and so the results are of limited use.

A review of endurance testing was compiled by Plint and Alliston-Greiner [20]. In it standard methods of testing EP additives were reviewed. Test machines were grouped under two headings: group 1 machines have a fixed surface in contact with a rotating surface, and group 2 machines have the two mating surfaces rotating. All test rigs can be compared by important parameters such as geometry, stress, velocity and frequency of stress cycling. The effects of lubricants in endurance testing are given by Kleinlein [21] working for the German bearing manufacturer FAG. An attempt to lower the cost involved with endurance testing is given by Morrison et al. [22]. This

technique attempts to use a small number of specimens in conjunction with SEM analysis of bearing surfaces to detect failure modes in bearings. Tests were carried out on a synthetic oil lubricant in a pump bearing.

2.2.3 Failure prediction models

Eleven failure prediction models are reviewed by Tallian [23] identifying common life-influencing variables and relations. In 1947 and 1952, Lundberg [14] and Palmgren [15] published their two influential papers on the load carrying capacity of rolling bearings. In these papers they defined the standard equations relating the load carried by a bearing to it predicted life. The simplified equation relating survival probability S, to Lundberg - Palmgren life L_{LP} for an assembly of one or more contacts is given by:

$$-\ln S(L_{LP}) = \left(\frac{C}{P}\right)^{-p\beta} L_{LP}^{\beta} \qquad (2.1)$$

The life centres around the C/P ratio, C characterises the load carrying capacity of a component of a given material and geometry. P is the equivalent applied load. The Weibull dispersion exponent is usually set at $\beta = 1.1$, with $p = 3$ for ball bearings and $p = 10/3$ for roller bearings.

The ISO standard was introduced in 1977 [24] when the Lundberg - Palmgren model was extended to include life adjustment factors a_1, a_2, a_3 for reliability, material and operating conditions.

$$L = a_1 a_2 a_3 \left(\frac{C}{P}\right)^{p} = a_1 a_2 a_3 L_{\mathrm{LP10}} \qquad (2.2)$$

Since then improvements in the quality of steel, as described by F. Hengerer [25], and advances in heat treatment methods have meant that bearings today have a greater life than that predicted by the standardised theory. Ioannides and Harris [26] have built on classical ideas to formulate "The New Life Theory" of bearings. A fatigue load limit is introduced which represents the load below which fatigue will not occur. The a_2 and a_3 life adjustment factors were combined to produce the a_{SKF} coefficient. Wuttkowski and Ioannides [27] have described the development of life prediction equations from Lundberg -Palmgren to the SKF New Life theory.

The SKF New Life equation:

$$L_{SKF} = a_1 a_{SKF} L_{\mathrm{LP10}} \tag{2.3}$$

The Schlicht et al. [28] model was published in 1986, and was adopted by the FAG catalogue in 1990. Bearing failures are taken to be nearly exclusively surface in origin, the critical stress is the Von Mises stress. Plastic flow and residual stresses arising in the load cycling are important factors.

$$L_x = a_1 a_{23} f_t \left(\frac{C}{P}\right)^{-p} \tag{2.4}$$

Keer et al. [29][30] published two papers on crack propagation research models for a 2-D fracture-mechanical model of rolling/sliding contacts. Traction, crack growth direction and hydraulic effects in cracks are covered. The model predicts that life is shortened if the crack is in the same direction as rolling, and the life is increased if the crack is in the opposite direction to rolling. Bearing life calculated using this equation is orders of magnitude lower than any of the engineering prediction models for similar Hertzian pressure. A more sophisticated three dimensional crack propagation model was researched by Hanson and Kerr [31]. A fatigue stress limit is assumed, with a discontinuity of crack growth at that stress. The predicted life at a Hertzian stress of 2 GPa is in the order 10^7 cycles which is closer to that of engineering models.

A study of plastic cumulative strain in a strain hardened material under contact stress cycling by was published by, Bhargava et al. [32]. The stress verses plastic strain curve is a cliff curve rising steeply from zero at a shakedown limit stress and flattening towards horizontal near twice that stress. Spalling lives are predicted from the plastic strain levels. Blake and Cheng [33][34] studied a crack propagation model for spur gear. Contact pressure, crack initiation angle, traction coefficient, slide/roll ratio and the lambda ratio are calculated for carburized test roller and gear sets. All life predictions are less than 10^6 cycles and thus are very conservative estimates of life.

2.2.4 Failure distribution

Considerable scatter can occur in bearing fatigue life, this is partly due to the inhomogeneities found randomly in the material, and to the varying solid debris that may pass through the contact zone. The bearing steel is a matrix with a number of defects being acted on by an applied cyclic stress. As the cycling proceeds, irreversible changes occur near the defects and spalls form at the most severe defect. Defect severity and density are randomly distributed, hence spalling life has a degree of scatter.

The wide scatter makes predicting the life on an individual bearing nearly impossible. Bearing life predictions can only be assessed accurately when a large number of bearings are tested under similar conditions. Failure lives are then arranged in order of increasing failure times and the results are plotted on Weibull distribution paper. On this graph log t (x-axis) is plotted against log.ln[1/(1/$F(t)$)] (y-axis).

Weibull Distribution: $$F(t) = 1 - \exp\left[-\left(\frac{t}{T}\right)^{\beta}\right] \qquad (2.7)$$

Where:

	F(t)	is the failure probability
	t	is the time to failure
	T	is the time when 63.2% have failed
	β	is a measure of scatter and corresponds to slope of line through plotted points

2.3 BEARING STEELS

The elemental composition of bearings has remained nearly unchanged since the start of the 20th century, 1% carbon and 1.5% chromium being typical. The heat treatment of AISI 52000 steel is described in the ASM Metals Handbook [13]. A Special vacuum melting process is used to minimize inclusions. This process minimises residual austenite content in the steel and ensures dimensional stability.

AISI 52100 steel can be through hardened up to 13mm, for larger sections a modified 52100 steel can be used. Kroon and Nutzel [36] also reported on bearing steel development, with decreases in inclusions obtained with electro-slag remelting. Improvements in bearing steel have been described by Hengerer [25]. Non-metallic inclusions in bearings generate local stress concentrations and are potential points for crack initiation. Heat treatment by soft annealing gives good machining properties. Oxygen and macro inclusions have steadily decreased since the 1950s. Basic metallurgical problems such as cleanliness have been solved.

Christ et al. [37] carried out push-pull fatigue tests on three variants of 52100 steel with slightly different compositions and heat treatments. Under high stresses, changes to the microstructure can occur such as decay of martensite to ferrite. Changes in residual stresses and a decay of retained austenite can also occur. The retained austenite decomposes considerably in the first loading cycle, from 11% to 4%. The transformation from austenite to martensite can cause volumetric changes of 5%.

Morgan [38][39] reported on plastic deformations in rolling and static contacts. Torrance [40] discusses grinding burn in 52100 steel, if the temperature of the surface rises above the tempering temperature the steel softens and this is known as temper burn. Torrance found [3] grey matter containing phosphorus was found in the cracks. Hollox et al. [41] used martensitic heat treatment on 52100 steel keeping the steels free from surface and other defects. His study looks at new developments and their effects on predicting life. Below a certain stress level the life of the bearing is nearly infinite. Zaretsky et al. [42] reported on hardness and its effects on life. Maximum fatigue life and load capacity achieved when rolling elements are 1 or 2 points (Rockwell C) harder than the races.

2.3.1 Bearing damage - classifying failures modes

Early work on failure modes concluded that the primary mode of failure was by surface initiation. Lanchester [43] in 1921 proposed that pitting was due to a welding tearing process. Way's [44] classic paper on pit formation, describes v-shaped pitting starting at the surface. He thought pitting could be prevented by using adequate lubrication and that mating hard and smooth surfaces provided the best resistance to

pitting. Fatigue spalling can be sub-classed by spall origin, surface or subsurface. Surface distress is characterised by a high gloss of the metal and an obliteration of the original finishing marks. Surface distress originates from a plastic deformation of the asperities. In the advanced stages of this failure small pits form on the burnished surface. As large amounts of small pits form on the distressed surface, this type of phenomenon is sometimes called micro-pitting.

Bearing failures are primarily classified according to their place of origin. Littman and Widner [45] have summarised spalling failure in the following way; (1) Spalling originating under the surface due to non-metallic inclusions or unconfirmed origin and (2) Spalling originating at the surface due to debris dents, handling nicks, surface flaws or surface inclusions. Tallian [46][47] has classified rolling contact failure according to their failure modes: wear, plastic flow, fatigue and bulk failures. A common failure mode between hard steel surfaces is contact fatigue. Contact fatigue is classified as spalling or surface distress. Spalling fatigue is described as a crater-like depression in the original rolling surface. Spalling in some literature is referred to as pitting or flaking. Action must be taken to control the most critical failure mode by setting acceptable limits.

Martin and Eberhardt [48] found surface distress around grinding furrows. They identified potential nuclei in RCF. In very clean steels fatigue normally starts at a surface defect. Deformation bands and orientation are found in areas of high shear stress. Borgese [49] developed a technique for making fractographs of spalls. Spalls are not formed over one cycle, but metal is removed in several stages to form a spall.

Scott and Blackwell [50] reported that subsurface cracks occur at a depth near where maximum shear stress occurs. Spalling originating at the surface is caused by a stress concentration, a breakdown in lubrication or an asperity contact near a metal defect. In 1979, Citlan and Sailbel [51] proposed a new mechanism of pitting corrosion. They highlighted the importance of specific ions, called "Zeta Potential" in the lubricant which migrate to the tips of the cracks and through the surface of the solid causing volumetric changes that leads to blistering and pitting.

Zhou et al [52], wrote a paper on micro-pitting which reported on the micro-crack initiation, propagation and surface pitting. Cracking is assumed to occur when the accumulated strain energy of the dislocation reaches a critical level. A 3-D crack propagation model was used to predict pitting life in rolling contacts. Polk and Rowe [53] used an optical method to measure the extent of cracking in specimens which have failed under rolling contact conditions.

2.3.2 Wear in rolling contact fatigue

Friction occurs when two mating surfaces move relative to each other. The introduction of a lubricant in bearings can reduce friction considerably but metal to metal contact will eventually cause wear. Wear is the loss of material along the running track of the bearing elements, which produces a series of small craters, known as micro-pitting. Abrasion or roughening of the surface is usually caused by hard particles such as dust, grit or sand entering the contact area. Abrasion of asperities can uncover fresh metal surfaces which are free from surface oxides and therefore more susceptible to attack by additives. Barwell [54] and Spikes et al. [55] have compiled good reviews on wear mechanisms.

Suh's [56] delamination theory describes thin plate-like particle formation. The theory states that friction forces are caused by the effects of asperity deformation, ploughing and adhesion. Subsurface deformation is caused by cyclical loading, and this causes the nucleation of voids at a distance underneath the surface. Voids can coalesce to form a crack that runs parallel to the surface. The crack propagates to the surface producing a flake like debris. The flakes have a length to thickness ratio of 10:1, up to one million flakes can be generated in 200 cm^3 of lubricant. Tallian [57][58] wrote two papers on life prediction in contaminated lubricants, where wear debris continually builds up causing quicker failures.

Archard [59] calculates the wear volume to be the product of the real area of contact, the sliding distance and the coefficient of wear. Rowe presented [60] a model of adhesive wear for boundary lubrication. The wear rate is expressed as the volume of material lost per unit sliding distance and is related to the real area of contact. The rate of adhesive wear and the ratio of load to hardness have been extended to include a

lubricant on the surface. This model considers the heat of adsorption to be the controlling factor in the effectiveness of a boundary lubricant.

2.3.3 Cracking in bearings

The fatigue life of a bearing can be divided into three stages, crack initiation, crack propagation and fast fracture. The crack initiation time depends on the micro-structural details of the steel, especially the distribution of hard inclusions. At present no model has been developed to predict this initiation period. The propagation period can be predicted using Paris' empirical law.

Salehizadeh and Saka [61], using finite elements have calculated the time it takes for a crack to reach a critical spalling length. Stress intensity factors, for straight cracks subjected to pure mode II loading and branched cracks subjected to mode I and II loading, were calculated. Subsurface cracks initiate around non-metallic inclusions or carbide particles. The crack, must reach a critical length and reach the surface before spalling can occur.

Torrance [62] in a metallographic survey of pitted tracks lubricated with hydraulic oil found that many surface defects and subsurface cracks were found in specimens that had failed by pitting. None of the cracks showed signs of propagating to form pits. The cracks however were seen to contain a substance which was rich in phosphorus, measured quantitatively by electron microprobe analysis. The pitting may have been started by corrosion. Surface-nucleated cracks may propagate to form pits through hydraulic action, as oil is forced into the crack by a pressure caused by the movement of the rolling elements.

2.3.4 Optical and SEM analysis

The tools used in the examination of failed specimens are important to researchers. Osterlund and Vindsbo [63] paper looked at phase changes in bearing steels, by comparing micrographs taken with LM and SEM methods. A greater number of features were identified clearly using SEM, such as, primary carbides and martensite. Phase changes in fatigued bearings were also identified with micro-graphs. Torrance [52] draws attention to the difficulty in near surface metallography, extreme care must

be taken during preparation stages to avoid damage to the metal. Werker and Voskamp [64] used x-ray analysis to characterize distress on bearing surfaces. Voskamp [65][66] used x-ray diffraction to identify bearing material response to loading. He discovered the preferred crystalline orientation in narrow subsurface regions. Material response to loading can be divided into three phases: shakedown, steady state and instability. The preferred orientation develops in the third stage from the accumulation of micro yield. Deformations accumulate at newly formed weak points initiating fatigue failure. Bartz [67] reviewed failures in rolling contacts caused by inadequate lubrication. Dizdar and co-worker [68][69][70] have used GD-OES glow discharge optical emission spectroscopy to analyse quantitatively the elemental structure of film formation in boundary contacts. Elemental concentration profiles can be plotted to depths as small as 10 (nm).

2.3.5 Hydrogen embrittlement effects on bearing steels

Industrial oils are known to contain small quantities of dissolved water in the range 50 to 500ppm. Water molecules are smaller than lubricant and additive molecules and can readily diffuse into the tips of micro-cracks where decomposition can occur on surfaces leading to the production of hydrogen. Subsequent embrittlement can promote crack propagation and branching. Effects of water and oxygen in rolling contact lubrication have been studied by Schatzberg and Felsen [71]. Tests were carried out using a 4-ball machine, the lubricant contained controlled concentrations of water and oxygen. Corrosion was found to increase with increasing water concentration and this caused a reduction in fatigue life. Dissolved oxygen also resulted in a small but measurable reduction in fatigue life.

Ciruna and Szieleit [72] conducted 4-ball tests using AISI 52100 and 440C steels impregnated with hydrogen, and found that the fatigue life was inversely proportional the hydrogen content in the steels. Ioannides and Jacobson [73] have studied the reduction in bearing life due to contamination caused by reaction. Particles depending on their size and hardness were found to be capable of penetrating the lubricant film giving local stresses and increased wear. Small concentrations of water (0.01%) were found to reduce the life of the bearing by half. Wan et al. [74] report that the deterioration of lubricants due to oxidation can influence the life of a bearing and is a

dominant mechanism in hydrogen embrittlement. FTIR was used to investigate the influence of a S/P additive package on the oxidation process of a base oil. The results showed that this package increased the rate of oxidation. Acidic compounds that can cause corrosion of bearing surfaces were formed by oxidation. Hydrogen was also produced by the oxidation process that could initiate hydrogen embrittlement.

2.4 OIL ADDITIVES IN LUBRICANTS

A lubricating motor oil typically contains between 90-95% of a bulk component called base oil and 5 - 10% of reactive chemicals called additives. The base oil determines the physical properties of the oil, and the additives can alter the chemical behaviour under harsh conditions. According to Forbes [75] there are two groups of additives:

a) Additives used to alter the physical properties:
   - anti-foamers: prevent or reduces stable foam formation.
   - viscosity improvers: reduce the rate of change of viscosity with temperature.
   - pour point depressants: lower the pour point of oil.

b) Additives used to alter the chemical properties:
   - detergents: remove oxidation products from lubricated surfaces.
   - corrosion inhibitors: protect metal surfaces from corrosion.
   - anti-wear: reduce rapid wear in metal-to-metal regimes.
   - extreme pressure: prevent seizure under high loading and temperatures.

When lubricating films collapse, due to surface wear, boundary lubrication may exist in the contact. Additives became increasingly important during the development of the IC engine. High temperatures were experienced at contacts and pressures were extreme. Boundary layer films are important when the lambda ratio falls below a value of 1. When metal-to-metal contact occurs the additive's behaviour becomes increasingly important.

2.4.1 Chemistry

Lansdown [76] describes the complex chemistry of modern lubricants as a "witches brew of additives". Anti-wear additives are generally sulphur and/or phosphorus

containing organic compounds added to oils to reduce wear at moderate temperatures and pressures. They form thin organo-sulphide or phosphate films, which often produce a polishing effect on surfaces. Extreme pressure additives are organic compounds with at least one non-metal element usually sulphur. Wong et al. [77] looked at changes in the density of lubricants due to increases in pressure and temperature. Oils are said to be a complex mixture of compounds, with a wide range of boiling points.

Research into the chemical influences of additives on fatigue life usually involves a comparison between static and dynamic experiments. Rounds [78] has compared TCP and ZDDP using dynamic friction and static immersion tests. Seven additives were tested at various loading and temperature conditions. Under dynamic conditions the amount of phosphorus on the surface increased exponentially with increasing temperature. The temperatures at which reaction film gained an appreciable thickness were found to be similar. There was a sharp increase in thickness at 350F (176 °C). Additive decomposition in the bulk oil generally occurred at the same temperature as detectable oil oxidation. Thus additive decomposition may be triggered by oil oxidation products.

In another paper, Rounds [79] studied the influence of steel composition of two case hardened and five through hardened steels. In low alloy steels more surface coatings formed on surfaces, with the composition of the oxide layer being the controlling factor. The magnitude of the steel effect depended on the nature of the additive and the oxygen level available. Additive decomposition was found to be promoted by oxygen, but was unaffected by the composition of the steel. The study looked at two case hardened steels and five through hardened steels in dynamic friction, fatigue and immersion tests. Static beaker testing showed a high increase of phosphorus on surface at temperatures of over 450F (232 °C). The critical temperature for sulphur was 350F (178 °C).

Cameron [80] has theorised that the reactivity of steels is enhanced by the phase transformation from retained austenite to martensite. This occurs for bearing steel in the temperature range 350-400F (178-204 °C). Effects of oxygen on surface coating

formation were studied, on low alloy steel the surface layer is usually iron oxide but alloying elements can contribute to the film. Parker and Zaretsky [81][82] tested fatigue life of eight steels using five-ball tests. They found a decrease in fatigue life with an increase in total weight percentage of alloying elements. Of the steels tested at high stresses and high temperatures SAE 52100 was found to be the best. Barber [83] tested phosphorus compounds using a 4-ball machine and found increases in the weld point compared to when base oil are used .

Traditionally reaction films produced by additives were thought to have thicknesses of a few nanometers. In 1985 Lacey et al. [84][85] reported on the thick film concept. Using a ball on a glass disc apparatus at oil temperatures of over 100 °C, thick films were seen to grow during the test period of 3 hours. These films were not seen when a base oil was used. A discolouration was seen on the test ball, which was not removed by ultrasonic cleaning. Using EDAX analysis, large amounts of phosphorus were found in the track. This thick film has large implications on the Lambda ratio for the contact. In this study the lambda ratio changed from 0.2 to 0.8 during the test, thus providing a greater protection against wear.

The chemical nature of the thick films was investigated in the second paper. The phosphonate ester used in the dynamic tests were found to form viscous "wax-like" reaction products when reacted with iron powder. A good example of the confusion that surrounds the used of additives is the study by Phillips and Quinn [86]. Tests carried out with disc-on-disc apparatus. When the D ratio (similar to the Lambda ratio) was below 1.5, the use of additive reduced pitting life, with D ratios above 1.5 the opposite occurred. This paper shows the importance that the contact parameters can have while using the same lubricant. Galvin and Naylor [87] used rotating bending cantilever tests to eliminate the effects of friction and wear. A Wohler fatigue rig was used, where a specimen immersed in a lubricant was rotated while having a constant load applied. Mineral white oil was tested against oils containing phosphorus. A decrease in life and fatigue limit was observed when the white oil was not used. At stresses above the fatigue limit some specimen lives were only 10-12% of those found with the white oil. Sheasby et al. [88] studying additive interactions in

steels and ceramics found that the conditions in which additives perform well can be very restricted.

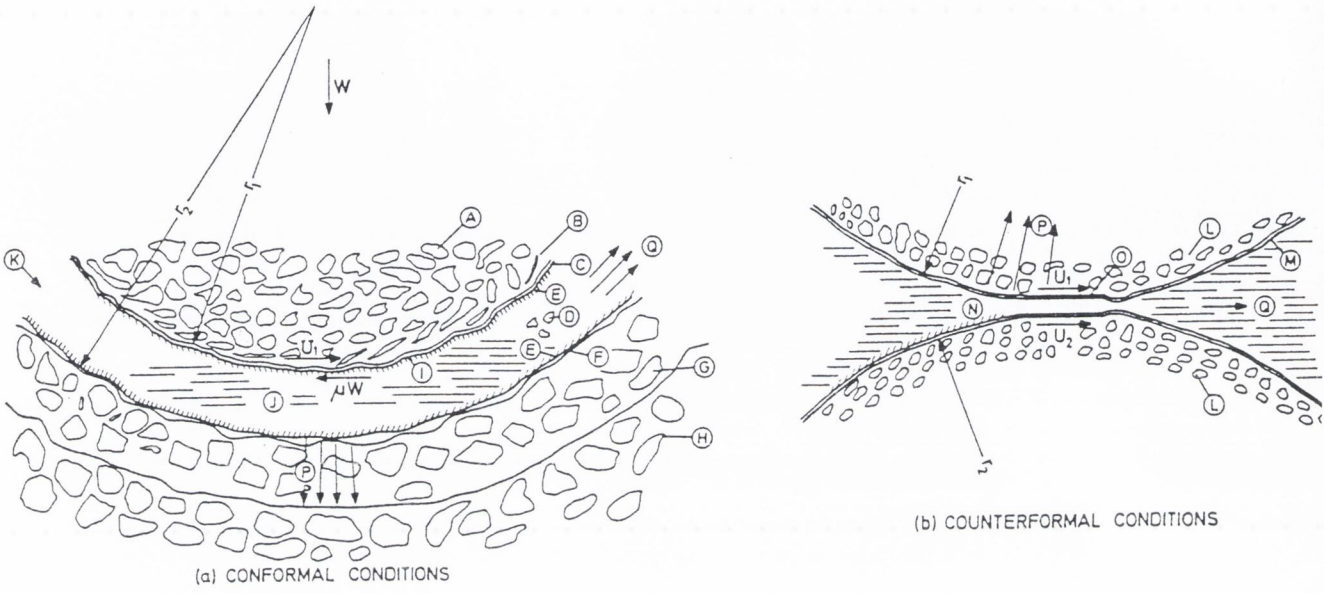

KEY	FEATURE	DISCIPLINES INVOLVED
A	SHAFT MATERIAL - HARD OR SOFT	METALLURGY
B	MICROSTRUCTURE MIXED WITH OXIDE	ELECTRON PHYSICS
C	OXIDE LAYER	INORGANIC CHEMISTRY
D	FOREIGN PARTICLES IN LUBRICANT	MICROSCOPY
E	SURFACE PROFILE- WAVENESS AND ROUGHNESS	METROLOGY
F	EMBEDDDED MATERIAL AND WIPED SURFACES	APPLIED MECHANICS
G	BEARING MATERIAL - SOFT	METALLURGY
H	STEEL BACKING	METALLURGY - STRENGTH OF MATERIALS
I	ABSORBED OR REACTED SURFACE LAYER	PHYSICAL CHEMISTRY
J	LUBRICANT - FILM THICKNESS	ORGANIC CHEMISTRY - HYDRODYNAIMICS
K	AMBIENT ATMOSPHERE	CHEMISTRY - PHYSICS
L	HARDENED MATERIAL	METALLURGY
M	REACTED FILM (FROM EP ADDITIVE)	CHEMISTRY
N	LUBRICANT - FILM THICKNESS - PRESSURE	ORGANIC CHEMISTRY - APPLIED MECHANICS
O	ELASTICALLY DISTORTED SURFACE	THEORY OF ELASTICITY
P	HEAT CONDUCTED ACROSS SURFACE	HEAT TRANSFER
Q	HEAT CONVECTED IN LUBRICANT	THERMODYNAMICS

Figure 2.4 Factors affecting tribological situation - from F.T. Barwell [54]

2.4.2 Additives ZDDP/TCP

Spikes and Cameron [89] tested dibenzyl disulphide in friction tests. Additive reactions on the test specimen were measured using a radio-tracer technique. The concentration of sulphur on the metal surface was found to increase as temperature increased, this was matched with a reduction in friction co-efficient (0.27 to 0.12) at 165 °C. Georges et al. [90] generated films with pin-on-disc tests, the reactions of the ZDDP additive in tribological contacts were found to be complex. Anti-wear films are

produced in the contact zone by tribo-chemical reactions. The paste produced by the surface products is thought to be the principle factor in wear characterisation.

Khorramian et al. [91] studied the effects of additives in automotive engines. Scuffing in the crankcase caused reduced life and increased fuel consumption. Mild, or oiliness agents were found to protect against wear. Full EP additives prevented welding scuffing and galling. ZDDP's main function is wear prevention. Cann et al. [92] studied the formation of thick films by the reactions of ZDDPs on metal surfaces using a high frequency reciprocating device. Anti-wear additives are recommended in mixed lubricating regimes. EP additives are more appropriate in boundary regions were the lubricant film breaks down. The thermal decomposition products are found to react with the metal surfaces forming thin organic films. Films formed with high concentrations are found sometimes to be unstable and can increase wear and friction.

So and Lin [93] studied films produced by ZDDPs, concentrations of sulphur and phosphorus were highest in the rubbed areas. They came up with an anti-wear theory, additive decomposition was followed by absorbtion of products onto the rubbed surfaces, forming a chemisorbed film. Two surfaces with different hardnesses can react differently. Three layers are thought to exist, from the surface out, a reaction film, a chemisorbed film and a gel on the outside. Rosado [94] has shown that under boundary conditions fatigue life and wear are affected by temperature and lubricant type. He found statistical differences between oils tested on M50.

Gauthier et al. [95] studied the iron phosphate formation in the film seen by other authors. Bieber et al. [96] studied the impurities in TCP, they were believed to be acid phosphates and chlorophosphates. Gallopoulos and Murphy [97] studied the interactions between ZDDP and oil dispersants.

2.4.3 Mechanisms

Forbes [98] investigated how EP additives react with metal surfaces to form inorganic coatings that prevent welding. Forbes and Battersby [99] investigated anti-wear properties of dialkyl phosphates using a 4-ball tests, adsorption tests and an oxidation test. They found that the best additive is the one that reacts the fastest when surfaces

are exposed. Phosphorus was recommended for anti-wear conditions and sulphur for extreme pressure regimes. Allum and Forbes [100] considered the differences that the reaction mechanisms of organic sulphur compounds can have in mixed region and boundary regions. In mixed lubrication wear scars show very little sulphur but the boundary region shows high amounts of sulphur. In further 4-ball tests, wear scars were produced with various roughnesses. Sulphur was found on the centre of the scars (30% wt) using electron probe analysis giving sulphur distributions. Cracks were visible at right angles to the direction of sliding. The mechanism suggested was that disulphide absorbs onto metal surface, followed by cleavage of the S-S bond occuring with the formation of an iron mercaptide layer.

Tallian [101] defined modes of failure caused by wear, galling, plastic indentation, heat imbalance and rolling contact fatigue. Fatigue is a gradual reaction to repeated loading. Cracks grow to a critical length and then failure occurs. He gave factors for life prediction as a function of, design geometry, material and its condition, surface, load, chemistry of the lubricant and degree of sliding. Lundberg and Palmgren [102] considered the case of maximum alternating shear stress, with no traction. Failures start at the point of maximum shear stress. Weibull statistics were used to analyse the life results. Cantley [103] devised a method for predicting the effect of lubricant chemistry on fatigue life. In ring-on-block tests a few additives had negative effect on life. Scott [104] found that in the 4-ball test, high stresses and high concentrations of additive reduced life.

Rowson and Wu [105] tested using an Amsler twin-disc rig, and found that at 30 °C sulphur was detrimental but at 100 °C it was beneficial. A possible solution could be the formation of a sulphur acid at the oil lower temperature. Correlation between the D ratio and time to first pitting confirmed this. Begelinger and DeGee [106] studied thin film lubrication in sliding point contacts of 52100 steel. They found that with pin-on-disc tests the load carrying capacity with base oil was significantly lower than when oils containing di-esters were used.

In 1965 Godfrey [107] investigated the mechanisms of TCP and proved that iron phosphates form on ferrous surfaces. No evidence was found to support theory that

TCP reduces wear by the formation of an iron-iron phosphorus eutectic. Hall [108] looked at organo-phosphorus compounds and compares them to TCP. Reactions were carried out on 440C and 52100 steel, the 440C steel was seen to be the least reactive of the two. The 4-Ball tester was again used, and most phosphates were seen to reduce wear. Davey [109] investigated the effects of additive concentration on wear. Phosphides were seen to be better than phosphates as EP additives producing smaller wear scars in 4-ball tests. Higher concentrations of additives promoted chemical attack on surfaces. There was a suggestion that sulphide films may facilitate the attack of the phosphorus additive.

2.4.4 Film formation

Mills [110] found thick films could be formed by ZDDP which turned solid at temperatures of between 90 °C and 250 °C. Fowles et al. [111] found that an unidentified "organic phosphonate" could react and give a thick film at 80 °C. Debies and Johnston [112] used SAM analysis to study thin films produced by boundary lubrication. Elements attributable to the additives were found on the wear surface. Auger images showed a highly inhomogeneous distribution of surface elements, this was thought to be caused by the spread of debris on the surface. The debris was composed of metal particulates, hydrocarbon and additives residue. Dimnet and Georges [113] modelled the surface damage caused by reaction products, due to scratching. Wear in boundary lubrication is seen to be caused by a ploughing action caused by lumps of colloidal substances. When the relatively soft particle enters the contact inlet it deforms. Under contact pressure this layer of plastic material can cause scratching. Hamilton and Woods [114] studied the reactivity of sulphurized terpene hydrocarbons at temperatures between 125 °C and 275 °C. They report the formation of iron sulphide at the rubbing surface.

Godfrey [115] looked at the chemical composition of the film formed on steel by EP additives. The EP film was defined as the reaction products layer which was insoluble in hydrocarbon solvents. He concluded that the sulfurized mineral oil promotes oxidation of steel under EP conditions. Iron sulphides are the major constituents of the film. Organic silicon compounds were also present in the film. They cause a decrease in friction and wear. Fowles [116] has found that organic phosphonates can

form thick chemical films within the rolling track in an EHD contact. The film is sheared as it is formed leading to a reduction in traction. Failure analysis is hampered by the destruction of the evidence. Forbes and Upsdell [117] and Sakurai [118] tried to relate reactivity and load carrying capacity.

Georges et al. [119] found that a colloidal paste was formed when oxides, adsorbed lubricant and additives are mixed together in the convergent contact. Depending on conditions the paste can cause abrasive wear or be a protective layer, more evidence of additive interactions being a complex phenomenon. The films have a complicated structure as shown by Godfrey [120]. Tallian wrote two papers [121][122] on the effects of contaminants on bearing life, a theoretical one followed by an experimental one, and concluded, "Rolling bearing will survive without fatigue spalling for much longer if they operate in an extremely clean environment".

2.4.5 Temperatures

As temperature is one of the key factors influencing additive reactivity it is important to be able to estimate the temperatures in the contact. Bulk oil temperatures of lubricants are generally used in bearing catalogues to define safe operating conditions. Higher temperatures however are produced at the micro-asperity level where metal-to-metal welding and shearing takes place. Sethuramiah et al. [123] deal with EP lubrication as a temperature problem. Using the 4-ball machine with five sulphur compounds, they showed that two types of failure occurred. EP lubrication failure is first a lubricant failure at 290-390 °C. Beyond this the EP film may or may not support the load. There is a second critical temperature at around 700 °C which is a consequence of metallurgical failure. Salomon [124] estimates flash temperatures of 500-600 °C in four ball tests. Load is increased in steps and a period of high wear and friction is reached. Then a sudden decrease in friction is caused by the adhesion of iron oxides on the surface. Archard [125] developed an equation to estimate surface temperature from the wear conditions.

2.4.6 Early failures with additives

Recent papers have cast doubts on the usefulness of the widespread use of oil additives in bearings. Wan [126] found that in marginal lubricating conditions

(lambda=1.2) that a S/P package can reduce life by a factor of 4.5 compared with base oil alone. Post-test analysis showed differences in surface topography. In the test specimens lubricated with the additive, wear tracks were hardly visible and the surface roughness had decreased by a factor of three. Research from other labs [127][82] has suggested that additives can sometimes be detrimental to bearing life. The effectiveness of an additive depends on concentration, temperature, stresses and film thickness. Most studies have focused on high stress regimes which is not truly representative of a bearing in normal operation.

Wan used the SKF R2F rigs at Hertzian stresses of 3.3 GPa. and found a decrease in fatigue life when S/P EP additives were added to base oil. Immersion tests confirmed the reactive nature of the EP additives at 160 °C. Ball discoloration was evident using additive and absent with base oil alone. Four-ball tests showed that the EP additive had a high weld load but this test is not necessarily a good way of assessing additive performance. Wan [4] also carried out tests under moderate lubrication conditions (lambda=2) again EP additives caused a reduction in rolling contact fatigue life, this was attributed to the aggressive nature of the phosphonate additive. The tests were carried out with diphenyl phosphate (DPP) additive. Tests with additives showed a reduction in the steel barrel diameter by several microns as compared with minute changes when no additive was used. There was a L_{10} life reduction of around five when additives were used.

Khorramian et al. [91] in a review of synthetic additives, found that under high loads and temperatures, friction, wear, scuffing, and corrosion can occur. This may reduce engine life. Each additive has its own mechanism in reducing friction. Cautious and selective use of additives is necessary if additives are to be used effectively. Summers-Smith [1] considers additives to be responsible for failures in industrial systems. Sulphur caused early failures in silver bearings. Additives should only be used in systems were their use has been established as essential.

Parker and Zaretsky [82] also looked at effects of EP additives on life. He found that some additives were detrimental to fatigue life. The chlorinated-wax additive reduced life by a factor of 7. Sulphurized terpene additive reduced life by 50%. A recent paper

by Torrance et al. [2], (the foundation work of this thesis), showed that if the reactivity of additives in rolling contacts is high then there is a risk of a reduction in the fatigue life of the bearing. Ball-on-cylinder tests [129] have shown that fatigue life was reduced when the lubricant contained a commercial sulphur/phosphorus additive package. Wear volumes were compared for the two conditions.

2.5 REACTIVITY OF OILS ON METALS USING HOT-WIRE TESTING

In bearings it is often difficult to understand what chemical or physical reactions are taking place at contact zone because as the products are formed they are worn away from the surface. The thickness of corrosion is sometimes very small and this can also hinder analysis. Static tests have been developed where by hot specimens are plunged into oils, similar to quenching, and the reaction products are analysed. Rounds [79][130] compared dynamic friction tests and static immersion tests with TCP and DDP. Critical temperatures were found where elements such as sulphur and phosphorus were detected on the surface.

Levine and Peterson [131] heated metal discs to high temperatures and plunged them into solutions of free sulphur in cetane. Factors such as disc temperature, rate of cooling and extent of reaction were measured. In other tests by Godfrey [107], iron filings were heated in oil and then analysed to find how much iron was consumed in the reaction. The SKF reaction test involves putting ½ inch balls in beakers and heating them in ovens for 24 hours or 72 hours. The reactivity is ranked by the discolouration of the surfaces during post test inspection. The hot-wire technique measures the rate of corrosion on the surface of thin metal wires through resistance measurements. The rest of this section will examine this method in detail as it is a major part of the experimental work in this thesis.

Davey [132] found that the high temperatures experienced in contact areas caused the additive elements phosphorus, sulphur and chlorine to react. Using such additives is thought to decrease the metal-to-metal contact between the mating surfaces due to the reaction film formation and through the gradual smoothing of the surfaces due to chemical corrosion. Unreactive additives are known to give little protection against

scuffing, yet damage can also occur if the additive reaction is high and uncontrolled chemical corrosion occurs. It is important then to be able to select a correct additive type and concentration for specific applications.

2.5.1 Barcroft's hot-wire method

Oil additives are combined, in small concentrations, with lubricating oil used in gears and bearings to improve component life. The additives are known to react with the metal surfaces producing a film that effectively reduces asperity contact. If the additive becomes too reactive, damage may occur to the surface due to chemical corrosion. A technique was required to test additive reactions at normal operating temperatures, but also at higher temperatures found at the contact of asperities were shearing and welding take place.

In 1960 Barcroft [5] working at Shell Research Ltd., Chester, developed a static test method that quantifies the corrosive reaction oils and metals at high temperatures. The hot-wire technique involves heating a thin wire immersed in a lubricant and measuring the thickness of the surface that is corroded or consumed as the reaction occurs. As the hot-wire test is static the reaction products are not removed from the surface by wear mechanisms. It is therefore possible to learn more about the film formation caused by the additives used.

Predicting how additives react with metals at varying temperatures without having to do full-scale bearing fatigue tests could have great financial attraction to the bearing industry. The hot-wire technique could be used as an early warning indicator for new additive combinations appearing on the market. If the new additive appeared to be more reactive than known highly reactive additives caution should be shown. The technique can also identify temperatures at which decomposition takes place.

2.5.2 The hot-wire test technique

Barcroft's work involved measuring changes in resistance of an electrically heated thin wire immersed in a bath containing extreme-pressure additive. The wire was heated electrically by passing a current through it, after some time a film was formed caused by the reaction of the oil with the wire. The temperature of reaction was

estimated using the temperature/resistance characteristics of the material. The circuit used by Barcroft is shown in Figure 2.2.

The circuit consists of a measuring circuit (m) and a heating circuit (h) connected to an oil bath containing the additive of interest. P1, P2 and P3 are potentiometers used to measure the voltage changes in the circuit. The reaction wire (typically 30 mm in length) is clamped across terminals and heated by passing a DC current through it. The two circuits are connect using a double-pole two-way switch. This allows the heating circuit to be switched rapidly to measure the increase in resistance as the additive reacts to decrease the original wire diameter. The oil temperature was found to increase during the experiment. The resistance of the wire was therefore always corrected to 20 °C. For convenience the change of resistance was converted to a change of diameter of the wire expressed in Angstroms (10^{-10} m). The rate of reaction was expressed in Angstroms metal reacted/minute.

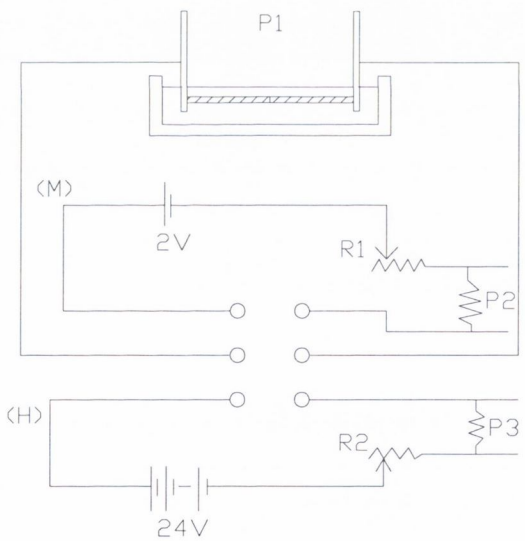

Figure 2.2: Barcroft's circuit for hot-wire testing

The test metals were chosen which showed regular changes of resistance with temperature. Wires were vacuum annealed for two hours at 600 °C to ensure that the metal electrical properties did not vary during reaction. When corrosion takes place, changes in wire resistance can more easily be measured if the initial resistance is high. Wires with diameter of less than 65μm or less are preferable, but the number of

metals that can be drawn to such diameters is limited. Barcroft identified several metals that could be used, stainless steel, mild steel, pure iron and pure silver.

The ability of the method to distinguish between the reactivity of EP additives depends on the sensitivity of the measuring device. The potentiometers used were capable of measuring changes of 1 in 10,000, which corresponded to a change in radius of about 1 nm. Allowing for errors, changes of 10 nm were readily detected. The temperature of the wire is found from the temperature/resistance characteristics of the metal. This temperature can change during the test as the bulk oil temperature rises. Barcroft quotes the average temperatures during the reaction period, this was said to be satisfactory provided the average temperatures do not differ by more than about 30 °C.

2.5.3 Analysis of hot-wire results

To help quantify surface reactions by relating the changes in the wire's resistance two assumptions were made.

a) The reaction film that built up on the surface was non-conducting, i.e. the wire thickness at any time was the original wire thickness minus the thickness of corrosion.
b) The surface reaction was uniform over the length of the wire, i.e. the film was of uniform thickness on the wire surface.

Using these assumptions an equation relating the change in wire radius to resistance changes was derived.

Barcroft's Equation:

$$\Delta r = \left(\frac{\Delta R}{\Delta R + R_0}\right)\left(\frac{r_0}{2}\right) \qquad (2.1)$$

Where:

r_0	=	original radius of wire
Δr	=	thickness of corroded metal
R_0	=	initial resistance of wire
ΔR	=	change of resistance due to corrosion

Barcroft's initial experiments used an EP additive where sulphur was the only reactive element. The rate of reaction between sulphur and the metal was expressed as:

$$\text{The rate of formation of FeS} = k.(Fe)(add) \qquad (2.2)$$

where: FeS = iron sulphide
k = constant
(Fe) = number of iron atoms on the wire surface.
(add) = concentration of additive

The surface area of reaction was small so the concentration of additive used in the reaction was assumed constant through the reaction. If the layer thickness is small, Barcroft assumed that the diffusion of metal through the film unhindered by the formation products therefore the equation can be rewritten.

$$\text{The rate of formation of FeS} = k.(\text{constant}) \qquad (2.3)$$

The Arrhenius equation was then used to describe the rate of reaction between the EP additive and the metal.

Arrhenius Equation: $$\log k = \frac{-E}{R_G T} + const. \qquad (2.4)$$

where: E = activation energy
R_G = the gas constant
T= absolute temperature

Thus:

$$\log_{10}[rate\_of\_formation\_of\_FeS] = \frac{-E}{R_G T} + const. \qquad (2.5)$$

The plot of $\log_{10}$[reaction rate] V 1/T was found to be a straight line except when phosphorus was used as the only additive.

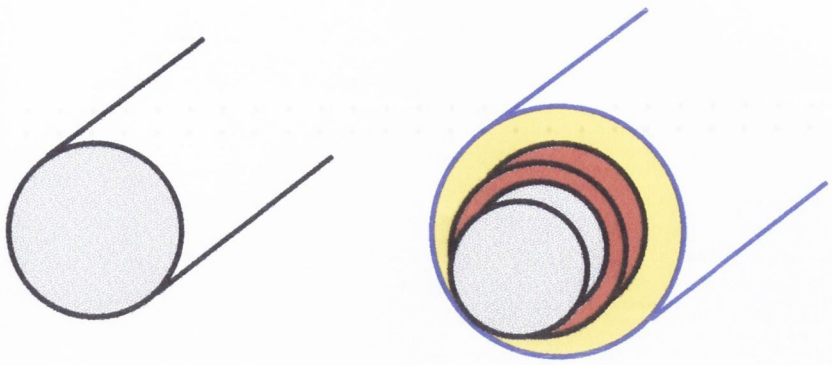

(A) (B)

Original wire: metal core (grey)

Reacted wire: reduced metal core (grey)
corroded metal depth (red)
reaction products (yellow)

Figure 2.3: Schematic diagram of iron wire, corrosion layer and reaction products film

2.5.4 Reactions of additives on metals

Additives containing sulphur, chlorine and sulphur/chlorine combinations were tested using the hot-wire method. The tests were carried out on a series of metals including steel, pure iron, bronze, gold, copper and platinum. Phosphorus was the only additive that was not found to obey the Arrhenius equation. In 1982 Barcroft [133] again used the hot wire technique to investigate the reaction mechanism of zinc dithiophosphate. The paper [134] found that additives of type ZDDP owed their effectiveness to a dual mechanism.

At temperatures between 200°C and 600°C the thiophosphate forms a deposit on the surface. The deposit also forms on non-reactive metals such as platinum and gold. At 600°C the thiophosphate reacts with ferrous metal surfaces to form mainly iron sulphate and some iron phosphate. It is argued that the effectiveness of the additive should be related to the additive's thermal stability, the more unstable the additive the greater the film formation and hence EP effectiveness. In practice it was found that the films produced using these additives contained zinc, phosphorus and sulphur. One theory postulates that the metal surface reacts to produce a Fe-P-S-Zn complex compound. Later it was found that the compound was the solid decomposition from

the thiophosphate. Wear rates in dynamic tests using the same additives were found to be inversely proportional to thermal stability of the additive.

In theory the conductivity of the metallic sulphates and chlorides are of many magnitudes lower than that of the metal. Wires were examined using SEM, a scalpel was used to break the brittle film away without damaging the wire underneath. EDAX was then used to examine the chemicals present in the films. X and R radiations were used to detect the elements of sulphur and phosphorus. The electron energy beam was 10 kV, however when the iron content was of interest a higher beam of 20 kV was used.

Interactions between ZDDP and metal surfaces are strongly influenced by the other additives present in the oil. Succinimide dispersants lower the extent of film formation of the thiophosphate but do not appear to change the film composition, whereas anti-rust agents alter the film composition but not the reaction rate. The extent of the reactions between these additives and the thiophosphate is temperature and concentration dependant. Half a dozen additives can be used in motor oil packages, this can lead to competition for reaction with the metal surface and cross interactions of additives are possible.

2.5.5 Sakurai's Investigations

Japanese Tribologists were quick to use the hot-wire technique, and to investigate the reaction mechanisms between additives and metals. The objective of Sakurai's work was to extend the knowledge of the mechanism of reaction between metals and hydrocarbons containing EP additives. In 1964 Sakurai et al. [6], from the Tokyo Institute of Technology, looked at the reaction between metal and hydrocarbon oils containing sulphur compounds. The reaction was controlled by the diffusion of reactants through the product film and parabolic corrosion rates were observed. This was a development of Barcroft's thin film assumptions. Sakurai also observed that the corrosion caused by white oil alone was nearly as high as by the solutions containing sulphur compounds. He found that corrosion generally increased with temperature, and that there was a relationship between the thickness of the iron corroded and reaction time.

The corrosion rate equation was:

$$(\Delta r)^2 = kt \qquad (2.6)$$

where: Δr = thickness of corroded iron

k = rate constant

t = reaction time

Sakurai concluded the following about reaction kinetics of corrosion "that the reaction was conceivably a kind of tarnishing reaction whose reaction rate was passivated by reaction products".

Summary of Sakurai's theory of Reaction Kinetics:

a) Diffusion of dissolved oxygen or sulphur compounds on the surface of the metal wire through the solution.
b) Adsorption of dissolved oxygen or sulphur compounds on the surface of the metal wire.
c) Surface reaction of metal wire - including oxidisation, sulphurization, and the conversion of iron oxide to iron sulphide.
d) Diffusion of iron-ion through formed film, the migration of iron through the iron oxide occurs by the diffusion of the Fe^{++} ions through cationic vacancies .
e) Surface reaction on the interface between the iron phase and the formed film.

2.5.6 Analysis of reaction products

Reaction products were investigated using x-ray analysis. Fe_3O_4 was identified on iron wires reacted in white oil, FeS was identified on wires which were reacted with elementary sulphur solutions. Stainless steel was also used as the wire material and reaction/corrosion rates were found to be lower than for iron.

A linear relationship between the cube of the thickness of the corrosion and the reaction time was observed. This corrosion equation is defined as the following.

$$(\Delta r)^3 = kt + k_0 \qquad (2.7)$$

In 1972 Sakurai et al. [135] carried out tests on the corrosion rate of iron wire subjected to tensile stresses using a variation of the Barcroft method. A weight was used to apply a stress-induced heterogeneity in the metal. When the wire was

subjected to a tensile stress the reaction rate between the metal and additive was shown to increase. Again the reaction mechanism was found to be very complicated and different for different additive types.

Further studies have been made of corrosivity and the correlation between chemical reactivity and the load-carrying capacity of EP oils on iron surfaces. EP agents are thought to react with the surface causing a solid film to build up and act as a boundary lubricant. Hot-wire tests were conducted using several EP additive concentrations. Fe_3O_4 again was found, Godfrey [107] has shown the formation of this product on steel surfaces lubricated with sulphur compounds. Oxidation and sulphurization may take place simultaneously as both elements are present in the solution. If a crack forms in the reaction products layer localized reactions on the metal can occur. This will cause a high increase in resistance which is not representative of the whole wire.

For hot-wire reactions with phosphorus additives the mechanism of reaction has been attributed to a polishing action via a iron-iron phosphide eutectic. Godfrey [107] found that films consisted of $FePO_4$ and $FePO_4.2H_2O$. Barcroft showed that thin films of 50 (nm) were sufficient to inhibit further reactions and identified Fe_2P as a product. The rate of the reaction, is determined by the chemical reaction with the iron surface and the diffusion of iron through the films formed.

Barcroft's corrosion equation is:

$$\frac{d(\Delta r)}{dt} = k(Fe)\cdot(additives) \tag{2.8}$$

Applying the Arrhenius equation:

$$\log\left(\frac{\Delta r}{t}\right) = -\frac{E}{RT} + const. \tag{2.9}$$

The effects of EP additives in various environments were investigated. Analysis of the reaction products showed that variations occurred due the atmosphere and the chemical structures of the sulphur compounds. Two different types of failure have been identified at different temperatures [130]. Oxide films were seen to reduce the

sulphurisation of the iron surface. It is known that there is an optimal film thickness to give smooth lubrication.

Recent tests by Han and Li, [8] have investigated chemical reactivity of binary additive systems using a four ball machine and hot-wire technique. The results showed that the anti-wear properties of the additives were strongly influences by a petroleum calcium sulphonate and hexadecamine salt of benzotriazole. The extreme pressure properties however were not effected. As lubricants contain more than one additive it seems sensible to try to quantify the interactions between different species. Results from the 4-ball tests showed that with additive combinations higher weld loads could be achieved, and the wear-scar diameter reduced. Hot-wire results at low reaction temperatures were not as ordered as Barcroft's higher temperature results. Retardation or passivation of the reactions was found. Run away plots are also seen where localised attack can accelerate reactions at grain boundaries ultimately causing the wire to break.

CHAPTER 3

3 ROLLING CONTACT FATIGUE TESTING

3.1 INTRODUCTION

The RCF test machines at the University of Bristol were designed originally to investigate the influence of grinding conditions on the fatigue lives of bearing materials. In this new research they were modified to investigate the effects of EP oil additives on the lives of the inner raceways of bearings at elevated temperatures. The first section of this chapter describes the Bristol test machines. Particular attention is given to the loading head where the balls are hydrostatically loaded against a rotating raceway.

A heater-controller system has been designed and added to the rig to elevate the lubricant temperature and promote additive activity. The second part of the chapter examines the test conditions. The test parameters, such as surface roughness, Hertzian stress and oil film thickness are discussed. Details of the 6305 ground inner raceway test specimen are listed. The properties of the lubricating oils are discussed and the test procedure is outlined. The oil film thickness and Hertzian stresses calculations for the Bristol rig are given in Appendix (A). Although complete standard bearings are not used in the Bristol rig, a life prediction calculation has been made.

The final section concentrates on the test conditions of the SKF R2F rigs. These test were carried out independently by the project sponsors. The results are used for comparison with the Bristol rig tests. The stress conditions in these tests are higher than in the Bristol tests, giving useful information on how additives behave under different conditions. Life prediction calculations are also given for the bearings under these conditions.

3.2 ROLLING CONTACT TEST MACHINE

The Rolling Contact Fatigue (RCF) machine, at the University of Bristol, was designed in the late nineteen seventies by Roger Stokes [129] to test the life of bearing steels machined under various grinding conditions. The machine shown in Figure 3.1, won a bronze medal award in the Institution of Mechanical Engineers Design Awards in 1979. Four rigs were built in total, their main features are listed below.

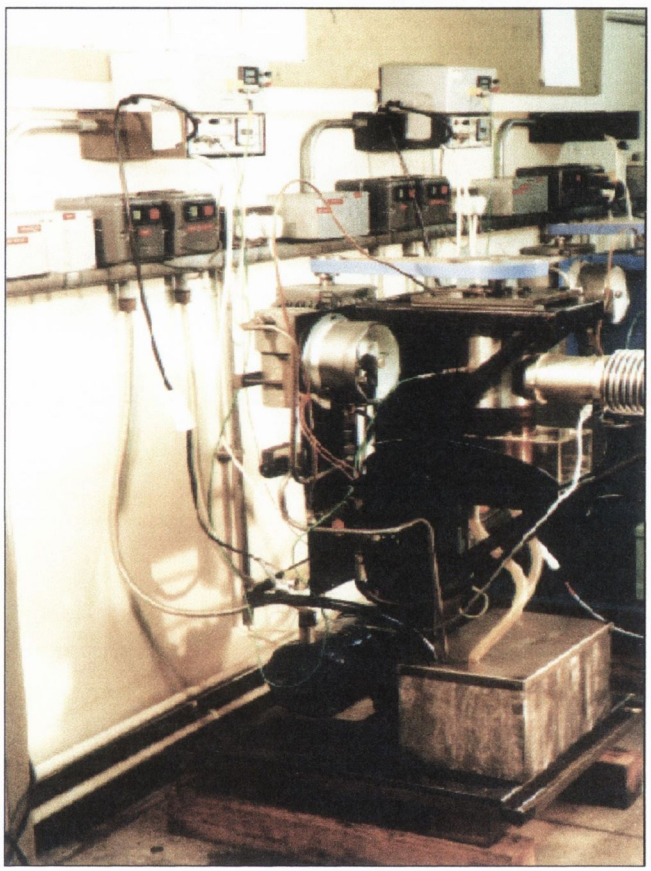

Figure 3.1 Photo of the Bristol rolling contact fatigue test rig.

The principal components of the test rig:

a) A high pressure two piston reciprocating constant delivery pump delivers oil at 2 litres per min, at pressures up to 25 (MPa).

b) The pump is protected from damage by a low pressure 25μm filter, this prevents any large debris particles entering from the sump.

c) An accumulator with a bladder pressure of 70% of the operating pressure was used to dampen out pressure fluctuations in the system.

d) A pressure relief valve is used to control pressure of the system.

e) A pressure reducing spool valve was used to control accurately the pressure applied to the loading head.

f) A high pressure filter was used to remove particles larger than 2-3 μm in diameter from the oil.

g) A pressure gauge measures pressure applied to the loading head. To ensure that pressure is constant during the test, upper and lower pressure limits can be set. Abnormal pressure changes cause electrical terminals to short, and the test is switched off.

h) The sump of 15 litres capacity allowed the oil to settle between circulation cycles. A sump accessory was added to the outlet hose to prevent bubbles circulating in the system.

i) Splash guards and a metal funnel are used to return the oil from the loading chamber to the sump.

3.2.1 Description of the gallery-chamber area

The specimen testing area is shown in Figure 3.2. Six balls were equally spaced around the specimen. The balls were held by replaceable loading sleeves made from nitrided En40B steel. The nitriding process produced surfaces with good wear properties. The sleeves were accurately honed to 11.122-11.124 (mm) giving a diametrical clearance of 10-12 μm. If the clearance was too large then too much oil could pass through the gap making it difficult to generate high pressures, conversely if the gap was too small the balls risked getting stuck. In the latter case sliding would result at the contact. The inner ring specimens were fixed to the spindle by using bearing fit Loctite.

The honed cylinders are sealed in the loading sleeve with Dowty O-rings to prevent leakage and hence pressure drops. The alignment of the balls and test specimen was achieved by using spacer rings underneath the loading sleeve. The accuracy of the alignment was monitored by examining the position of the wear track on the specimen

after a period of running. Spacer height adjustments were made to compensate for any wear track misalignments.

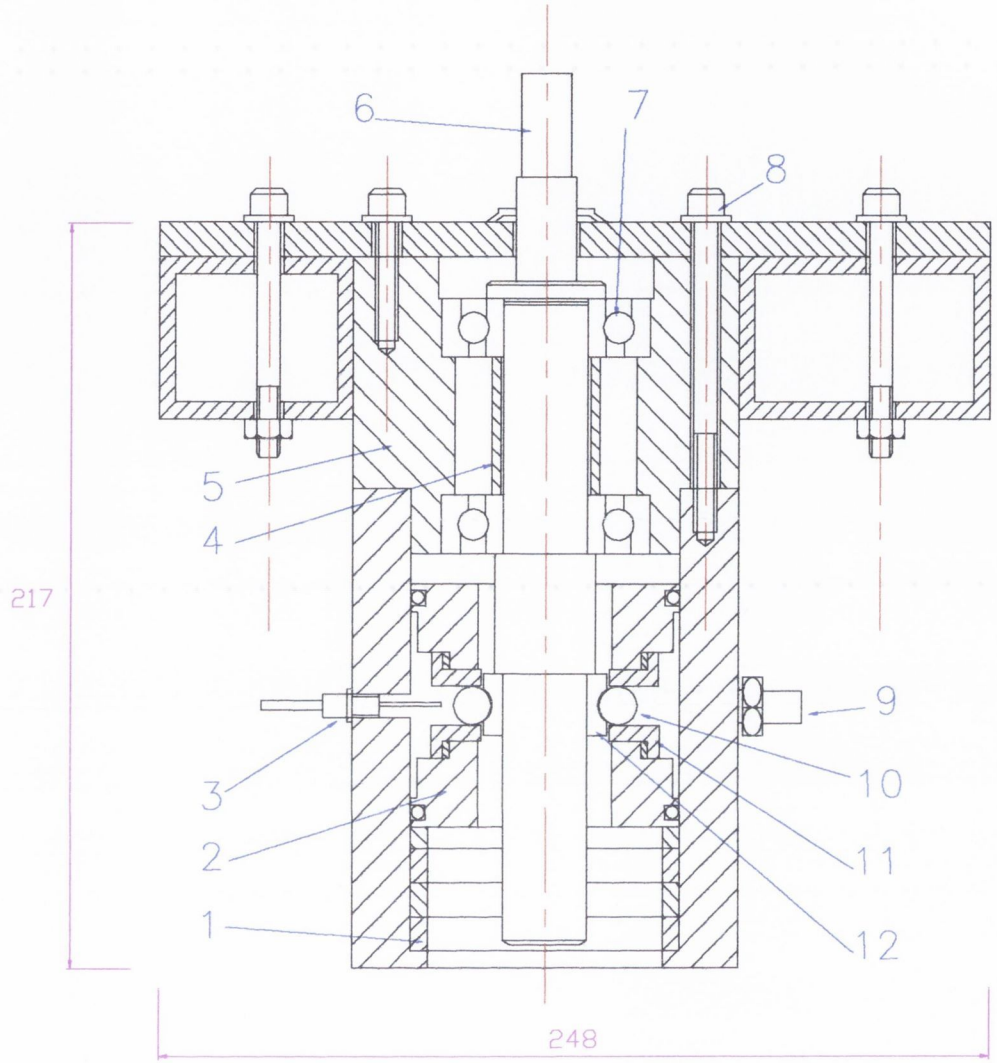

1. Spacers	2. Loading sleeve	3. Thermocouple	4. Spacer
5. Housing	6. Spindle	7. Support Bearings	8. Bolts
9. Accelerometer	10. Ball	11. Honed cylinder	12. Inner Raceway

Figure 3.2 The Gallery-Chamber Area

The rigs initially used cylindrical specimens where 20 tests could be carried out at different locations along its length. The cylinders were replaced by 6305 inner raceways for this study. This made the area of contact larger, therefore the maximum Hertzian stress was reduced from 4.7 to 2.2 (GPa). To compensate for this decrease in pressure the surface roughness of the specimen was changed. The lambda ratio was

decreased to make the specimens fail quicker and to promote surface interactions between the metal and lubricant.

New larger pulleys were fitted to the spindles to reduce the thickness of the oil film between the mating bodies. The spindle speed was governed by the pulley ratio used, the speed was reduced to 1000 rpm for these tests. The flat belt connected to the 3-phase induction motor provided a stress rate of 360,000 cycles per hour. An hour-meter connected to the spindle circuit recorded the total number of stress cycles for each test, from this measurements of fatigue life were taken.

3.2.2 Hydraulic loading of balls on specimen

As seen above the machine uses a unique lubrication method to apply the contact stress and to provide lubrication. As the pressure builds in the system the oil is forced through the annulus created between the ball and the loading sleeve. Careful honing and polishing is essential to keep this part of the rig in working condition. In cases where the ball was the first element to fail it was sometimes possible to recover the spalled material if it jammed in the annulus. The abnormal vibrations caused by such an event were detected using an accelerometer causing the rig to switch off.

This type of loading has advantages over more conventional methods of testing:

a) Under conditions of low flow the pressure behind each ball was constant, the ball in sleeve system allowed free rolling contact during testing.
b) The inertia of the loading mechanism would be very small and therefore large loads would not be created by small specimen imperfections.
c) The filtration system allowed a clean supply of lubricant to the contacts.

3.3 TEMPERATURE HEATER-CONTROLLER DESIGN

3.3.1 Heating element

To promote chemical reactivity in the lubricant and to simulate bearing conditions in practice, a heating device was added to the test rig. A temperature controller was designed to maintain the oil temperature at 70 °C. Each oil sump contained 15 litres of

oil and therefore it was important not to start any unwanted fires in the laboratory. To increasing the temperature of the oil three alternatives were investigated:

a) Heating the oil from the tank (sump) at the base of the rig.
b) Heating the oil in the galley by a heater element inside the rotating shaft.
c) Heating the oil by an induction coil element as it passed into the gallery.

The first method was seen initially to be the simplest one, but was rejected because it was felt that the oil temperature in the gallery would be too difficult to control from the sump. If the sump had been used as the heating source a stirrer would probably have been necessary to achieve an even temperature distribution. This may have added to the problem of oil foaming. The second idea was ruled out also as supplying an AC current near a rotating shaft presented problems. It would also have been difficult to find a heater with enough power to fit inside the shaft. The inner race would have been hotter than the oil so estimating the oil temperature at the contact would have be complicated.

The induction coil was felt to be the best method of heating the oil. An initial design of the heating cylinder was created, and a 2-D finite element model was created to help estimate the heating element power needed to keep the oil at 70 °C. It was decided that an 800 Watt square coiled cylindrical heater was the best option for this application. A suitable heating element was manufactured by, Elimatic Ltd. Cardiff. A cross section of the heater cylinder is shown in Figure 3.3.

To increase heat transfer to the oil as it passed through the heating cylinder, a series of 11 copper tubes (6mm diameter/ 80 mm length) were fixed inside the tube parallel to the flow of oil. This was found to reduce the power needed to heat the oil and prevented black decomposition (slack) being formed at the oil/cylinder interface. As a safety precaution the inner cylinders were pressure tested to 600 Bar for 15 minutes by Saunders and Weeks, Bristol. Temperature resistant Viton O-rings were added to the end-caps of the cylinders to prevent oil leaks. Aluminium cooling fins were mounted between the heater and the connecting hydraulic hose to preserve the hoses from thermal damage.

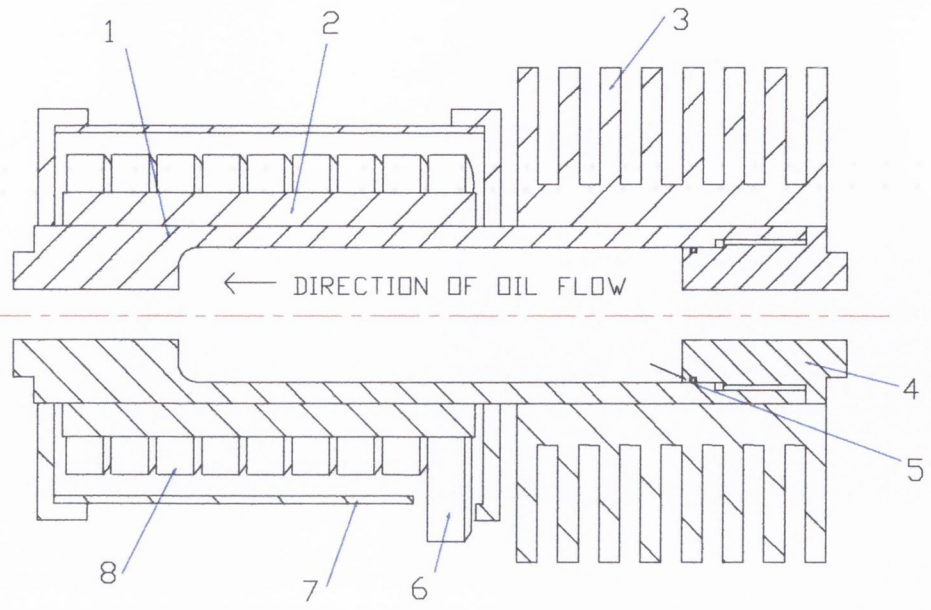

1. Inner Cylinder 2. Copper Spacer 3. Aluminium Fins 4. End Cap
5. Viton O-Ring 6. Power Cable 7. Heater Guard 8. Heating Element

Figure 3.3 The oil heater design (tube inserts not shown)

3.3.2 Temperature controller

A controller system was designed to monitor and maintain the temperature of the lubricant at 70 °C. A four digit, dual display controller C100FKO-7-AN supplied by TC. LTD. UK., was chosen for this application. The proportional integral derivative (PID) controller allowed a thermocouple to dictate the amount of power being supplied to the heater. The alarm safety setting ensured that the power to the heater was switched off if the oil temperature rose above a set upper limit, in this case 6 °C above the set temperature of 70 °C.

The input was supplied by a K-type thermocouple which measured the oil temperature just before it reached the raceway. The output was directed to a solid state relay which controlled the amount of power supplied to the heating element. Figure 3.4 shows the temperature controller and vibration box. Below Figure 3.5 shows a photo of the heater cylinder during testing.

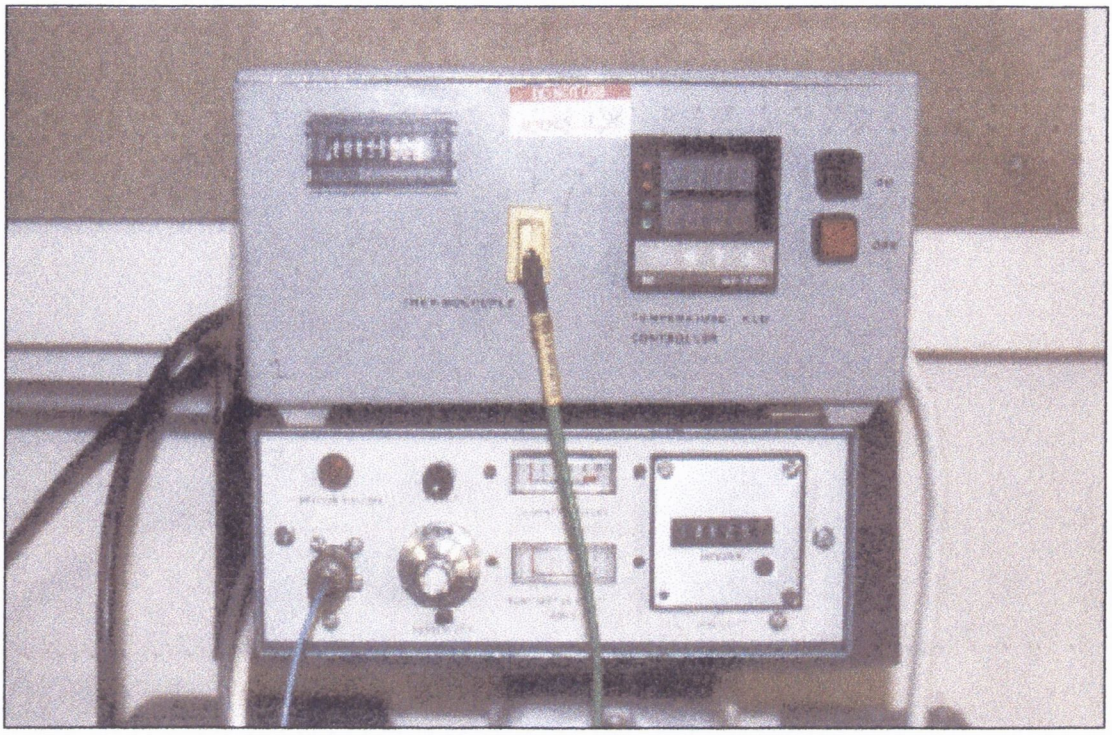

Figure 3.4 Photo of the temperature controller (above) and vibration box (below).

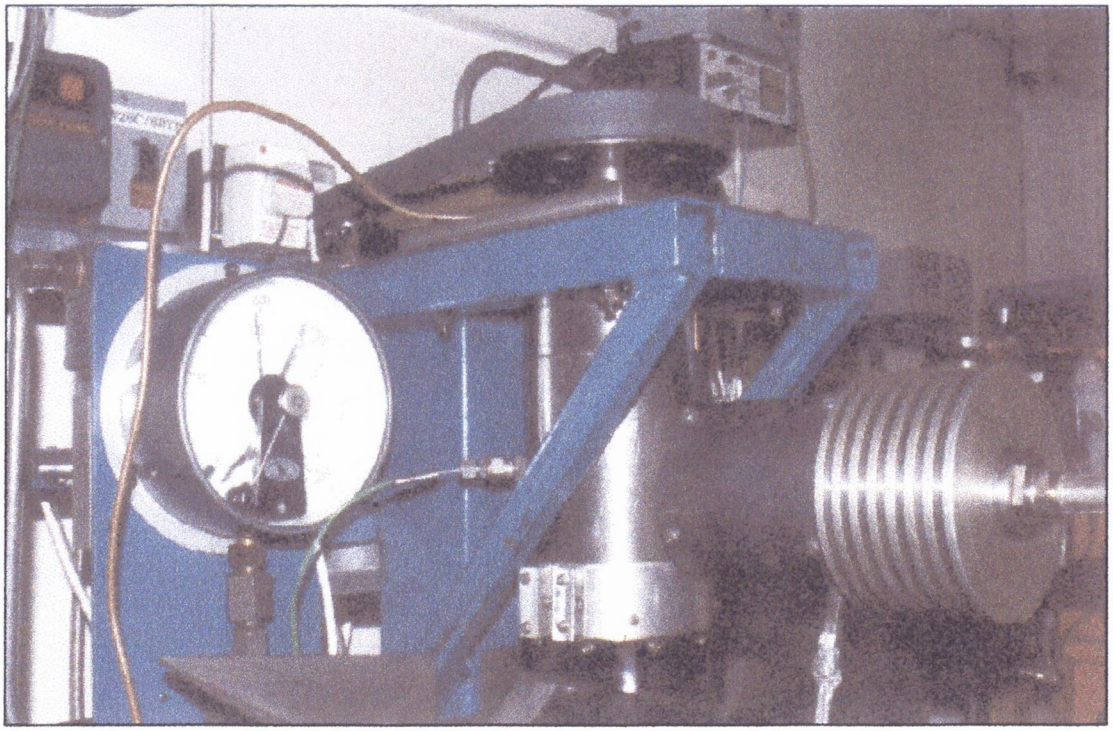

Figure 3.5 Photo of the oil heater, thermocouple, pressure gauge and pulley

3.4 TESTING CONDITIONS

3.4.1 The test specimen

A batch of unpolished 6305 deep groove raceways were supplied from a SKF factory in Italy. The ground finish raceways were chosen to accelerate the time to failure. The raceways were made from 52100 bearing steel. They had a composition of 1% carbon and 1.5% chromium, with the heat treatment described by Hengerer [25]. The specimen can be seen in Figure 3.6, with dimensions of 25mm inner diameter, 17mm height. The average roughness was measured to be 0.5 μm cla. giving a Lambda ratio of 0.4. Twelve specimens were tested for each oil tested. The results were then analysed using Weibull techniques. The balls used in the tests were 11.112 mm diameter balls of the same material. The information about the geometry and test conditions was used to calculate the contact stresses and film thickness, shown in Appendix (A). A summary of the main test conditions is given in Table 3.1 below.

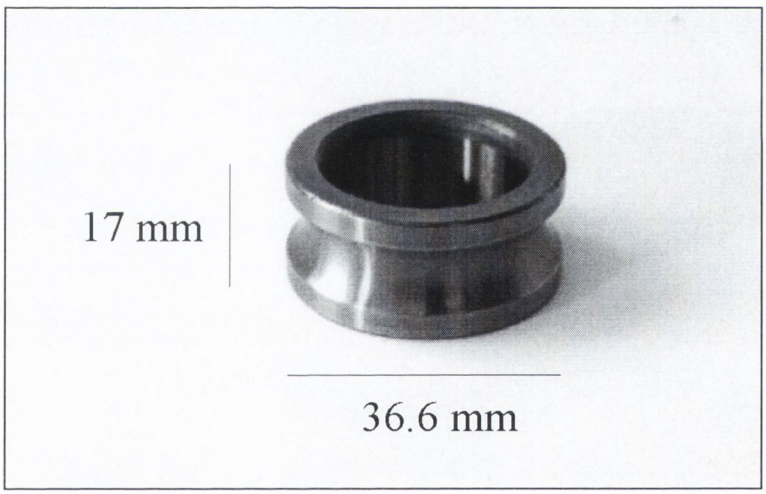

Figure 3.6 Photo of the ground inner raceway specimen

3.4.2 Test program at University of Bristol

The base oil used in the test was Shell Vitrea M100, a premium quality mineral lubricating oil refined to perform satisfactorily in applications where additive treated oils are not required. The oil has good oxidation stability, good demulsibility to quickly shed water and a high viscosity index that minimises changes in viscosity with temperature. This oil is the modern equivalent of the HVI 160 oil used by Stokes

[129]. The first twelve tests were carried out using this lubricant and the results were used as a base line against which other test results were compared.

The additive package was provided by Dr. K. Hole, Product Manager at Lubrizol International Laboratories, Derby, UK. The Lubrizol 5034A is a sulphur-phosphorus type industrial gear lubricant additive. It is recommended for use at 1.75% (wt) in suitable base oils to meet or exceed DIN 51517 Part 3 specifications. Twelve tests were carried out using both concentrations of 2% (wt) and 5% (wt) L5034A in Vitrea M100. For all tests with Vitrea, small quantities of anti-foam agent (L889D) 0.1% (wt) and anti-oxidant (L5172) 0.01% (wt) were added, provided again by Lubrizol.

The final set of tests were carried out using Shell Spirax AX 80W-90. Spirax contains a sulphur-phosphorus additive system, marketed by Shell to provide "an excellent load carrying capacity". It offers protection against rust, corrosion and foaming. This pre-formulated oil contains weight percentages of 1.8 % phosphorus, 0.1 % sulphur and 0.1 % nitrogen.

Lubricant	Weight of additive per litre base oil (g)	Temperature (Celsius)	Number of tests
Vitrea M100	natural traces	70°	12
Vitrea + 2% (S/P)	17.2	70°	12
Vitrea + 5% (S/P)	43.0	70°	12
Spirax AX 80W-90	pre-formulated	70°	12

Table 3.1 Summary of tests and lubricants used in Bristol rig

Lubrizol 5034A			
Density, kg/l @ 15.6 °C	1.00	Phosphorus (%wt)	1.9
Viscosity, cSt @ 40 °C	65.0	Sulphur (%wt)	19.1
Viscosity, cSt @ 100 °C	9.0	Nitrogen (%wt)	1.15

Table 3.2 Properties of Lubrizol L5034A (S/P) package

Summary of Test Conditions:	
Test specimen:	6305 ground deep grooved inner race.
Contact Pressure:	Max. Hertzian Stress: 2.2 (GPa) (100 bar on gauge).
Test lubricants:	Shell Vitrea M100
	Shell Vitrea M100 + 2% (S/P)
	Shell Vitrea M100 + 5% (S/P)
	Shell Spirax AX 80W-90
Surface roughnesses:	0.5 and 0.03 μm cla. (race and ball respectively)
Minimum film thickness:	0.17 μm
Speed:	1000 rpm.
Temperature of oil:	70 °C.
Test period:	672 hours (4 weeks) or until failure whichever is first

Table 3.3 Summary of test conditions for Bristol rig

3.5 EXPERIMENTAL DETAILS

3.5.1 Test procedure

To ensure that all fatigue tests were as similar as possible, the following test sequence was adopted.

a) The test balls and raceways were cleaned with acetone in an ultrasonic bath.
b) The raceway was fixed to spindle with loctite and allowed to cure overnight. To prevent the specimen from rusting the specimen surface was coated with a little oil.
c) The balls are loaded in the sleeves and checked to see if they could move freely.
d) The gallery was bolted to the frame and the thermocouple and accelerometer were then attached.
e) The pump was turned on and the oil allowed to flow around system, the yellow pressure valve was closed slowly until the pressure reaches 15 Bar.
f) The oil flow through each sleeve was checked and the splash guards mounted.
g) The spindle was switched on and the pressure was increased slowly until it reached 100 Bar.
h) The heater was turned on and the pressure adjusted to compensate for drops due to increases in temperature.

i) After the temperature stabilised after 30 minutes the accelerometer sensitivity was adjusted to 97%.

3.5.2 Film thickness calculations

To quantify the severity of the ball and race contact the Lambda ratio was calculated. This ratio relates the surface roughness of the mating bodies and the thickness of the film that separates them. The thickness of the film in the contact zone was calculated using the Hamrock and Dowson equation. The equation links the parameters speed, viscosity and pressure. The minimum film thickness equation is briefly shown below, in equation (3.1), see Appendix A, page 159.

$$H_0 = \left[3.63(U)^{0.68}(\alpha E')^{0.49}(W)^{-0.073}\left(1-e^{-0.68K}\right)\right] \qquad (3.1)$$

Minimum film thickness was calculated as 0.17 microns

Using the film thickness and the surface roughness values of the ball and raceway surfaces, the lambda ratio was calculated giving a measure of the metal-to-metal contact in the test rig.

$$\Lambda = \frac{h_o}{\sqrt{\left(R_{q1}{}^2 + R_{q2}{}^2\right)}} \qquad (3.2)$$

$$= \frac{0.17}{\sqrt{\left(0.5^2 + 0.03^2\right)}}$$

$$= 0.4$$

3.5.3 Hertzian stress calculations

Contact stresses are caused by the pressure of one solid on another over a small area of contact. In bearings, stresses are usually cyclical and are often repeated a large number of times. The geometries of the mating bodies, along with elastic deformation properties were needed to calculate an area of contact between the race and the ball. A summary of the main points in the calculation is given below.

Principle radii of mating	R_{11}	=	5.556 mm
surfaces:	R_{12}	=	5.556 mm
	R_{21}	=	-5.87 mm
	R_{22}	=	15.75 mm
Semi-major axis:	a	=	1.211 mm
Semi-minor axis:	b	=	0.157 mm
Load:	F	=	982.40 N
Maximum Hertzian stress:	σ_{max}	=	2.175 (GPa) compressive

More details in Appendix A, pages 156-158

Table 3.4 Summary of Hertzian stress calculations for Bristol rig

3.5.4 Life prediction for 6305 bearing

Because the Bristol rig uses slightly smaller balls than in the standard 6305 bearing the life is calculated using a stress based approach.

For a 6305 bearing, a load of 22.5 kN (C/P=1) gives a maximum Hertzian stress of 3554 MPa.

From Appendix (A):
At 100 (bar), the Bristol rig applies a load of 982.4 (N), which gives a maximum Hertzian stress of 2175 MPa.

To get a stress of 3554 MPa on the Bristol rig, it would be necessary to apply a load of 982.4 x $(3554/2175)^3$, so the C/P value is simply:

$$C/P = (3554/2175)^3$$
$$= 4.36$$

$$\text{Lambda} = 0.4$$

$$\Lambda = K^{0.69}$$

If Kappa, $K = 0.26$

The from the SKF catalogue:

$$a_{SKF} = 0.15$$

The expected L_{10} life would be:

$$L_{10} = \frac{0.15 \times (4.36)^3 \times 10^6}{1000 \times 60 \times 6}$$

$$= 35 \text{ hours}$$

3.6 EXPERIMENTAL DETAILS OF TESTS AT SKF ERC

A set of tests was undertaken using the R2F rigs in SKF ERC. The following section lists a brief description of the rig and a summary of the test program. The R2F rig is shown in Figure 3.7. A radial load of 12 kN was applied hydraulically on the 6206 ETN9 test bearings. The basic dynamic load rating was 19.5 kN, therefore the C/P ratio is 1.625. The shaft is supported by two large bearings and rotated by a flat belt at a speed of 2,500 rpm. The oil temperature was 80 °C and was filtered though a 3 μm filter. The oils used in the test program were Spirax AX 80W-90, TT 68, Volvo 97305 and Volvo 97307.

Lubricant	Weight of additive per litre base oil (g)	Temperature (Celsius)	Number of tests
Spirax AX 80W-90	pre-formulated	80°	13
TT 68	natural traces	80°	7
Volvo 97305	unknown	80°	8
Volvo 97307	unknown	80°	7

Table 3.5 Summary of tests conditions for R2F rig

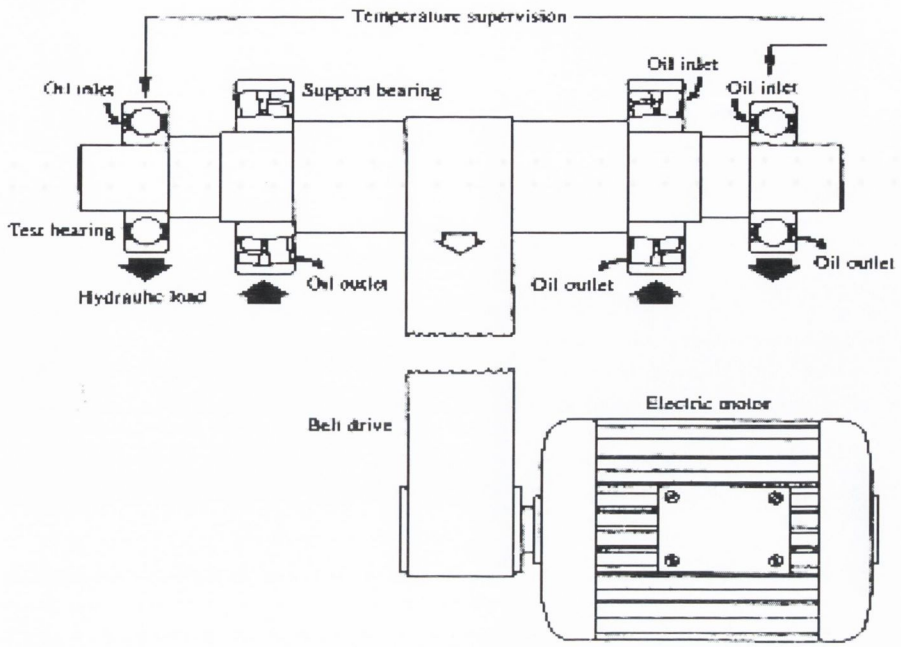

Figure 3.7 Diagram of R2F rig used for SKF tests

Principle radii of mating	R_{11}	=	5.556 mm
surfaces:	R_{12}	=	5.556 mm
	R_{21}	=	-5.73 mm
	R_{22}	=	17.5 mm
Semi-major axis:	a	=	3.427 mm
Semi-minor axis:	b	=	0.315 mm
Load:	F	=	9750 N
Maximum Hertzian stress:	σ_{max}	=	4.2 (GPa) compressive

note: radii quoted are approximate measurements made at TCD

Table 3.6 Summary of Hertzian stress calculations for R2F rig

3.6.1 Life prediction for 6206 bearings

Operating conditions:

TT68 oil viscosity @ 80 °C	=	14.5 mm^2/s
Shaft speed	=	2,500 rpm
Load	=	12 kN

From catalogue:

C = 19,000 N

P_u = 475 N

A) Basic life rating L_{10}

$$L_{10} = \left(\frac{C}{P}\right)^p$$

$$L_{10} = \left(\frac{19{,}500}{12{,}000}\right)^3$$

$$L_{10} = (1.625)^3$$

$$L_{10} = 4.29 \times 10^6 \text{ revs}$$

B) Adjusted life rating Lna

$$L_{na} = a_1 a_{23} L_{10}$$

$v_1 = 13.0$ mm^2/s viscosity needed for adequate lubrication

v = 14.5 mm^2/s operating viscosity

Kappa ratio, K=1.15

Combined life adjustment factor,

$$a_{23} = 1.1 \times 10^6$$

assuming clean operating conditions,

$$a_1 = 1$$

$$L_{10a} = 1 \times 1.1 \times 4.29 \times 10^6$$

$$L_{10a} = 4.72 \times 10^6$$

C) New Life

$$L_{naa} = a_1 a_{SKF} L_{10}$$

$$\frac{P_u}{P} = \left(\frac{475}{12000}\right) = 0.04$$

$$a_{SKF} = 1$$

$$L_{10aa} = 4.29 \times 10^6$$

Life in hours:

$$= (4.29)\left(\frac{1{,}000{,}000}{60(2{,}500)}\right)$$

$$= 28.6 \text{ hrs}$$

3.7 SUMMARY

The Bristol rolling contact fatigue machines were modified to test the ground 6305 inner races. Tests were carried out for a maximum of four weeks after which the test was suspended. The contact stresses were reduced using the raceway compared to the cylinders. To accelerate testing time ground specimens were used instead of polished specimens. The spindle speed was reduced to lower the oil film thickness.

To promote chemical reactivity a heating element added to the rig that raised and controlled the temperature of the lubricant. The power input to the heating element was controlled by a PID controller. A K-type thermocouple was fastened to the gallery chamber area to monitor the oil temperature as it passed into the contact zone.

Tests were carried out with four lubricant oils, one neat oil and three which contained S/P additives. The neat oil was Shell Vitrea M100, solutions containing 2% and 5% S/P additive were made by adding quantities of Lubrizol 5034A package. The other oil was Spirax AX 80W-90 this oil was seen to be reactive in the SKF reaction tests. The time to failure of each tests was recorded using an hour-meter. Failure was detected by an accelerometer which stopped the rig at a given level of vibration caused by pitting.

CHAPTER 4

4 THE HOT-WIRE RIG

4.1 INTRODUCTION

A hot-wire test was developed to assess the reactivity of oil additives on metal surfaces. The rig was similar to the one used by Barcroft [4] and Sakurai [5], where lubricant reactivity on metal surfaces was successfully measured at high temperatures. When oil/metal corrosion takes place the thickness of reaction films can be very small, making direct measurement difficult. The hot-wire method uses accurate resistance measurements to calculate changes in diameter of a metal wire caused by corrosion.

Metal wires were provided by Goodfellow Ltd. and Advent Scientific, UK. Iron and stainless steel wires were selected as they were available in an annealed state. The significance of this will be dealt with later. To test the reactivity of commercial oils and oil/additives mixtures a hot-wire test rig was constructed. The design of the hot-wire rig is described in detail below, the rig consists of four parts, the reaction bath, a heating circuit to initiate reactions, a measuring circuit to measure changes in the wire's resistance and a software interface to process voltage measurements.

The heating circuit, see Figure 4.5, comprises of a reference resistor and the reaction wire. Voltage measurements across a reference resistor are used to calculate the current passing through the reaction wire. The voltage across the reaction wire is also recorded. A visual basic interface in conjunction with a data acquisition card calculates the wire reaction temperature as the test proceeds. The measuring circuit consists of the reaction wire and a dummy wire both connected to a high precision Ohmmeter capable of measuring to 10μΩ. The dummy wire acts as a reference wire to monitor changes in bulk oil temperature during reactions.

An experimental program was designed to test a number of lubricants at various temperatures, from this an understanding of the relative reactivities of the lubricants was obtained. The lubricants used were the same as those used in Bristol RCF tests. Initial tests were made on mineral white oil to check that Barcroft's tests were repeatable. Shell Vitrea was used as a base oil with concentration of 2% and 5% Lubrizol S/P additive. Shell Spirax AX 80W-90 and the Volvo 97305 lubricants were also tested.

4.2 HOT-WIRE RIG DESIGN

The hot-wire test used in this study was a modified version of the type originally used by Barcroft in the 1960's. Barcroft realised that a simple way of getting temperature of up to 600 °C was to pass a DC current through a metal wire of small diameter. The power needed to do this could be provided by an ordinary bench top device. During heating, changes in resistance due to temperature, ΔR_T, could be calculated and this value provided a good estimate of the temperature of reaction. When the wire reacted the atoms close to the surface were consumed in the process, this caused a decrease in the diameter of the metal.

A decrease in wire diameter causes an increase in resistance, ΔR_D, by measuring this it is possible to calculate the corrosion in the wire. One problem remains, during a reaction, heat from the wire is transferred to the oil and the bulk oil temperature is increased during the reaction. Therefore at the end of testing if the wire has reacted and the bulk oil temperature has increased the change of reaction recorded is not only ΔR_D it is a sum of $\Delta R_D + \Delta R_T$. To find the true ΔR_D, Barcroft used a temperature correction factor. He measured the increase in oil temperature and compensated this back to a reference temperature of 20 °C. His paper [5] quotes temperature measurements with a sensitivity of 0.05 °C.

To start with, tests were conducted using this method, a mercury thermometer with an accuracy of 0.1 °C being used to measure the temperature variations. Temperatures throughout the bath were seen to vary even after the bath had been stirred. There was also a lag time for the mercury to settle. To overcome this measurement problem a new means of calculating the temperature compensation was sought. A second parallel wire of length 32.5 mm at a distance of 8mm apart were chosen for this task. The first wire was connected to a heating circuit and will be known as the reaction wire, the second is a reference wire to monitor changes in bulk oil temperature and will be called the dummy wire. During the tests the reacted wire is heated and corroded and changes of resistance are compared with the dummy wire which does not corrode, since its temperature never exceeds 30 °C.

4.3 DESIGN DETAILS OF THE HOT-WIRE RIG

The hot wire rig consists of four main parts, the reaction bath, the power circuit, the measuring circuit and the visual basic interface. The individual parts will be discussed below. Figure 4.1 shows the layout of the hot-wire apparatus pictured on a bench at the University of Bristol.

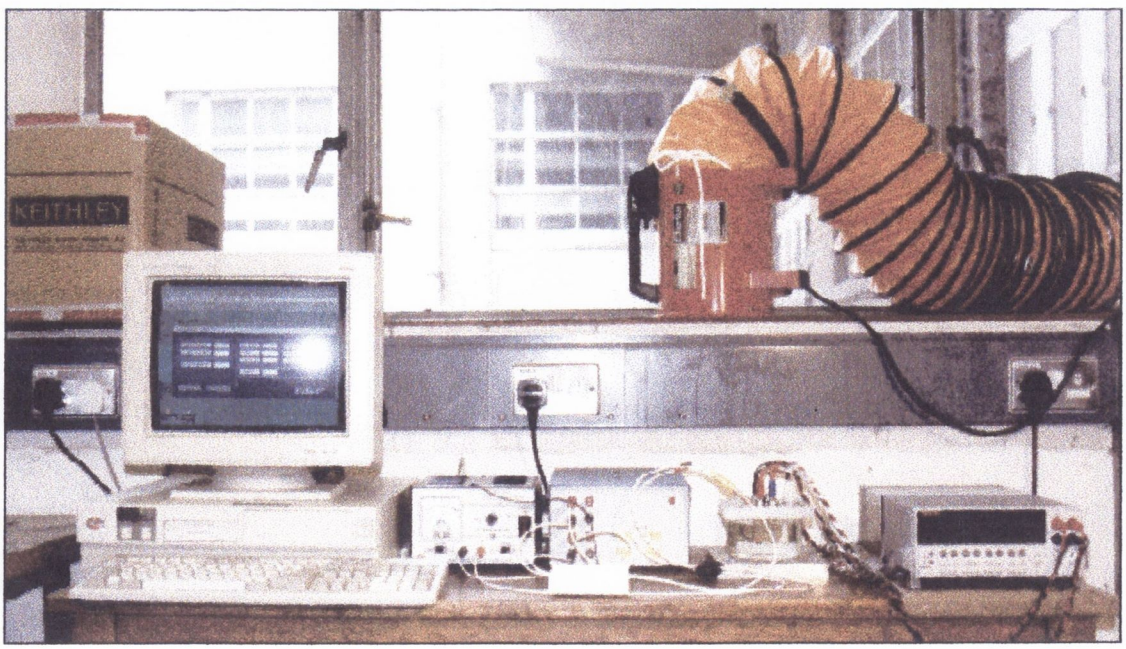

Figure 4.1 Photo of bench layout of the hot-wire rig

4.3.1 The bath

The reaction bath consists of a Pyrex basin with a volumetric capacity of 400ml. Two pairs of parallel clamping terminals are fixed to an electrically insulated nylon lid. The clamps were designed to give a good grip of the thin wires during reactions, heating and cooling. Any slippage of the wire would result in erroneous resistance measurements as the length of the wire could vary. An elongated hole was machined in the end of the clamp and a 0.5 mm slot was machined using spark erosion for high accuracy. The clamps are made from 12 mm square section 60/40 brass, so by tightening the bolts the wire is pinched making a good electrical contact. After the reaction the terminals spring back to their original positions and other sets of wires can be mounted.

The terminal blocks have 4 mm holes drilled at the top to connect the resistance measuring leads. The reaction pairs have 4 mm adaptors for connecting the heating circuit, see Figure 4.4. A nylon stirrer was fitted to the bath to mix the oil. To fix the bath the wire lid was bolted to an aluminium base. This prevented the wires from being disturbed during testing.

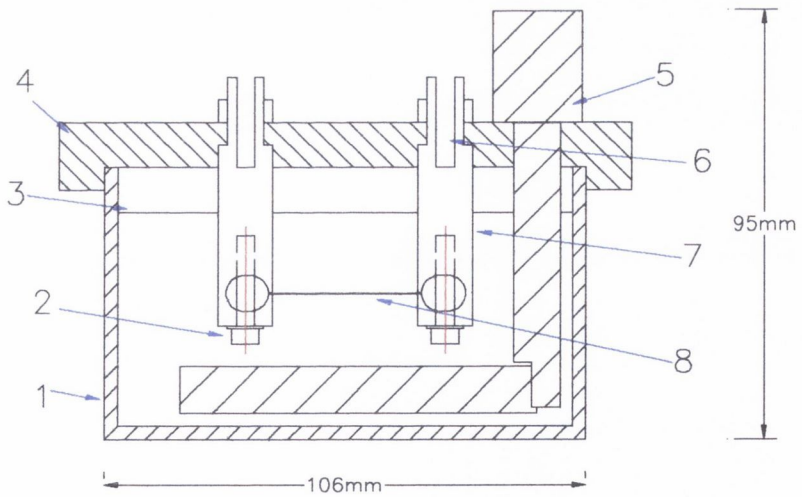

1. Pyrex Beaker	2. Bolt	3. Oil Level	4. Nylon Lid
5. Stirrer	6. 4mm Socket	7. Clamp	8. Wire

Figure 4.2 Front profile of the hot-wire bath showing clamping arrangement

4.3.2 Mounting the wire to the clamps

Before each test the clamps were immersed in a bath of acetone and cleaned ultrasonically to remove reaction products from earlier reactions. After drying the terminals were ready to have new wires mounted on them. The annealed wires were first cleaned in a basin of acetone and put in an ultrasonic bath for 30 seconds. The lid was fixed to a retort stand as in Figure 4.3. A small plastic weight (2.5 g) was fixed to the wire to provide a tension to straighten the wire. This applied a tensile stress of 12.5 N/mm^2 to the wire. The wire was passed over the side of the terminal, the wire was positioned carefully with tweezers. When the wire was in position the upper bolt was clamped, then the lower end of the wire was positioned and clamped. Excess lengths of wire which are not involved in the reaction are cut away with a sharp scalpel. The mounting procedure was repeated for the second wire.

The wires are now ready to be positioned in the oil bath. The lid is placed over the bath and the lid is held in place with two bolts which are screwed to an aluminium base underneath. The oil is stirred carefully and allowed to settle until all bubbles have travelled to the surface of the oil.

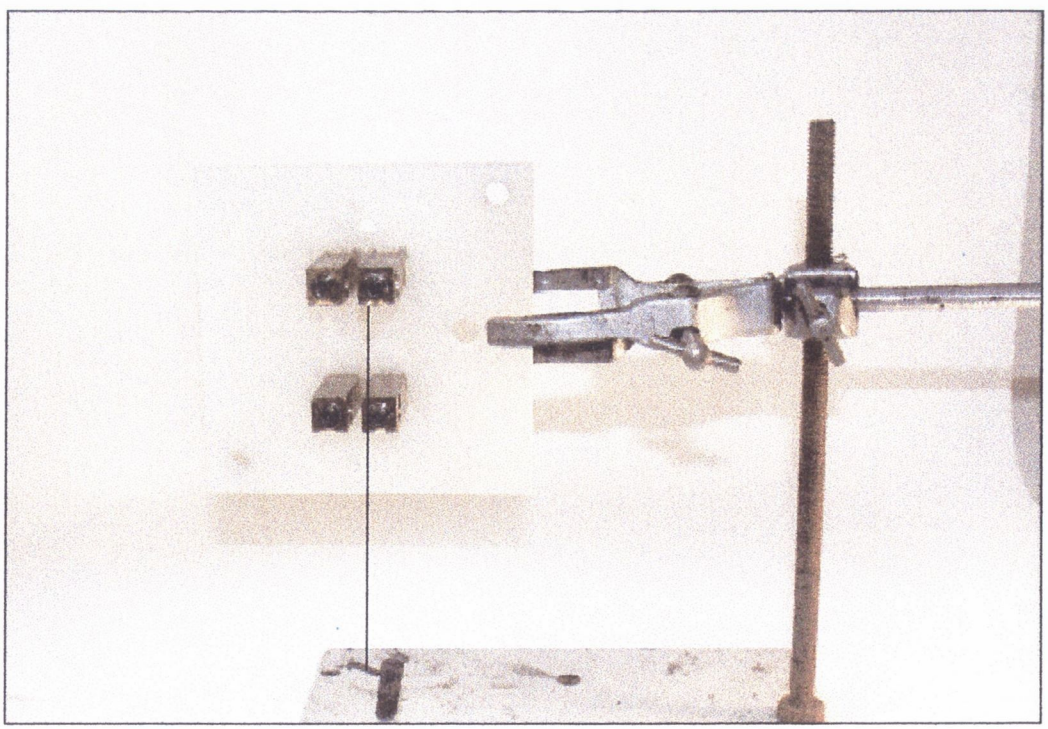

Figure 4.3 Photo of mounting wire to clamps

4.3.3 Extraction

Gas bubbles were observed to form on the wire during reaction. They tended to gather until a bubble was big enough to rise to the surface of the oil bath. To remove malodorous fumes caused by the decomposition of sulphur additives at high temperatures, an air mover was mounted over the reaction bath. During reactions the fan was switched on and odours were blown out of lab through a flexible funnel.

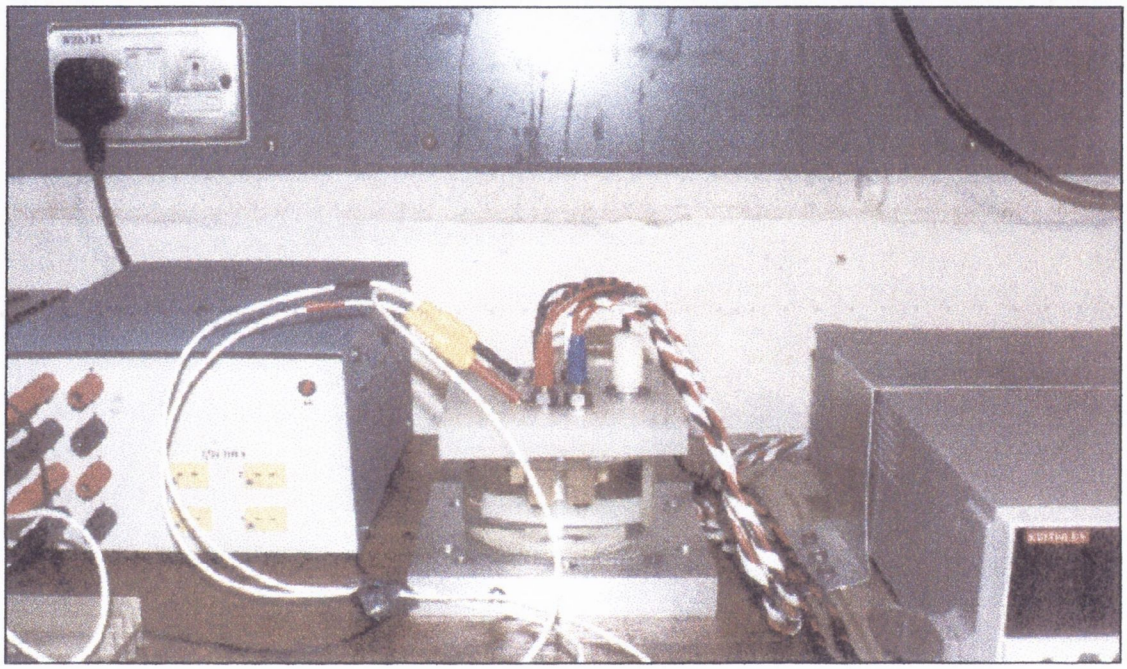

Figure 4.4 Photo of hot-wire bath showing positions of parallel wires

4.3.4 Heating circuit

The main feature of the heating circuit is a power supply capable of supplying constant currents to the wire. The voltage drop across a reference resistor (resistor A, 2.2 Ω) is used to calculate the current in the circuit. The reference resistor is mounted on a heat sink to eliminate variations in resistance due to temperature rises. The DC power supply is connected across the reaction wire terminals using 4mm adaptors allowing easy connection and disconnection.

At high temperatures the voltage drop across the wire was found to be high, so to remain inside the A/D card range (0-10V) it was decided that it would be better to divide the voltage in two by measuring the voltage drop between two resistors of high

resistance with are in parallel to the wire. Two 10kΩ resistors were chosen for this task. Voltage reading on channel 1 recorded the drop across the reference resistor and channel 2 measured the drop across the reference and half of the reaction wire. The voltage drop across the reaction wire was found by the following equation.

$$V_{wire} = (V_2 - V_1) \times 2 \qquad (4.1)$$

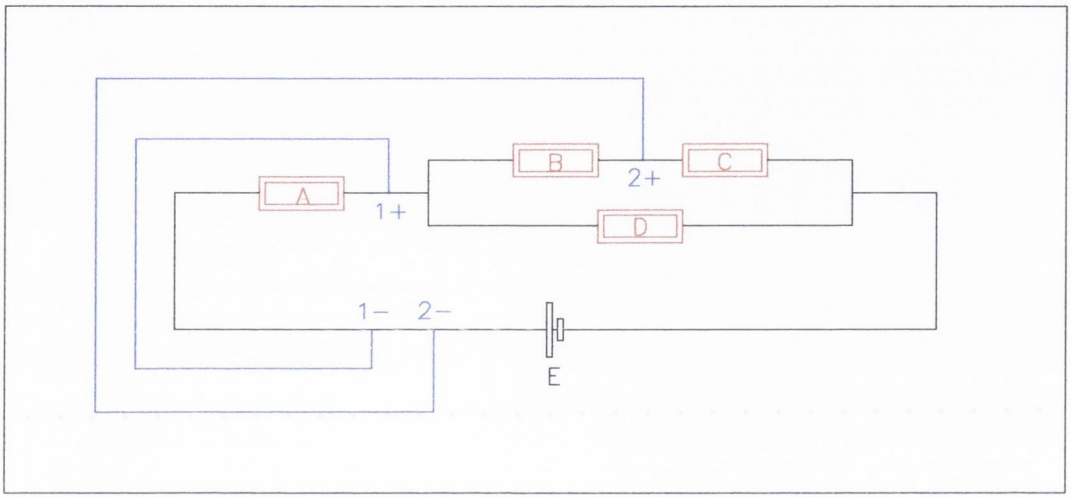

A. Reference resistor (2.2Ω) B. (10 kΩ) C. (10 kΩ)

D. Reaction wire E. DC Power supply

1-,1+. Voltage across A 2-,2+. Voltage across (A+ B) OR (A+ 0.5D)

Figure 4.5 Sketch of heating circuit and voltage acquisition points

4.3.5 The measurement circuit

The measuring circuit is used to record changes in wire resistance during the reaction period. A Keithley 2001 multimeter was used to measure resistance to an accuracy of 10 μΩ. The four-wire resistance measurement technique was used to achieve very accurate measurements. The measurement leads for the reaction wire are connected to the front display panel, while the leads for the dummy wire are connected to the rear. To avoid electrical noise interference the test leads were twisted. Switching between the two wires was facilitated by the front/rear input button on the right side of the front panel. The four-wire measurement technique is shown in Figure 4.6. A source current is passed from the input HI terminal to the input LO terminal.

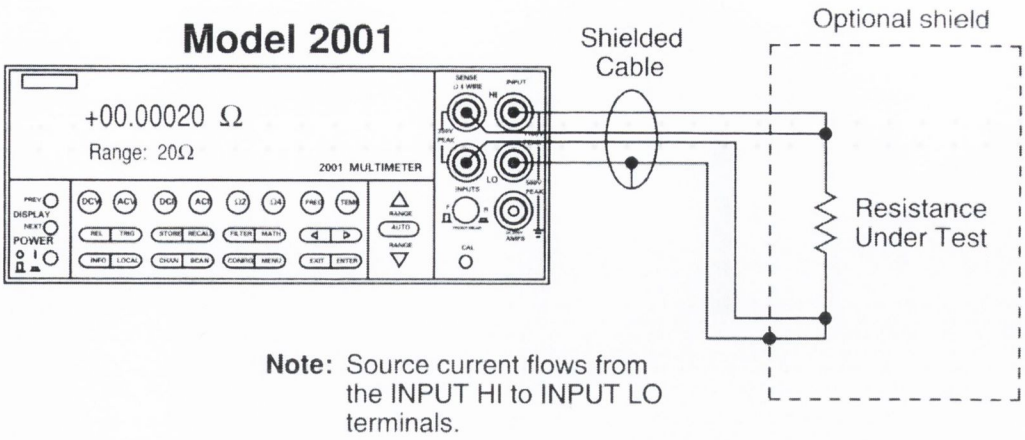

Figure 4.6 Four-wire resistance measurement

4.3.6 Logging equipment

To monitor the temperature of reaction during testing, visual basic software was developed. An Amplicon PC30AT analogue-to-digital (A/D) card measured two voltages in the circuit. The software used these values to calculate the percentage change in resistance of the wire. The reaction temperature of the wire was then found by using the resistance/temperature characteristic graph of the material.

Voltage was measured across a reference resistance, from this the current in the circuit was calculated. By measuring the voltage drop across the reaction wire and using Ohm's law the wire resistance was found. The resistance then converted to a temperature using the resistance-temperature function taken from Barcroft [5]. All measurements at the end of each test were written to the volts.csv file where the reaction temperatures could be easily plotted against time using excel or lotus 123 software.

Time (sec)	V1 (Volts)	V2 (Volts)	$I_{circuit}$ (Amps)	V_{wire} (Volts)	R_{wire} (Ohms)	Temp (°C)
1	2.007	8.825	0.912	13.636	14.945	453
2	2.010	8.825	0.914	13.631	14.922	450
3	2.007	8.825	0.912	13.636	14.945	453
4	2.007	8.825	0.912	13.636	14.945	453
5	2.010	8.828	0.914	13.636	14.927	450

6	2.000	8.779	0.909	13.558	14.914	449
7	2.002	8.799	0.910	13.592	14.933	451
8	2.005	8.813	0.911	13.617	14.942	452
9	2.005	8.806	0.911	13.602	14.926	450
10	2.002	8.799	0.910	13.592	14.933	451
11	2.002	8.796	0.910	13.587	14.928	450
12	2.002	8.794	0.910	13.582	14.922	450
13	2.000	8.794	0.909	13.587	14.946	453
14	2.000	8.791	0.909	13.582	14.941	452
15	2.002	8.791	0.910	13.578	14.917	449

Table 4.1 Example of output form visual basic interface

4.3.7 A/D card calibration

The PC30AT card is supplied with software to calibrate the card. The jumper settings on the card must be first selected in accordance with the voltage input range required. The program TPDEMO.EXE is then run. A reference voltage source stable within <1mV is attached to input channel 1 of the 50-way socket. Channel 0 is connected to ground for zero volts input. The software is then run to sample the voltages across channels 0 and 1. Zero volts are supplied to channel 0 and the variable resistor is adjusted to until the output reads 0.000 to 0.002/3. A voltage of +9.997 volts is applied to channel 1 and again the pot is adjusted until it reads from 9.995/6 to 9.998/9. These steps are repeated until the calibration is complete. Re-calibration is recommended every three months.

4.3.8 Visual basic interface

A computer interface was developed to allow convenient data logging of the voltage in the hot-wire circuit. Functions for reading voltages were provided by Amplicon and were incorporated in the program. The program recorded two voltages and from this the circuit current and the resistance and hence reaction temperatures were calculated. The current was calculated by measuring the voltage drop across a reference resistor. The voltage drop across the wire was then measured and knowing the current allows us to calculate the resistance of the wire. The temperature of the wire was then estimated from the temperature resistance function.

The inputs to the interface are sample number, sample rate and initial resistance of the wire. The program records two voltages and then calculates the current, resistance and temperature. The results the displayed on the screen in real time and all results were recorded to a (.csv) file. The sample rate needed calibration as the calculation and recording slowed the process down. A sample rate of 860 ms provided sampling at a rate of 1 per second. The temperature of the wire was calculated by comparing the percentage increase in resistance of 20 °C to that of the reaction temperature.

The results were put into a file called volts.csv where the temperature of reaction was plotted. The changes in resistance due to corrosion were not recorded by the VB interface. Reactions had to be suspended and the oil allowed to settle before these measurements could be recorded. After each test the file name was changed so that it would not be overwritten during the next test. As the interface displayed temperature of reactions as the test proceeded it was easy to control this temperature by adjusting the power output from the power supply.

4.4 TEMPERATURE / RESISTANCE CHARACTERISTICS OF THE HOT-WIRES

Resistance measurements were used to estimate the wire temperature during the reaction. Resistance/temperature characteristics for stainless steel and iron wire were taken from the original graphs used by Barcroft [5]. Temperature was plotted against percentage change in resistance for both metal in the temperature range 0-600 °C. Second order polynomials were fitted to the curves to give resistance/temperature functions. These functions were used by the visual basic interface to estimate reaction temperatures. Graphs are plotted in Figures 4.7 and 4.8.

Iron wire $$Y = -0.0013X^2 + 2.009X + 29.066 \quad (4.2)$$

Stainless Steel $$Y = 0.0774X^2 + 8.666X + 29.066 \quad (4.3)$$

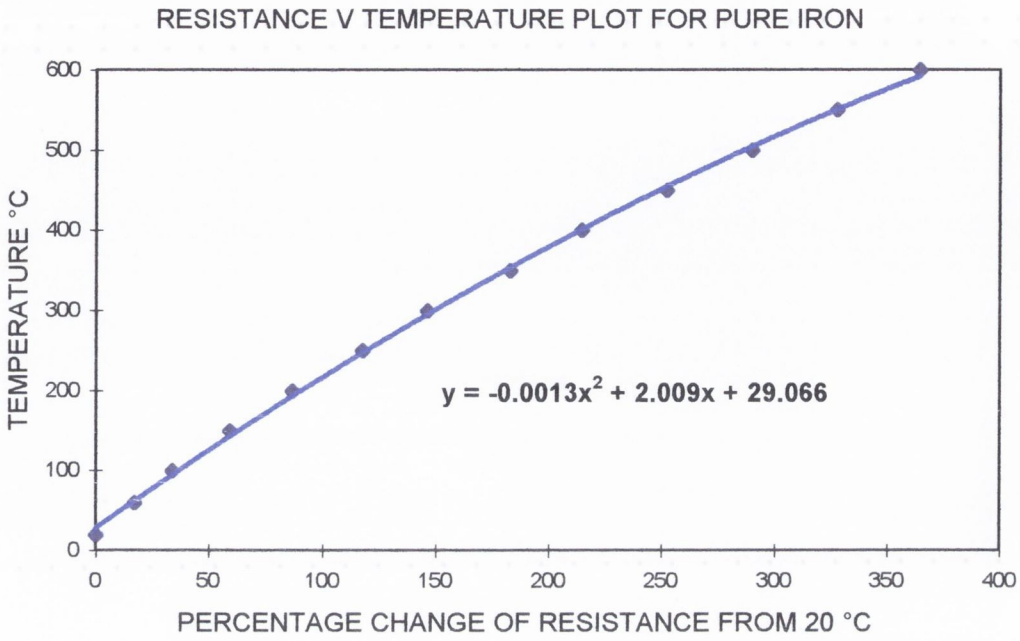

Figure 4.7 Resistance/temperature characteristics of pure iron

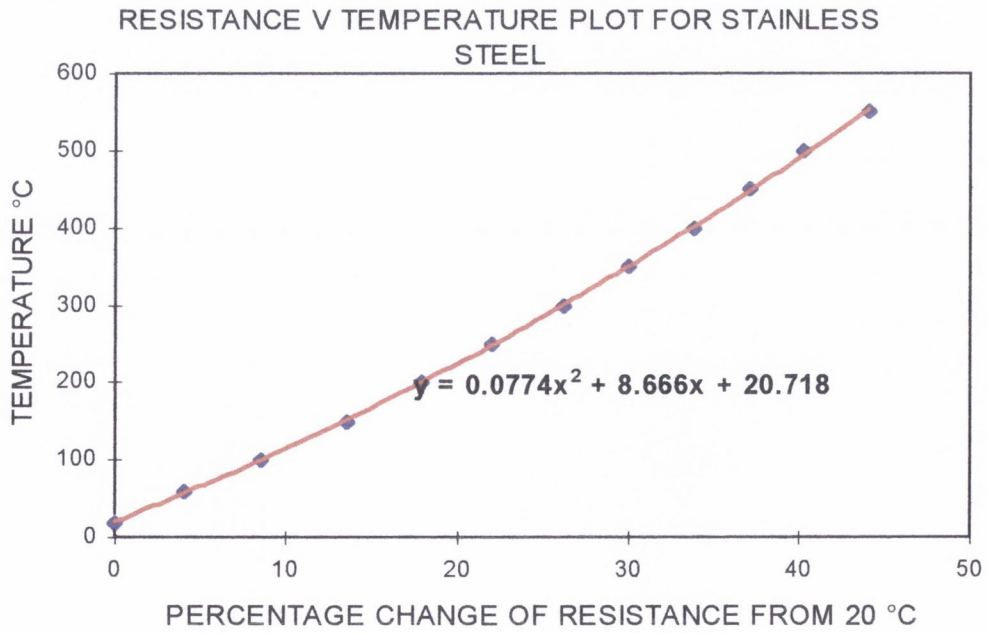

Figure 4.8 Resistance/temperature characteristics of stainless steel

4.5 EXPERIMENTAL DETAILS

4.5.1 Test procedure

The wires used in the hot-wire bath test had a diameter of 50μm. They were chosen as high temperatures were achievable using a conventional DC power source. Stainless steel was selected because of its high resistivity value $70x10^{-8}$ (Ωm). Initial resistance values were typically 10-11 (Ω). Changes due to corrosion were magnified to allow more sensitive monitoring of changes. Iron wire was also used because it had the disadvantage of having a lower initial resistance $10x10^{-8}$ (Ωm) but the nature of the oxide film on the surface made it more reactive than stainless steel. The wires were vacuum annealed at 650 °C for 2 hours to give stable resistance/temperature characteristics during the tests. Each test followed the same procedure as follows:

a) Two lengths of wire (200mm) were cleaned with acetone in an ultrasonic bath for thirty seconds.
b) A small weight was attached to the wires to provide a small tension to the wire during the clamping.
c) The wires were clamped across terminals and placed in oil basin and allowed settle for a period of ten minutes. See Figure 4.3.
d) The initial resistances of the wires were recorded, a 4-wire resistance measurement technique was used with Keithley 2001 multimeter accuracy 10 μΩ.
e) Before each reaction test was started the Ohmmeter was switched to the dummy measurement and 4-wire leads connected to the reaction wire were disconnected at front interface of the multimeter.
f) The heating circuit was connected to the reaction terminals.
g) The visual basic program was run and initial values for sample number, rate and initial resistance of the reaction wire were set.
h) Data sampling was then started and the power required to obtain the desired reaction temperature was applied.
i) The changes in wire temperature were monitored during the reaction, the power was adjusted to keep the it at the desired temperature.
j) When the test was finished, the results file (volts.csv) was saved under a new name and as an excel file (newname.xls).

k) A uniform oil temperature distribution in the bath was achieved by stirring the oil gently, care was taken not to disturb the wire connections.

l) Finally, the heating circuit was disconnected, and the 4-wire leads were replaced to measure the change of resistance.

To monitor reactions during the test period, each test was subdivided into six parts. Initial reactions were generally found to be high so special attention was given to the first five minutes. After the initial reaction the wire were seen to stop reacting or to continue to react linearly with time. Reactions were not measurable at temperatures under 300 °C. Tests were carried out at 25 °C increments to the highest temperature of interest 450 °C.

4.5.2 Annealing of the wires prior to testing

The wires used in the experiment are 50 μm in diameter, these small diameter are achieved by wire drawing. When a metal is drawn it is cold worked by plastic deformation. A small amount of mechanical energy used to deform the metal is stored in the metal. Subsequent heating will cause annealing to start, through recovery and recrystallization. Recovery is the term given to a series of structural changes as follows: the annealing out of point defects, the rearrangement of dislocations, subgrain formation and growth, and the formation of recrystallization nuclei. Following recovery recrystallization occurs by the nucleation and growth of new grains, which are essentially strain-free. Annealing the wire stabilises the metal properties, especially the electrical resistivity. It is important that the only changes in resistance in the hot-wire test are caused by temperature changes or corrosion.

4.5.3 Calculating changes in wire diameter

When a wire is heated, the resistance increases due to the changes in resistivity. If the wire is corroded and metal atoms are consumed, there is another smaller increase in resistance due to the decrease in the wires diameter. The changes in resistance due to corrosion are similar to that produced by a one degree Celsius of the wire temperature. This makes it difficult to measure corrosion effects as the wire temperature is governed mainly by the bulk oil temperature which can fluctuate during testing. Barcroft used a technique of temperature compensation to overcome this problem. All of his resistance measurements were corrected to 20 °C. This involved accurate temperature measurements of the bulk oil temperature to 0.05 °C. In order to avoid having to make such accurate temperature measurements a second wire was added to the basin to act as a compensation wire. Using this technique we isolate changes due to corrosion without having to make an absolute temperature measurement.

$$\Delta R = R_3 - \left(\frac{R_4}{R_2}\right)(R_1) \tag{4.4}$$

When the change in resistance has been calculated we are then in a position to calculate the change of diameter corresponding to this change in resistance.

$$\Delta r = \left(\frac{\Delta R}{R_1 + \Delta R}\right)\left(\frac{r_0}{2}\right) \tag{4.5}$$

where R_1 = initial resistance of the reaction wire

R_2 = initial resistance of the Dummy wire

R_3 = resistance of reaction wire after reaction

R_4 = resistance of dummy wire after reaction

ΔR = change to resistance due to corrosion

Δr = change in radius, depth of corrosion

r_0 = original radius of wire

4.6 CHANGES OF RESISTANCE AND CHANGES IN WIRE LENGTH

To verify if the changes in wire resistance relate to the actual temperature of the wire an additional experiment was devised. An increase in wire temperature not only causes an increase in resistance but an increase in length too. This change in length was used as an independent means of comparing resistance and temperature. To carry out the test an apparatus was developed which used a wire clamped at one end that was free to expand around a brass pulley when heated.

A vertical oil flow was created in a glass tube of diameter 10 mm, oil was pushed from a reservoir by a piston weight. A 100 (mm) wire was mounted between two brass terminals as seen in Figure 4.9. The wire was clamped at the top of the tube, the lower end was passed around a brass radius and passed over a pulley with a weight inducing a tension in the wire. The heating circuit from the hot-wire rig was connected across the terminals, and was used to cause a thermal expansion of the wire.

The wire was heated to temperatures of 100 (°C), 200 (°C) and 300 (°C) by passing DC currents of 1.3 (A), 1.5 (A) and 1.7 (A) through the circuit. The extension of the wire was found by measuring the displacement of a white marker on the wire with a microscope. The extension in wire length was converted to a temperature using the thermal expansion coefficient properties of the material. The results, Figure 4.10, were plotted against the theoretical extensions calculated from the resistance measurements of the wire at temperature.

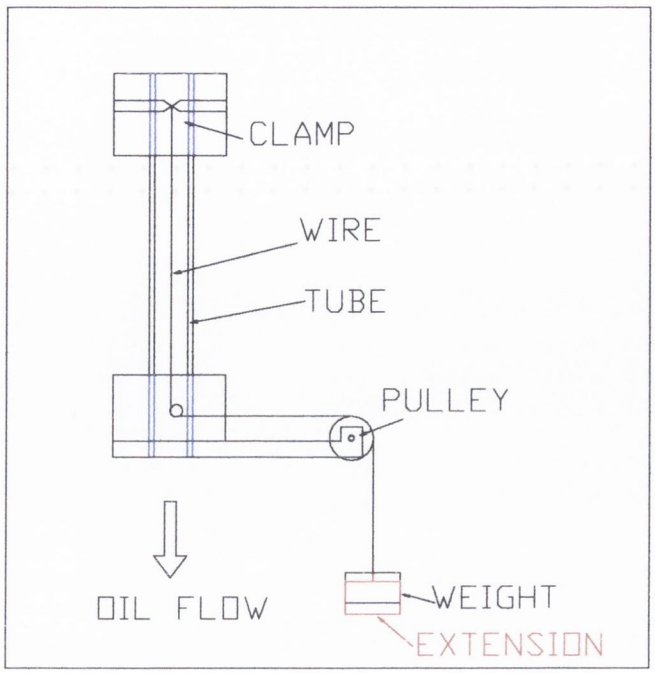

Figure 4.9 Schematic diagram of wire extension apparatus

The results show that there is a close relationship between the two temperature estimates, which confirms that using resistance measurements to estimate reaction temperatures is experimentally acceptable.

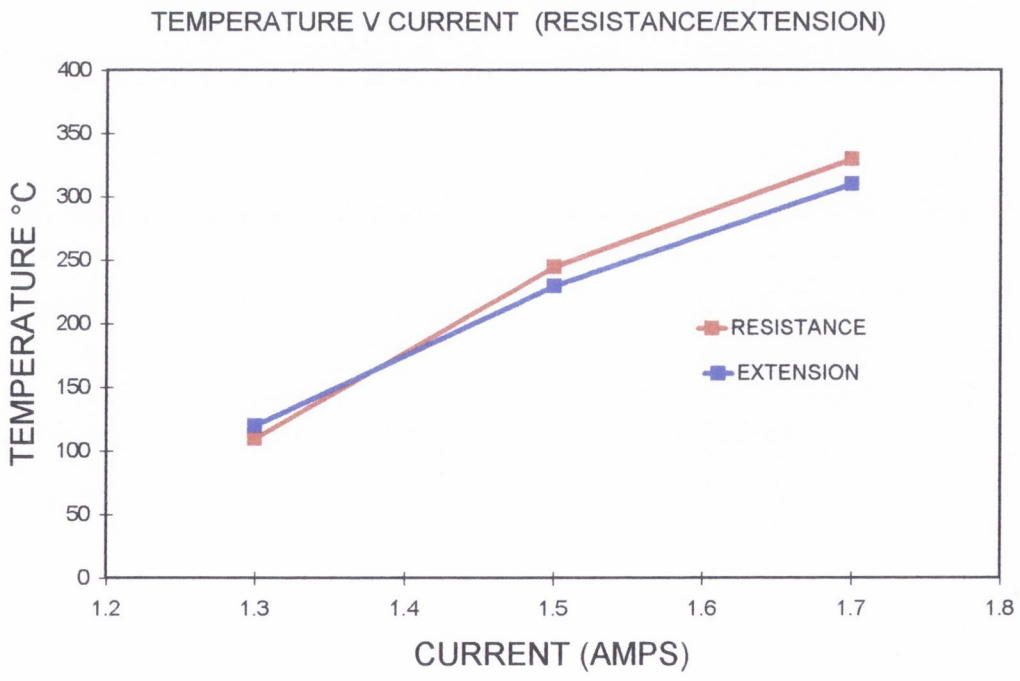

Figure 4.10 Graph showing temperature versus current for temperature prediction

4.7 VALIDATION CHECK OF TEST RIG

To ensure that the rig worked accurately some of Barcroft's experiments were repeated. The tests chosen were repeats of the stainless steel in white oil tests outlined in paper [5]. Reaction temperatures for these tests were high namely 400-650 (°C). The wire was reacted for 10 minutes after which time the $\log_{10}$ of the average reaction rate (Ang/min corrosion) was plotted against 1/T (absolute temperature in Kelvins). From Figure 4.11 it is seen that the reaction rate of the stainless steel and white oil is lower than that of the white oil containing additives.

Figure 4.11 shows the results of two of Barcroft's tests, the blue and red points show results for dibenzyl disulphide and sulphurized sperm oil respectively. Superimposed are the results of new tests carried out in Bristol with white oil only. The reaction rate when the white oil is used is lower than when additives are used. These results indicated that for high temperatures the new Bristol two wire rig worked well.

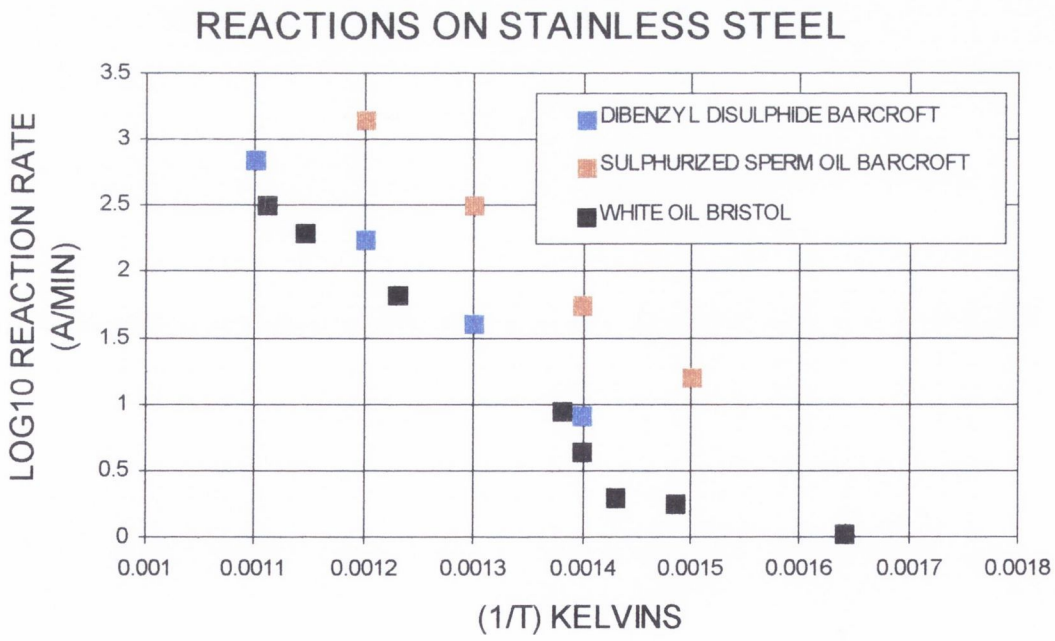

Figure 4.11 Comparison of Barcroft results and hot-wire tests at Bristol

4.8 SUMMARY

A hot-wire test rig has been designed and manufactured to test the reactivity of additives with metals. The rig uses two wires instead of a single wire used originally by Barcroft. The test rig has investigated reactions at lower temperatures than have previously been used in published works.

The hot-wire rig consists of four parts, the bath, the heating circuit, the measuring circuit and the VB interface. Special clamps were designed to hold the wire in a fixed position during testing. A precision Ohmmeter was used to allow accurate measurements of resistance changes.

Metal/additive reactions on the surface of the wire causes a reduction in the diameter of the metal wire. A decrease in wire diameter causes an increase in resistance. The reaction is assumed to be uniform over the length of the wire. The reduction in radius can be used to calculate the reactivity of the additive. The relationship between the changes in resistance and the oil/metal reactivity is given in this chapter.

To check if the temperature of reaction calculated by the heating circuit was accurate an independent test was devised. The thermal expansion of the wire was measured using the pulley system. This extension was converted to a temperature using the co-efficient of thermal expansion for the material. The two sets results corresponded quite well, proving that the resistance measurement technique was accurate.

To automate testing, a visual basic interface was developed to calculate the temperature of reaction. The program employed temperature/resistance functions to convert the wire resistance values to reaction temperatures. All results were recorded into a (.csv) file which could be processed using excel.

CHAPTER 5

5 ROLLING CONTACT FATIGUE RESULTS

5.1 INTRODUCTION

The results of the fatigue test programs carried out at the University of Bristol and at SKF ERC in The Netherlands are presented in this chapter. As bearing failures are of a random nature, Weibull analysis is used to quantify their failure lives. This study uses the software package "Minitab" to process the fatigue results. Statistical analysis of this type allows researchers to determine if significant improvements in bearing life are found by using a particular additive. The known test conditions were used to make bearing life predictions. These predictions are compared to results from the fatigue tests.

After failure life times have been examined, it is important to examine the failure modes of the specimens. In this study, bearing failure modes were investigated by optical and scanning electron microscopy. Changes in surface roughness were found on the Bristol specimens. The originally ground inner ring specimens were found to be polished during testing. This lowered the surface roughness of the specimen and improved the lambda ratio, allowing the bearings to survive for longer.

Oil oxidation and degradation have been examined using FTIR analysis. The Volvo 97305 oil produced a sludge that increased oil contamination, this dramatically lowered the bearing life. The sludge was found to contain several constituents and is examined later in section 5.7. FTIR analysis was also used to test for oxidation in oil samples taken from the Bristol rigs. The analyses were carried out by Mr. Albert v.d. Kommer at the ERC.

5.2 FAILURE DATA - WEIBULL ANALYSIS

Weibull analysis is a method of modelling data sets containing values greater than zero. Weibull analysis can make predictions about a product's life and compare the reliability of competing product designs. In this study the product life will be the life of the bearing until failure and competing design factor will be the type of lubricant used in the bearing test. The L_{10} life of a bearing is the standard life rating, it is calculated from a series of fatigue tests carried out under identical conditions. Since bearing failure is a statistical phenomenon, the L_{10} life is defined as the life that 90% of bearings can expect to survive under similar operating conditions.

Confidence levels indicate the reliability or accuracy of a life prediction. Large numbers of bearing tests give the best life estimates, and the confidence intervals are more accurate.

The Weibull shape parameter, called β, indicates whether the failure rate is increasing, constant or decreasing. A $\beta<1$, indicates a decreasing failure rate, this means that a high percentage of bearings are failing during a 'burning in' period. A $\beta=1$ indicates a constant failure rate. And finally a $\beta>1$ indicates an increasing failure rate, that the bearings are failing as they wear out.

The Weibull characteristic life, called α, is a measure of the spread of the distribution of data. α happens to equal the number of cycles at which 63.2 per cent of specimens have failed.

Tests were suspended after a censor time of 4 weeks. A complete sample where all units have failed yields greater precision. Type I censoring occurs where the censoring time is pre-specified as in the case of the Bristol rigs.

5.3 RESULTS OF FATIGUE TESTING USING THE BRISTOL RIGS

As discussed in Chapter 4, tests were carried out on sets of twelve 6305 inner races with the four oils listed in Table 5.1. Ground raceways with a surface roughness of 0.5 μm (cla) were used to accelerate the time to failure. The fatigue lives in hours of the Bristol tests are presented in Table 5.2. Some of the tests lasted longer than cut off period of 4 weeks and were suspended. The suspended test results are typed in bold lettering. The results are plotted on a Weibull chart in Figure 5.1 to compare the relative performances of the oils.

To characterize the effects of the EP additives on the bearing surfaces the failure modes have been investigated, the failure modes are defined as they are encountered during the discussion. In section 5.6 the changes in surface roughness of the ground races are examined to see how the contact conditions vary during the test.

	Lubricant
(1)	Shell Vitrea M100
(2)	Shell Vitrea M100 + 2% (S/P)
(3)	Shell Vitrea M100 + 5% (S/P)
(4)	Shell Spirax AX 80W-90

Table 5.1 Test oils for Bristol Rig

5.3.1 Weibull analysis of Bristol results

The results were processed using the "MINITAB" statistical software package. Most of the tests failed before the 4 week time limit, except in the case of the tests with Spirax. With the Spirax oil, 7 out of 12 tests were still running after 4 weeks, and were suspended. At first glance the Spirax oil did seem to give improvements in bearing life. To test whether the lives were significantly different, the results were plotted on a Weibull graph with 90% confidence interval limits. On the Figure 5.1, the confidence intervals are represented by the dotted lines. The confidence intervals display the amount of uncertainty associated with the life estimates. The confidence intervals are normally large when the sample number of failed specimens is low.

Test Number	Vitrea + 0% S/P	Vitrea + 2% S/P	Vitrea + 5% S/P	Spirax AX 80W-90
1	156.45	78.25	105.50	134.30
2	158.97	238.96	168.08	342.26
3	185.76	253.46	168.66	378.86
4	193.19	279.29	192.51	398.89
5	236.98	312.72	197.00	462.94
6	247.55	327.15	239.57	**623.24**
7	286.85	399.58	274.13	**654.82**
8	340.41	429.32	281.07	**659.70**
9	364.30	580.74	343.25	**671.25**
10	382.27	610.73	422.51	**671.82**
11	468.98	**671.39**	475.29	**671.01**
12	**671.63**	**719.39**	**749.92**	**681.69**

Table 5.2 Failure times in hours for Bristol tests, suspended tests in bold lettering

Looking at Figure 5.1 there are significant differences between the Vitrea and Vitrea/additive mixtures. The confidence intervals overlap, and this is evidence that the lives are not statistically different. Looking at Vitrea + 5% (S/P) and Spirax, a small over lap is observed for the L_{10}. The overlap does not exist for the L_{50} and therefore the differences in results do have some significance. The Spirax is a pre-formulated lubricant containing sulphur and phosphorus.

The Vitrea oil with or without additives did not have significantly different bearing life. Under these conditions no benefits were seen to accrue from using concentrations of the Lubrizol 5034a package.

A high proportion of the tests using Spirax exceeded the maximum test time of 4 weeks and were suspended. For simplicity, the suspended results were treated in the statistical analysis as normal failures. To get truly accurate estimates of the bearing life with Spirax oils the tests would have had to be allowed to continue until failure. This was not possible due to the time restraints.

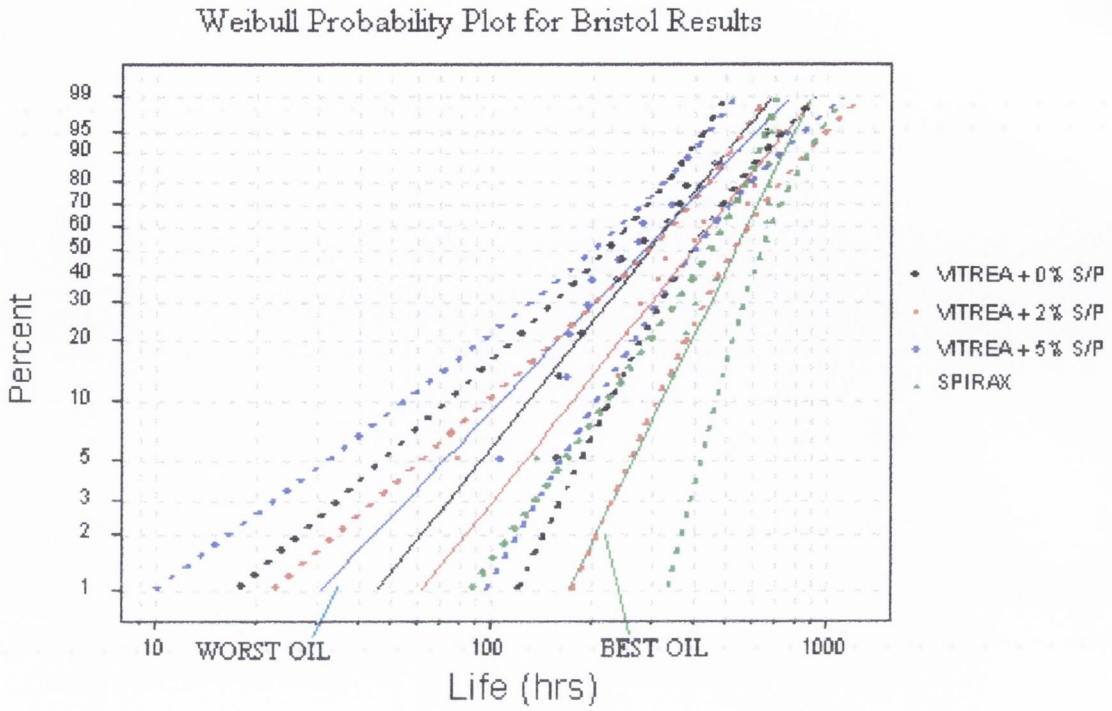

Figure 5.1 Weibull analysis of Bristol test results

5.3.2 Failure modes with Vitrea Oil (Base Oil) - Bristol tests

Examination of the failed inner rings and balls have shown that two failure modes are common when using Vitrea base oil. Surface distress of the inner ring - initiating spalling, and micro-pitting of the balls were the modes of failure. The two failure modes are defined below.

To define micro-pitting, it is first necessary to define micro-cracking. Micro-cracking is caused by continual cyclic stressing that exhausts the plasticity of the material. Cracks which tend to run parallel to the surface form as a result. As these micro-cracks grow, the surface becomes undermined to a depth of a few microns and multiple micro-pits form.

Surface distress is defined as micro-scale spalling fatigue. It is failure of rolling contact metal surfaces by the formation of (a) glazed surface areas (b) asperity scale micro-cracks and (c) asperity scale micro-spall craters. Surface distress occurs in the presence of a sufficiently low EHD film thickness to roughness ratio. The surfaces are not totally separated and there is contact at asperity level. Surface distress produces a

distinctive glazed appearance on metal surfaces. The most hazardous consequence of surface distress is spalling fatigue. In the absence of other surface defects, surface-origin spalling initiates from surface distress.

Examples of these types of failure are shown in Figures 5.2 and 5.3. The first micro-graph shows surface distress and pit formation on an inner ring. The original grinding marks can be seen in the top right hand corner of the photo. They are missing in the centre where polishing has occurred during the test. The second micro-graph shows pitting on one of the rolling elements. Micro-pitting is visible on the extremes of the horizontal track. Other failures, using the same oil, also showed surface distress and micro-pitting. In certain cases, five dark lines were seen on some of the wear tracks on the inner rings. It is possible that these are the result of grinding burn that happened during the manufacturing process. Circular micro-pitting was found on some balls, probably caused by contact between the ball and the loading sleeve. This micro-pitting appeared at the poles of the balls, at points furthermost from the wear track.

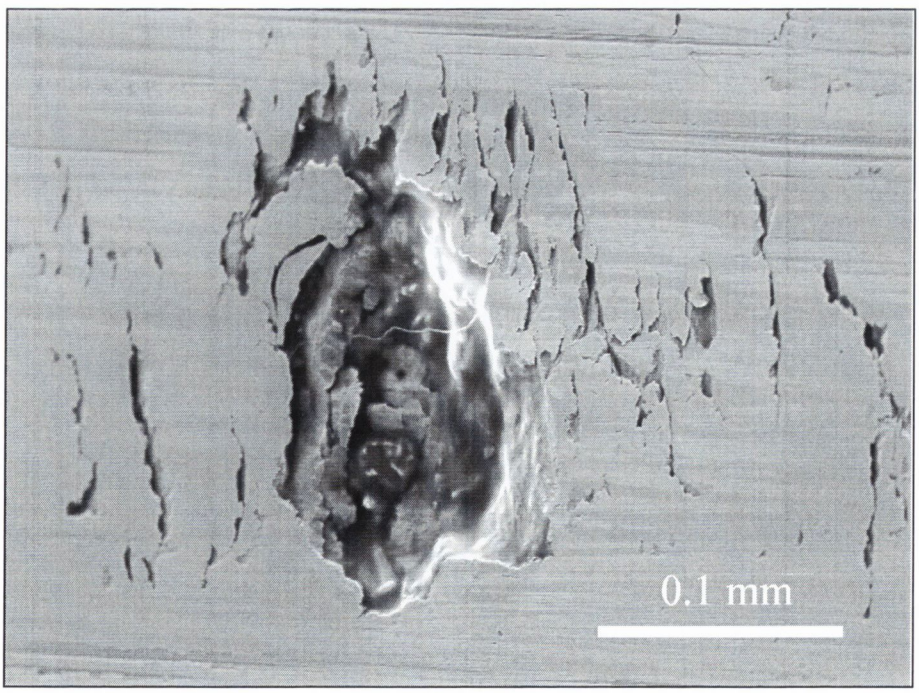

Figure 5.2 Spalling and surface distress on inner ring (Vitrea + 0%) (719 hrs)

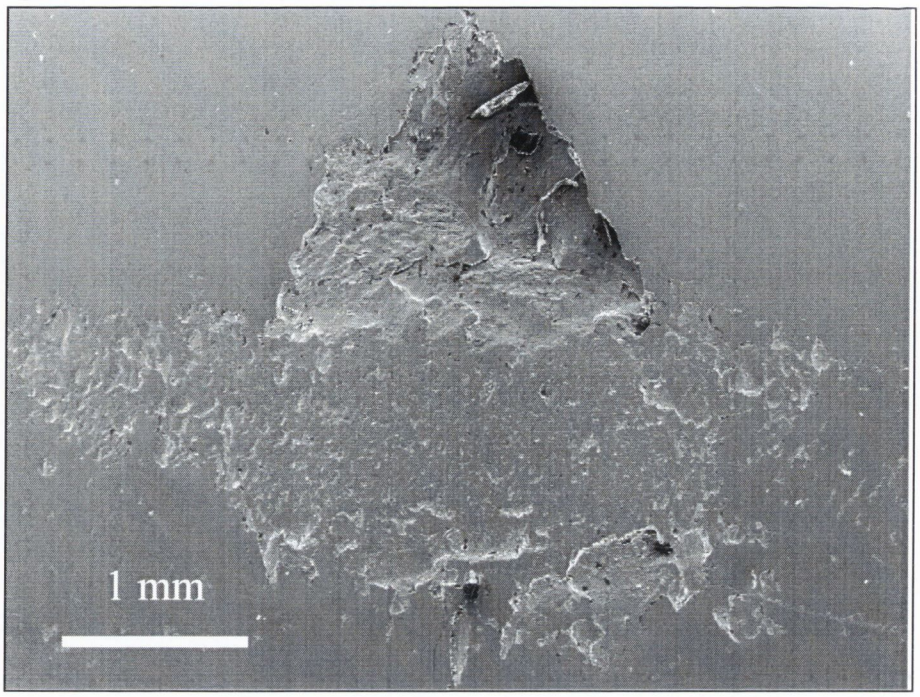

Figure 5.3 Micro-pitting on rolling element (Vitrea + 0%) (468 hrs)

5.3.3 Failure modes with Vitrea Oil + 2% (S/P) - Bristol test

Vitrea + 2% (S/P), in terms of survival times, performed second best of the of the four oils in the Bristol rigs. The failure modes of surface distress on the inner ring and micro-pitting on the balls were again found. Of the ten failures, six failed due to rolling element failure, two due to inner ring failure and two due to combinations of both. Figures 5.4 shows damage on an inner ring, that has been tested for a period of 610 hours. Surface distress has produced pitting on the surface.

Figure 5.5 shows a rolling element from the same test. In the case of the rolling element, subsurface failure caused by a non-metallic inclusion is suspected. The pit is localised, a flake of debris close to the removal stage is visible in the lower right hand corner of the micro-graph.

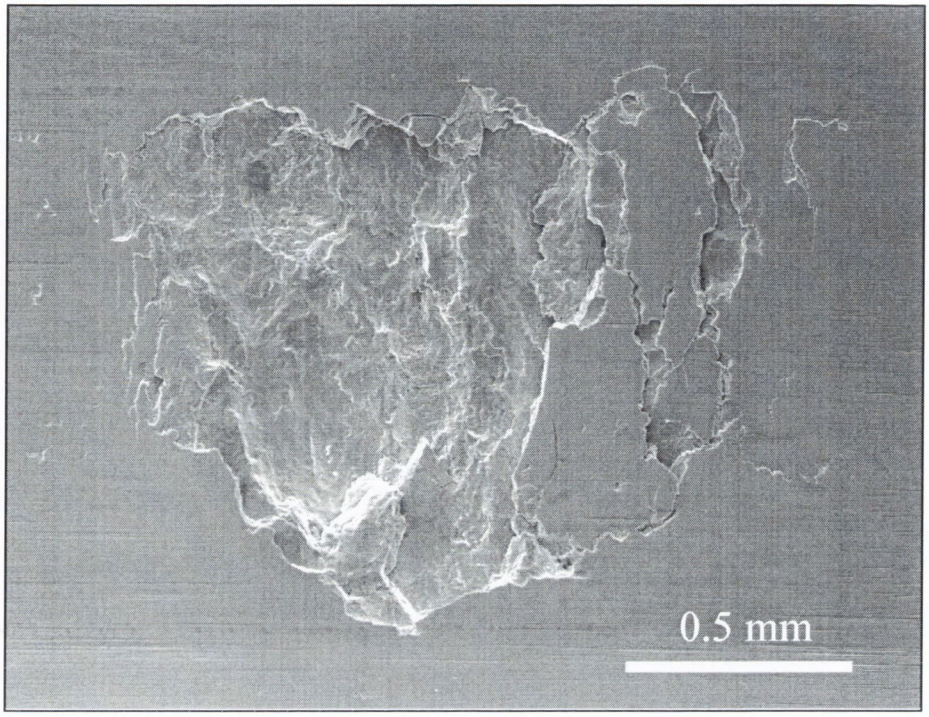

Figure 5.4 Surface initiated pitting on inner ring (V+2%) (611 hrs)

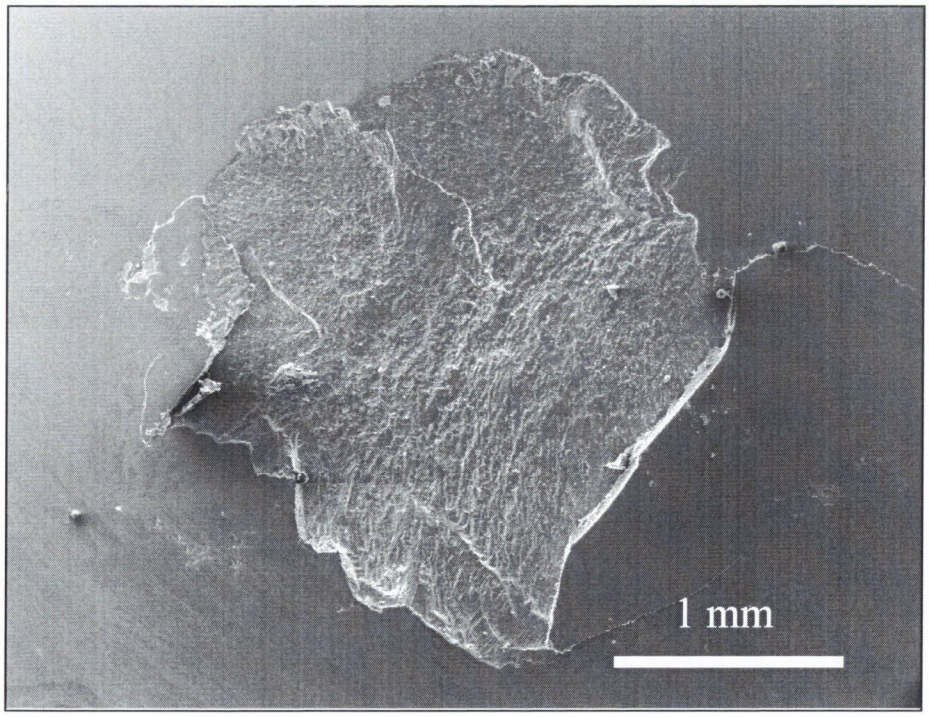

Figure 5.5 Sub-surface spall caused by defect (V+2%) (611 hrs)

5.3.4 Failure modes with Vitrea Oil + 5% (S/P) - Bristol tests

In section 5.3.1 we have seen that Vitrea + 5% (S/P) gave the shortest lives of the four oils. The failure modes were similar to those seen with the other oils used in the Bristol rig. Combined failures were found where the inner race and the rolling elements both experienced damage before the test was suspended by the vibration level. Surface distress on the inner ring was seen in 4 of the 11 tests that failed. The primary failure mode was surface distress on the rolling element. Dark tracks were formed on the surface, two or three distinct tracks were typical. In some cases the ball had changed axis and a secondary set of rings could be found.

Circular shaped micro-pitting was found on a number of balls, this is thought to be due to contact between the sleeve and the ball. Another explanation is that a hard particle was trapped in the clearance area between the ball and the sleeve - causing localised pitting. When the inner rings were examined five dark tracks were again seen on the surface. As the number exceeded the usual three (as seen on the balls) it was felt that these marks possibly originated at the time of manufacture.

Figure 5.6 shows typical pitting on the inner ring caused by surface distress. The ground finish has also been replaced with a more polished surface, this means that the lambda ratio is increasing from its initial value of 0.4 during the test.

Figure 5.7 shows advanced stages of pit formation on the surface of an inner ring which has been tested for 475 hours. The debris particle has broken in two as the metal is subjected to cyclical loading. Again polishing of the centre of the track is evident.

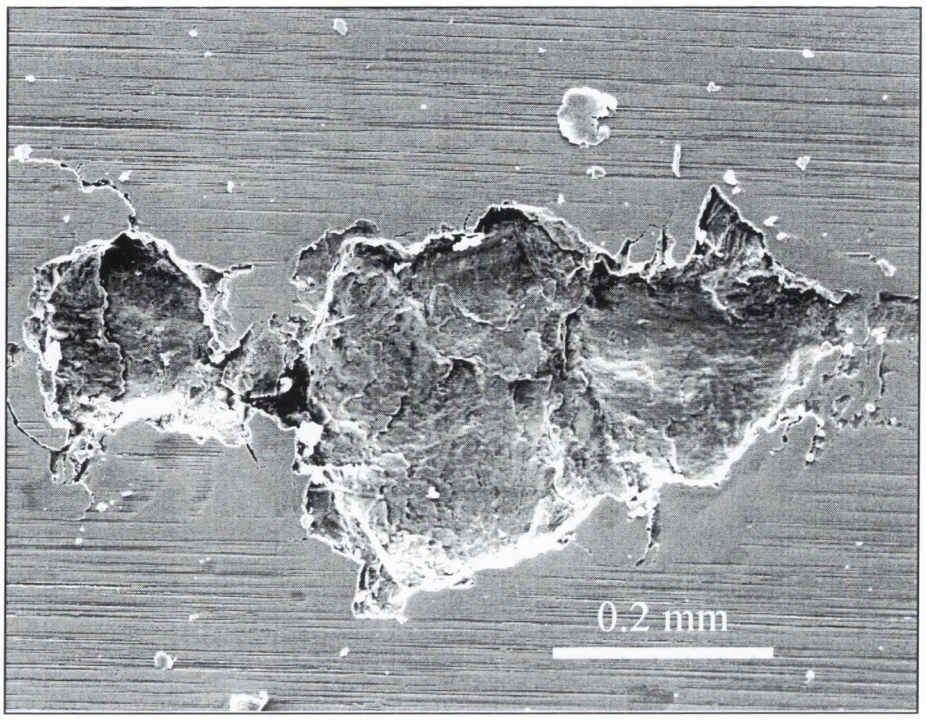

Figure 5.6 Surface initiated pitting on inner ring (V + 5%) (475 hrs)

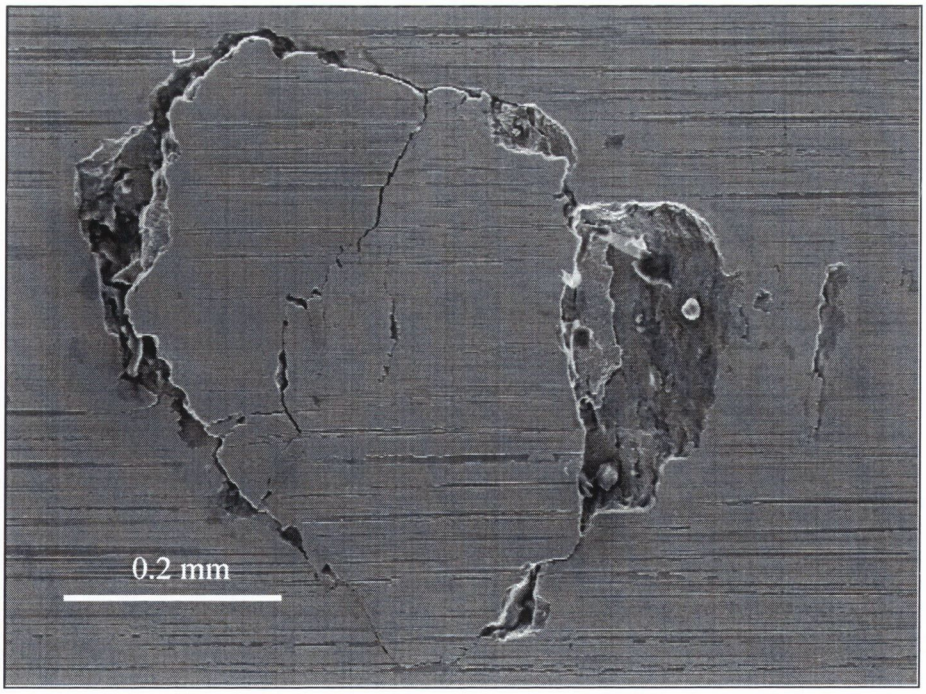

Figure 5.7 Advanced pit formation on inner ring (V + 5%) (475 hrs)

5.3.5 Failure modes with Spirax 80W-90 oil - Bristol tests

Seven of the twelve tests lasted the 4 week period. Of the 5 that failed, one inner ring had surface distress with shallow pits and the others had rolling element failures. Discolouration tracks on the rolling elements were not found using this lubricant. This could be due to a different type of reaction mechanisms caused by the Spirax oil. The high survival rate means that the life of the bearings tested under these conditions is being underestimated. In a more sophisticated approach the data is taken as being suspended. This however makes the confidence intervals wider, making the task of distinguishing between the oils more difficult.

5.4 RESULTS OF FATIGUE TESTING AT SKF ERC

The fatigue tests carried out by SKF served as a valuable comparison of lubricant effects at higher stresses and lambda ratio. The oils used in the R2F fatigue tests are listed in Table 5.3. The TT68 oil is the base oil used. The Spirax oil was the same grade used in the Bristol rigs, containing sulphur and phosphorus. The Volvo oils, with unknown compositions, produced an unusual failure mode: bulk cracking from the inner bore will be discussed later. In the case of the Volvo 97305 oil, sludge formation was found in the oil system and failures occurred at an ever increasing rate with the increase of this contamination.

	Lubricant
(1)	TT68 base oil
(2)	Volvo 97305
(3)	Volvo 97307
(4)	Shell Spirax AX 80W-90

Table 5.3 Test oils for SKF R2F rig

5.4.1 Weibull analysis of ERC results

Table 5.3 shows the oils tested in the R2F rigs. As mentioned in the literature review sufficient numbers of bearings must be tested to obtain meaningful statistical data. The number of tests carried out in ERC varied between 7 and 12. The times to failure given in hours are presented in Table 5.4. The lives in bold lettering signify that the

test was suspended. Some tests were suspended because of high level of contamination found.

Figure 5.8 is the Weibull distribution plot for the ERC tests. The base oil TT68 performed the best, followed by Volvo 97307, Spirax and Volvo 97305. The 90% confidence intervals of the base oil and Volvo 97305 do overlap. This is the test to see if there are significant differences in oil performance. The overlap indicates that there is no difference. A greater number of tests with the Volvo 97305 could refine the intervals, but as the bearings were taken from a limited single batch this was not possible.

Test Number	TT68	Volvo 97305	Volvo 97307	Spirax AX 80W-90
1	**390**	**39**	99	51
2	394	39	382	111
3	574	101	575	137
4	**790**	191	1513	141
5	938	416	1696	182
6	1300	902	**1696**	209
7	1342	1004	2387	**240**
8		1700		**319**
9				713
10				735
11				780
12				**1132**
13				1233

Table 5.4 Failure times in hours for ERC tests

The build-up of contamination in the oil during the test series meant that the bearings were not tested under identical conditions. In this case the co-efficient of cleanliness is becoming increasingly smaller each time a new test is started. The final couple of tests were carried out in a highly contaminated system. The longest lives were seen when using the base oil. The TT68 and the Volvo 97307 oils have similar lives, but as seen above the failure modes are significantly different.

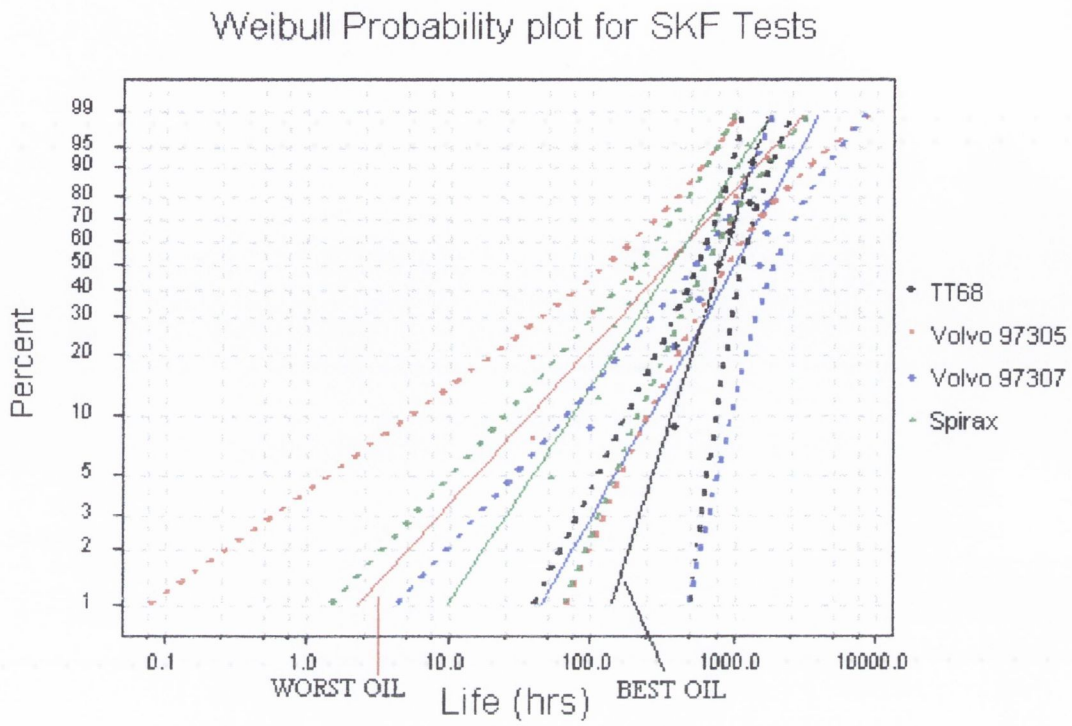

Figure 5.8 Weibull analysis of SKF ERC test results

5.4.2 Failure modes with TT68 oil - R2F tests

Failures were seen to be subsurface initiated deep spalls. The majority of the spalling occurred on the inner rings, with only one on an outer ring. One of the spalls was in an advanced state making it difficult to characterise. Subsurface initiated failures usually occur in three stages:

a) There is usually a straight leading edge on spalls near the point of initiation. The crack normally propagates perpendicular to the surface.

b) Crack propagation parallel to the surface occurs in the area of maximum Hertzian stress. Inclusions can sometimes be found at these points using SEM.

c) After the crack has reached the surface and the spall has formed, propagation on the surface can occur in both directions but mainly in the rolling direction.

Figures 5.9 and 5.10 show the typical subsurface failure modes. The rolling direction in each case is left to right. Denting can be spotted arising from the over-rolling of hard debris particles that have been removed from the surface. Debris damage usually indicates the rolling direction of the bearing elements, debris dislodged from the spall site is rolled by the passing ball over the surface of the raceway causing a characteristic

damaged surface. This mode of failure is associated with crack formation close to inclusions at depths where of maximum shear stress occurs.

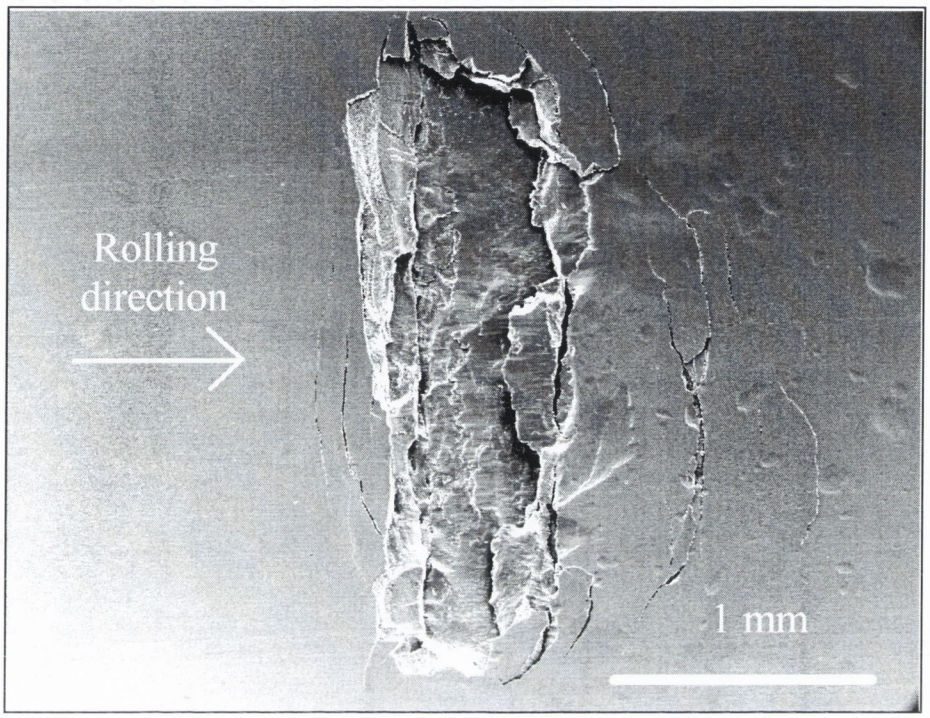

Figure 5.9 Subsurface initiated deep spall on inner ring (TT68) (1342 hrs)

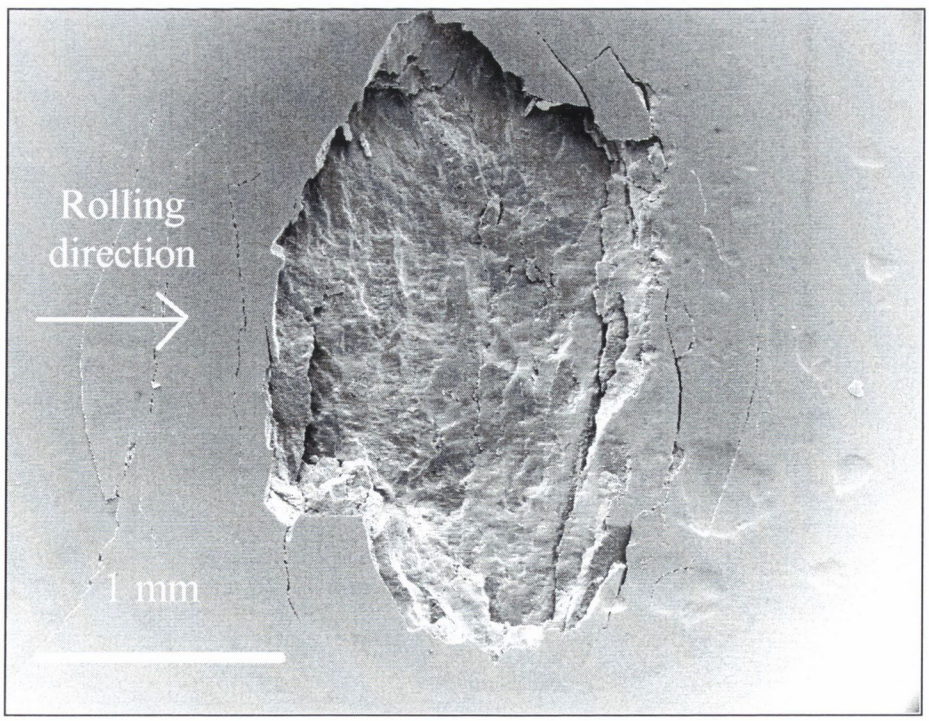

Figure 5.10 Subsurface initiated spall on outer ring (TT68) (574 hrs)

5.4.3 Failure modes with Volvo 97305 oil - R2F tests

Severe damage was seen on bearings under these conditions. Five of the seven failures were seen to have initiated at the bore, with three of these resulting in bulk cracking across the entire inner ring. Fretting of the inner bore was observed. Cracks were also found which propagated to the surface and thus initiated the large spalls seen on the optical and SEM photos. Fretting on the inner bores is most likely to be caused by some sliding between the bearings and the shaft during endurance testing.

Fretting wear is an adhesive wear process taking place in a nominally static contact under normal loads and microscopic surface-parallel relative motion. Fretting occurs usually at fit interfaces that transmit radial loads. In this example, the inner bore and the rotating shaft of the R2F rig, are at the interface. The fit must be tight enough so that rapid spinning of the fitted part is prevented, but slow creep or slipping can occur at the interference fit. The result of this motion is the formation of loose wear particles, which oxidise and cause a tightly adhering layer in the interface. The appearance of these oxidised marks vary in colour from dark red to black.

Abnormal sludge formation was observed in the oil lubricating system when Volvo 97305 oil was used. The time to failure of these test bearings was seen to decrease as the contamination increased. Table 5.5 shows the failure times in the test order. A FTIR analysis was undertaken to identify the composition of the sludge. This study is discussed later in this chapter in section 5.7.

Test No.	Failure time (hrs)	Failure mode
7	1004	IR, crack
8	1700	IR
14	902	IR
18	416	IR
21	191	IR
26	101	IR
30	39	IR
31	39	suspended

Table 5.5 Decreasing times to failure with Volvo 97305 oil

Figures 5.11 and 5.12 are optical photos showing the catastrophic damage caused by the bulk cracking from the inner bore being over-rolled. In both cases subsurface initiated damage caused by fretting corrosion at the bore was found. Very large oval shaped spalls were observed, but the inner ring crack is not visible in the micro-graphs.

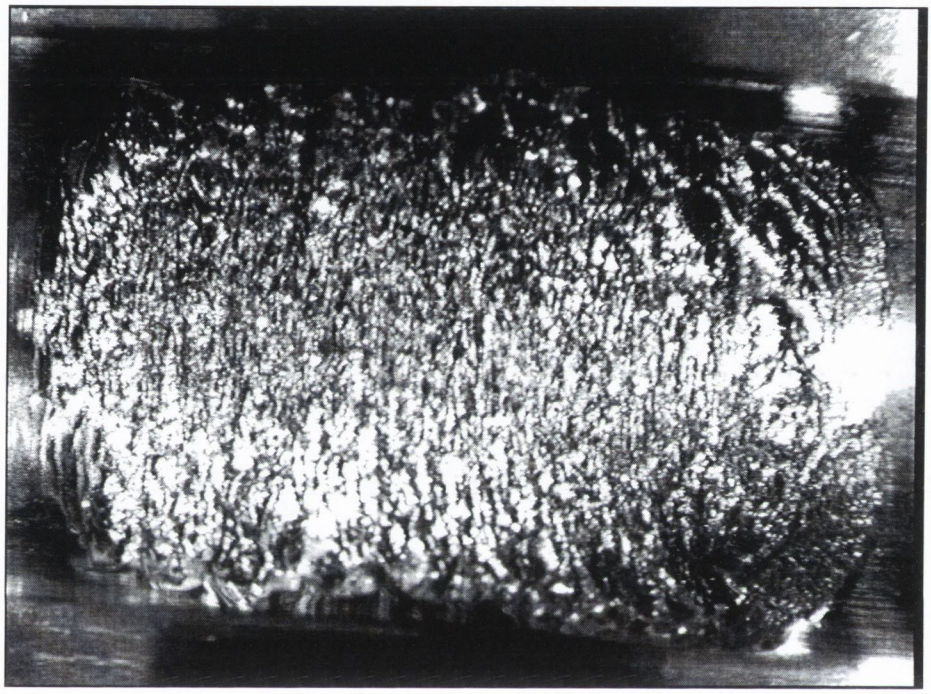

Figure 5.11 Subsurface initiated large oval spalling on inner ring (Volvo 97305) (39 hrs)

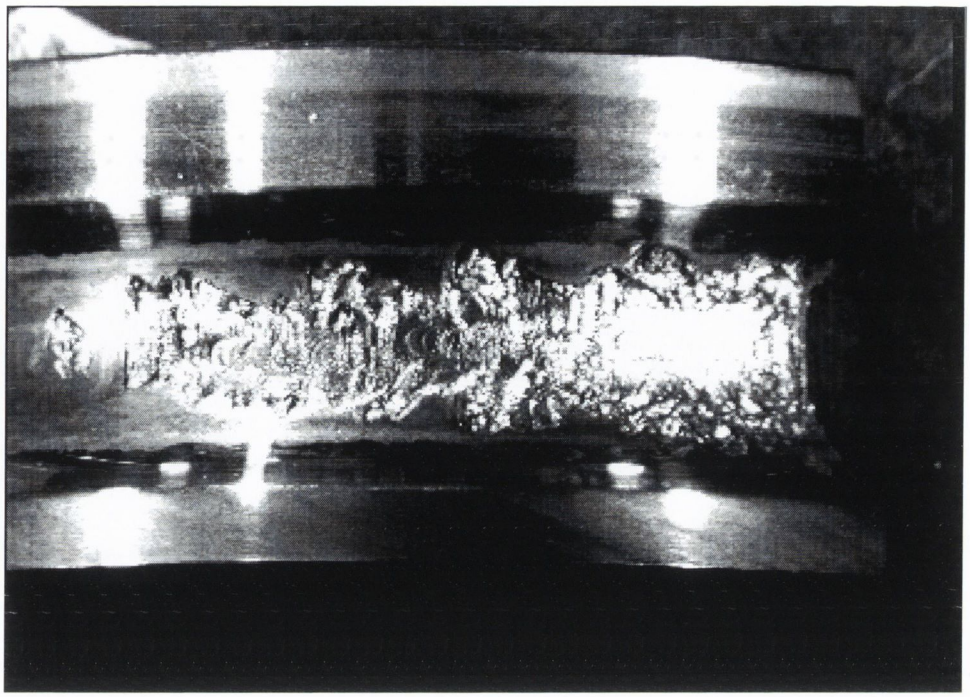

Figure 5.12 Subsurface initiated damage, bulk crack through inner ring (Volvo 97305) (1700 hrs)

5.4.4 Failure modes with Volvo 97307 oil - R2F tests

Fretting was again found in the inner bore, causing cracking and eventual failure by large spall formation. Figures 5.13 and 5.14 show similar damage to that seen using the Volvo 97305. The damage spans the width of the inner ring track which is 12 mm. Figure 5.15 shows a schematic diagram of the crack growth to the surface and the subsequent ball over-rolling of the through crack leading to the spalling found. Subsurface damage was seen in four inner rings and one ball from the Volvo 97307 tests. Sludge formation was not found with these oils.

Originally set-up problems were blamed for the unusual failure modes. It was thought that the shafts of the test rigs were made with a lower hardness than specified. Other test results have been uncovered that show that the shafts involved in testing the Volvo oils behaved normally. It has been concluded that the oil probably contributes to this failure mode.

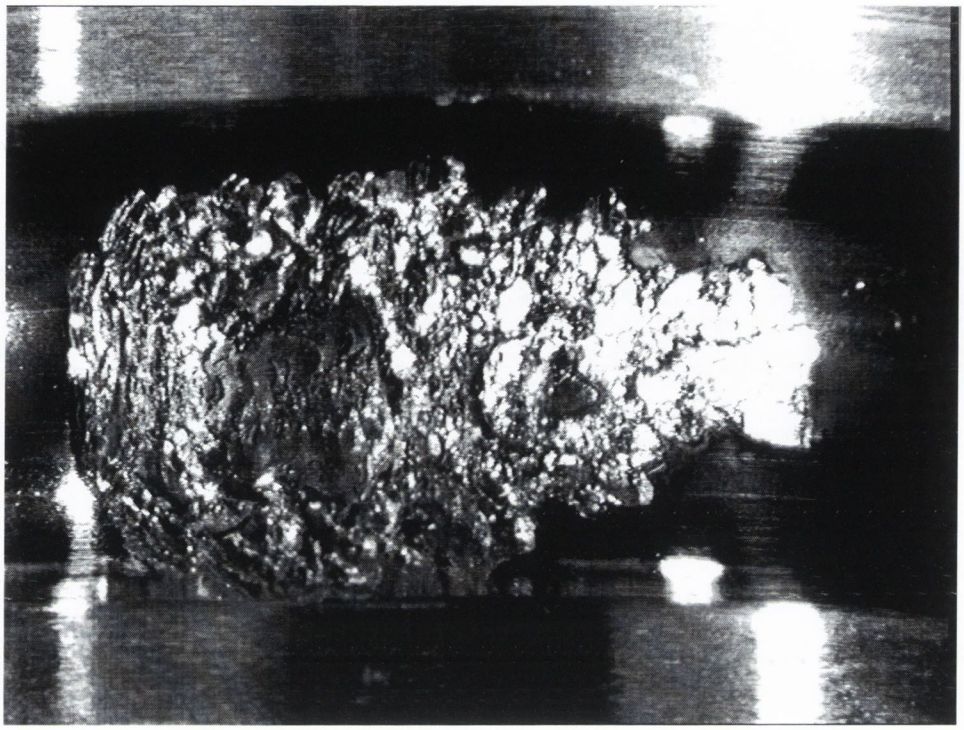

Figure 5.13 Fretting from inner bore causing large spall (Volvo 97307) (382 hrs)

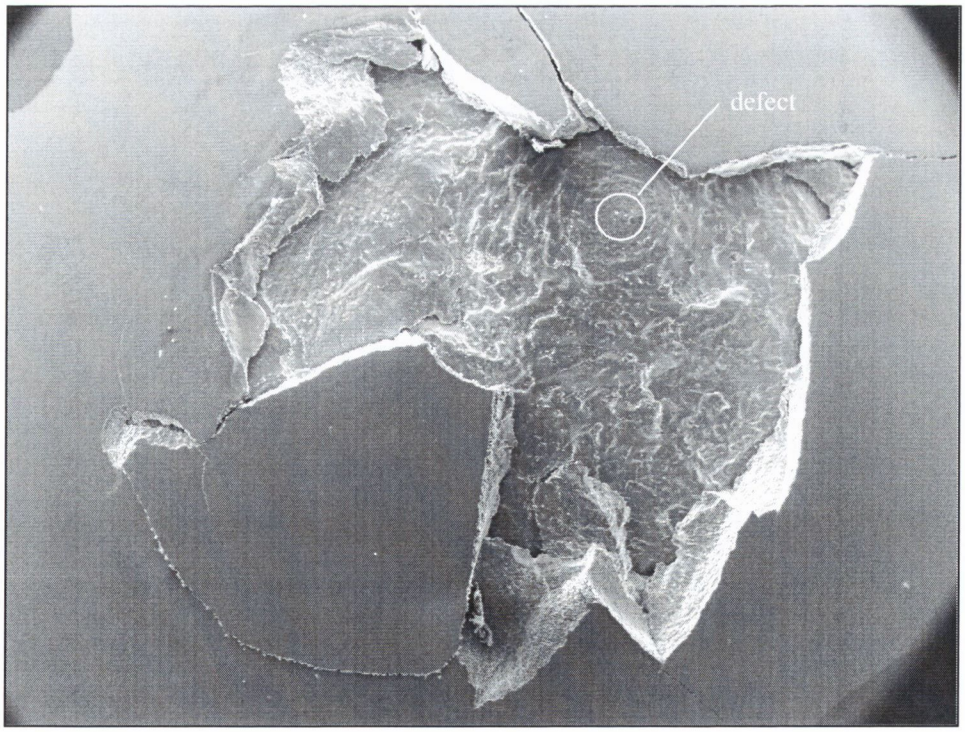

Figure 5.14 Subsurface initiated damage on rolling element (Volvo 97307) (575 hrs)

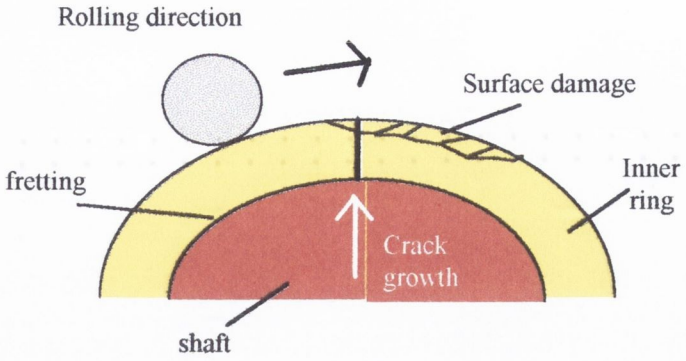

Figure 5.15 Schematic diagram of catastrophic damage caused by Volvo oils

Figure 5.15 represents the failure mechanism seen when using the Volvo oils. Bulk cracking of the inner ring is caused by fretting at the shaft. Subsequent surface damage was caused by the balls rolling over the crack. Debris is removed in stages, the pit grows mainly in the rolling direction with a small amount of pit removal on the near side of the crack.

5.4.5 Failure modes with Spirax AX 80W-90 oil - R2F tests

Using Spirax, half of the failures investigated were found to originate in the subsurface region, and four occurred on inner rings. For the remaining failures two surface initiated and two subsurface initiated spalls were found on the rolling elements. The surface initiated spalls on the balls were found to occur near indent defects. Surface initiated damage is characterised by a v-shaped spalling, usually arising from one of three types of defects:

a) Nicks: Damage on balls typically, which usually occurs during manufacturing or assembly.

b) Fragmented: A defect caused by hard particles. The surface is normally spotted because of the contact with the hard particles, for example hard particles from grinding or sand in oil.

c) Smooth: Defects caused by particles softer than bearing steel.

Figure 5.16 shows subsurface initiated damage on an inner ring causing the deep spall across the top quarter of the photo. The rolling direction in this instance is top to bottom. The second photo, Figure 5.17 shows a subsurface spall with the rings or semi-circles showing propagation from axis A-A. There is possible secondary surface initiated damage starting at the leading edge, point B. Rolling element failures were

not seen when base oil alone was used as the lubricant. This phenomenon is suspected by the bearing industry to be one of the factors contributing early failures in bearings.

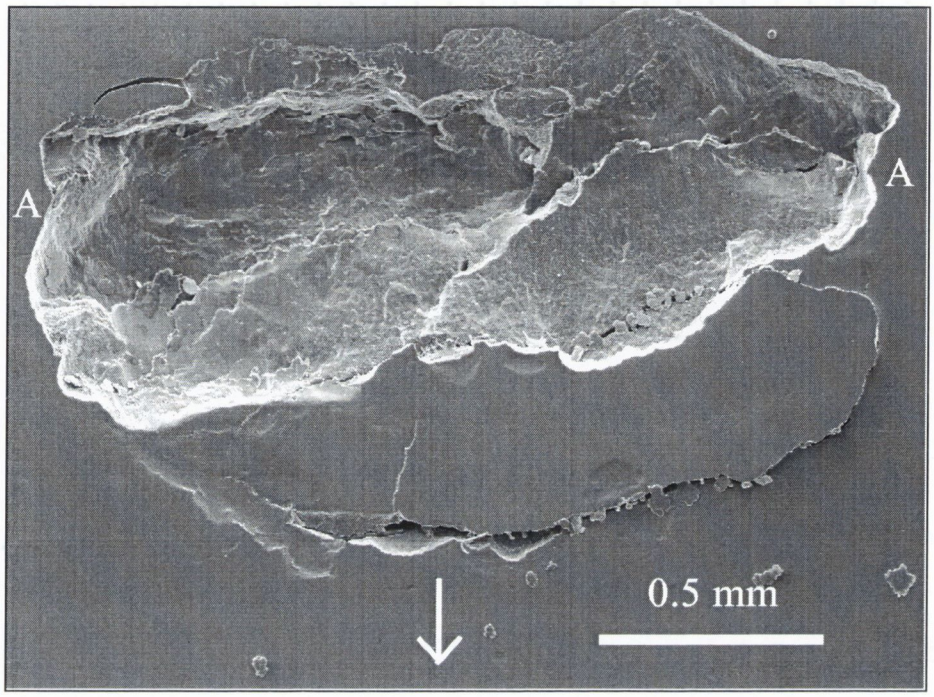

Figure 5.16 Deep subsurface spall on outer ring (SPIRAX) (209 hrs)

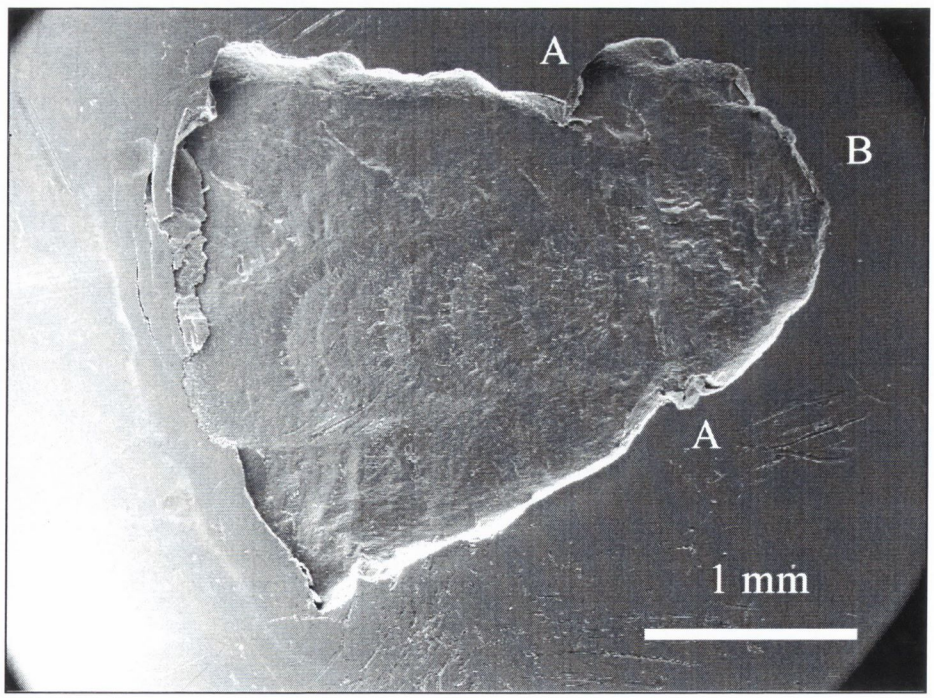

Figure 5.17 Subsurface initiated pit on inner ring (SPIRAX) (780 hrs)

5.5 SUMMARY OF FAILURE DATA

A summary of the fatigue results with the L_{10} and L_{50} lives is given in Table 5.6. The upper and lower 90% confidence intervals are also shown to help discuss differences caused by the test additives. A detailed summary of the statistical results is listed in Appendix (C). For the Bristol results the L_{50} upper CI for the Vitrea and Vitrea + 5% is lower than the Lower CI for Spirax oil. Looking at the L_{10} values there is no CI overlap between Vitrea + 5% and Spirax. There is a small overlap between the Vitrea neat and Spirax. This is evidence that under this set of condition Spirax does enhance bearing life.

TEST RIG	LUBRICANT	No.	L_{10}			L_{50}		
Bristol	Vitrea M100	12	74	130	226	221	297	398
Bristol	Vitrea + 2 % S/P	12	96	172	309	294	393	525
Bristol	Vitrea + 5 % S/P	12	54	105	204	199	282	401
Bristol	Spirax AX 80W 90	12	219	320	467	445	532	635
ERC R2F	TT 68	7	180	369	575	557	798	1144
ERC R2F	Volvo 97305	8	5	36	247	125	328	842
ERC R2F	Volvo 97307	7	66	250	942	523	990	1871
ERC R2F	Spirax AX 80W 90	13	24	72	212	206	357	618

Table 5.6 Summary of Weibull distribution parameter estimates 90% confidence interval with lower and upper limits

In the R2F tests the confidence intervals were quite large, making overlaps inevitable. The base oil TT68 and the Volvo 97305 produced longer lives than the Spirax and Volvo 97305. As discussed earlier the Volvo 97305 tests were strongly influenced by the sludge contamination in the oil system. In a case like this it is difficult to compare results as the tests were not carried out under identical conditions.

5.6 CHANGES IN SURFACE ROUGHNESS IN BRISTOL TESTS

The ground races used in the Bristol tests were found to have a more polished surface after testing. This polishing had the effect of increasing the lambda ratio thus making running conditions less harsh by a type of "running-in" period. To quantify the change in the roughness, measurements were made using a "Zygo" scanning white-light interferometer. A reference unused bearing was tested first to check the manufacture's claims that the original roughness was 0.5 μm cla. The series of bearings examined and their running times are listed in Table 5.7.

	test number	lubricant	Test time (hrs)	Average Ra (μm)
1	-	-	0	0.442
2	N14	Vitrea	719	0.216
3	N26	Vitrea + 2%	719	0.139
4	N20	Vitrea + 5%	422	0.208
5	N45	Spirax AX	654	0.208

Table 5.7 Roughness measurements of selected bearings

Examples of the 3-D surface profile are shown below in Figures 5.18 and 5.19. The instrument uses a function that flattens the 0.27 mm by 0.36 mm scanning area of the wear track. The roughness values for the used bearings range from 0.45 to 0.20 (μm). This change in roughness causes a change in the Lambda ratio for the Bristol tests. Suggestions have been made that the polishing process occurs quite rapidly, maybe in the first hour. This may be the case, but since none of the tests failed inside a comparatively short period it was not possible to check.

Since the surface roughness has effectively halved, it is likely that the asperities above the average line have been worn away and the valleys remain accounting for the roughness.

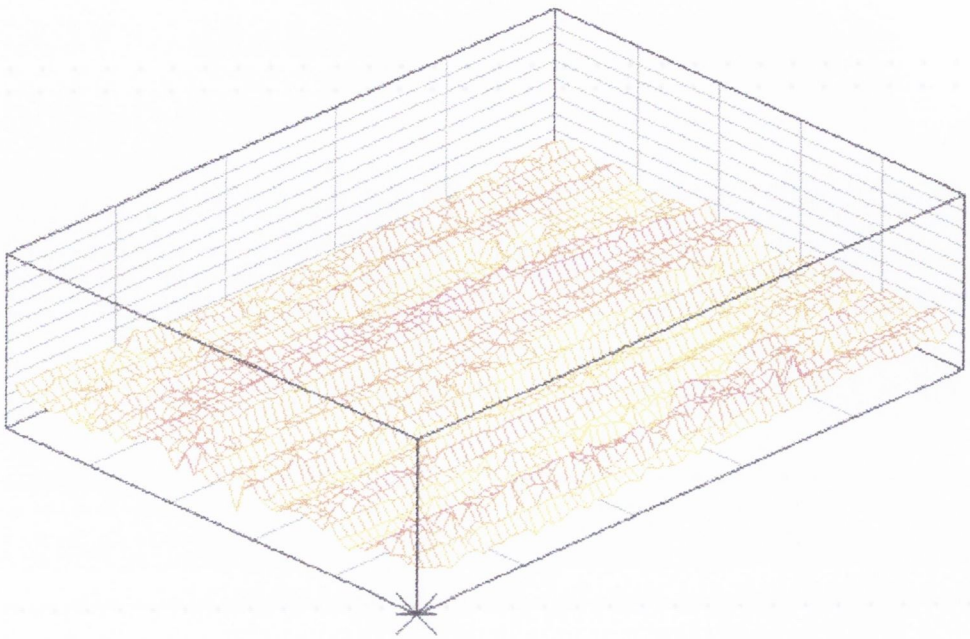

Figure 5.18 3-D surface roughness profile of untested ground raceway

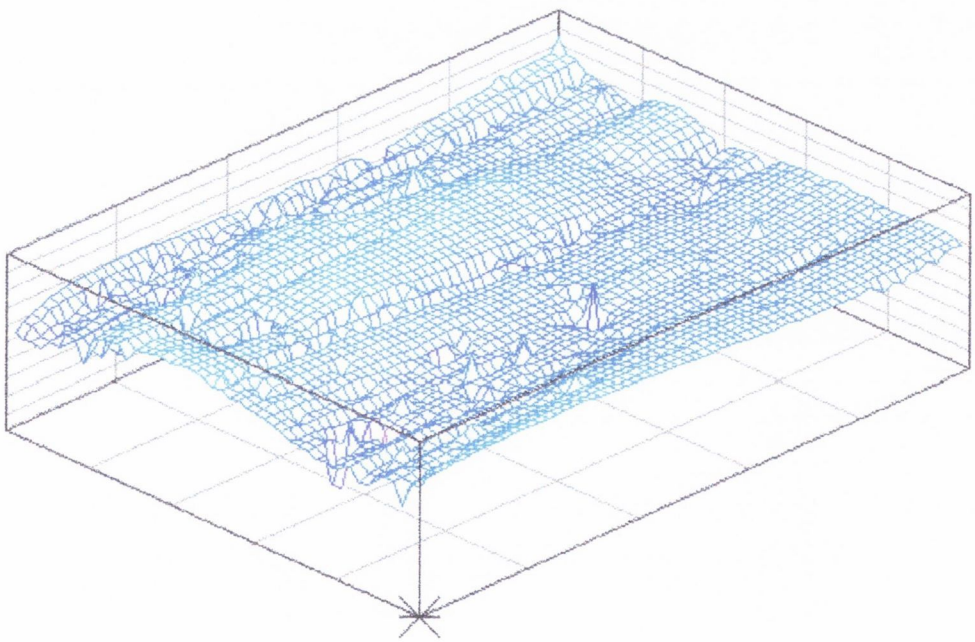

Figure 5.19 3-D surface roughness profile of raceway tested for 719 (hrs) with Vitrea+2% (S/P) polishing is evident

5.7 FTIR ANALYSIS OF OILS

Two FTIR analyses were undertaken as part of this project to identify changes in the lubricants used in fatigue testing. The first was to identify whether there had been any oxidisation of the oils used in the Bristol rigs during testing. The second analysis investigated the sludge found in the oil system of the R2F rigs when Volvo 97305 was used. Table 5.7 lists five oils samples taken from the Bristol rigs and tested for oxidation. Oils 1 and 3 had been used for a period of one week before samples were taken. A characteristic peak for the Lubrizol LZ5034A additive was found in the oil samples at 1749 cm^{-1}, shown in Figure 5.20. This band was likely to be caused by sulphurized esters. The peak is higher in the 5% oil than the 2% oil. After the oils have been tested for 4 weeks the oxidation peaks were seen to increase. The oxidation levels were found to be generally low, with oxidation levels increasing with higher S/P concentration.

	Lubricant
1	Vitrea + 2% (S/P)
2	Vitrea + 2% (S/P) + 4 weeks
3	Vitrea + 5% (S/P)
4	Vitrea + 5% (S/P) + 4 weeks
5	Lubrizol LZ5034A - additive package

Table 5.7 Oils tested for oxidation using FTIR analysis

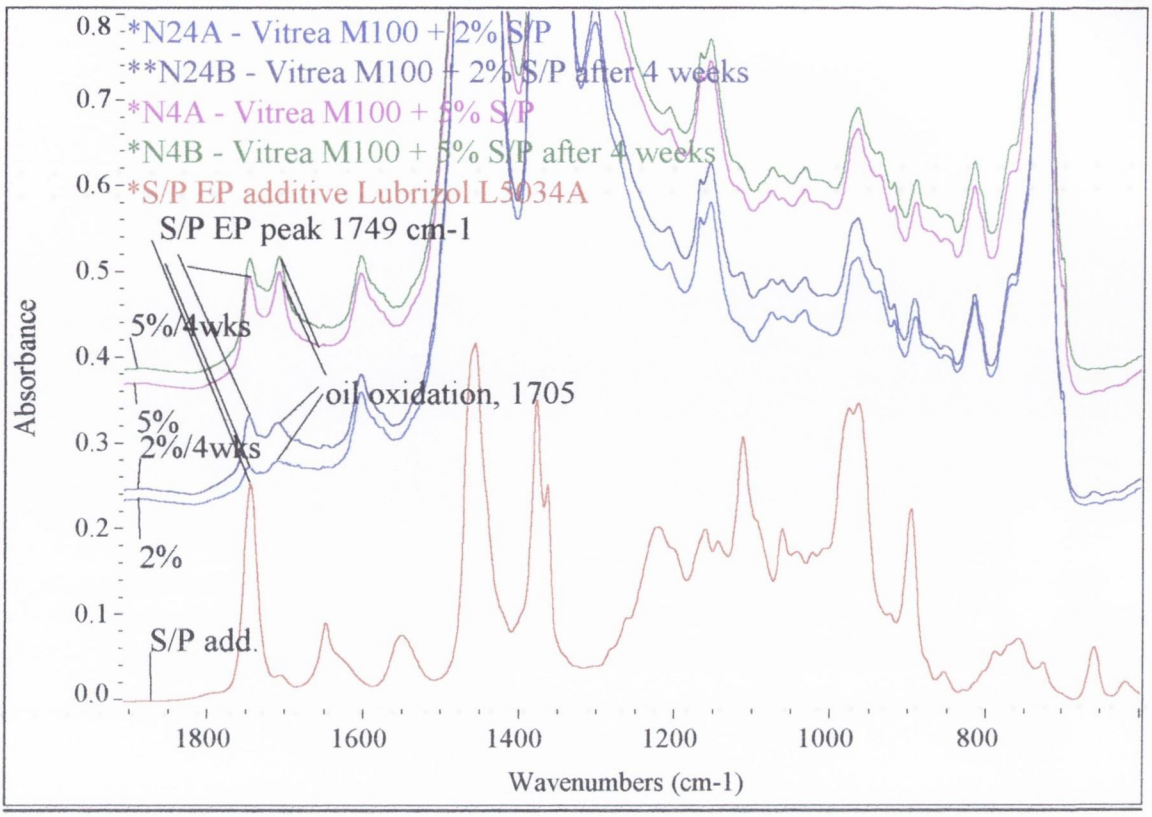

Figure 5.20 FTIR analysis on Bristol oils

5.7.1 Examination of sludge from Volvo 97305 tests

The Volvo 97305 produced a sludge in the oil system of the R2F rigs during testing. A study was undertaken to identify its components. The sludge was divided into several components for inspection. Part of the sludge was dissolved in petroleum ether. The dispersion was filtered over normal filter paper yielding a powder residue. A part of the sludge did not dissolve and stayed behind in the container. This was called the non PE soluble part. The PE was separated by vacuum evaporation of the solution resulting in a residue - the PE soluble part. The separated parts: the powder, the PE soluble part and the PE non soluble part, were analysed by FTIR. The PE soluble part consists mainly of oil. The non PE soluble part contains a mixture of soot and acid like material. The powder is a mixture of iron oxide and decomposition products of ZDDP. The decomposition was probably caused by high temperatures (>130 °C).

5.8 CONCLUSIONS

Bristol failures were caused by surface distress and micro-pitting of the inner raceway and rolling element respectively. These types of failures were seen whether additives were or were not used. Micro-pitting on the balls could have been caused by hard particles becoming stuck in the loading sleeve. Circular pitting could indicate that the ball was spinning on an axis in contact with the sleeve.

Spirax AX 80W-90 was seen to improve the life of the bearings in comparison to the Vitrea solutions, seven out of twelve tests were suspended after a time limit of 4 weeks. If the suspended tests are taken as suspended in the Weibull analysis then the confidence intervals tend to get large. The only way to get a proper result would have been to test to failure.

In the R2F tests, rolling elements did not fail when base oil alone was used. The mode of failure for the TT68 oil was found to be the classical subsurface spalling associated with non-metallic inclusions. Spirax produced failures in both the inner rings and the rolling elements. It looks as though Spirax reduced life in these conditions.

The Volvo oils produced uncharacteristic failure modes, fretting at the inner bore caused bulk fractures to propagate to the surface of the inner ring. Subsequent over-rolling by the balls caused very large spalls to form. The Volvo 97305 oil produced a large quantity of sludge in the system. The lives of the bearings were seen to reduce rapidly as the contamination of the lubricant increased. Oil interaction between the test shaft and the inner bore of the bearing could influence the premature failures.

5.9 SUMMARY

Twelve 6305 ground DGBB inner rings were tested to fatigue using the Bristol rigs with each of the following oils, Vitrea (base oil), Vitrea + 2% (S/P), Vitrea + 5% (S/P) and Spirax AX 80W-90. The initial lambda ratio was low at the start of these tests with a value of 0.4. Spirax was seen to increase the life to failure of bearing under these conditions.

The failure modes of the Bristol rig included pitting/spalling caused by surface distress on the inner rings. This was to be expected considering the contact conditions. Micro-pitting was found on the rolling elements. No distinct failure modes were seen for any specific single lubricant.

Tests were carried out at SKF ERC with the R2F rig with 6309 bearings, various tests were done with TT 68, Volvo 97305, Volvo 97307 and Spirax AX 80W-90. The stress conditions for these tests were more severe than in the Bristol rigs. The failure modes in both Volvo oils were unusual, fretting on the inner bores caused bulk cracking in the inner rings. Subsequent over-rolling of this crack led very large spalling.

Comparing the two sets of results, the Spirax oil appeared to increase the bearing life in the boundary lubrication regime of the Bristol rigs. In the R2F tests the Spirax caused a decrease in life. This curious effect has been seen before, as described in Chapter 2, where the operating conditions dictate whether a lubricant is beneficial to life or not. If these trends are genuine then there is no need to use this type of additive where metal-to-metal contact does not take place. The decomposition products, discussed in Chapter 6, associated with additive decay probably contaminates the contact precipitating premature failures. Evidence of this was seen with the Volvo 97305 oil.

5.10 SPECIAL ACKNOWLEDGEMENTS

Bearing failure modes were examined at the electron microscopy unit in TCD. Images were also taken at SKF ERC. Examinations of these micro-graphs were carried out with Mr. Gunner De Wit from the endurance testing section at SKF-ERC. His expertise, in the investigation to identify failure modes, was well appreciated.

Many thanks to Mr. Albert v.d. Kommer who carried out the FTIR analysis also at SKF-ERC.

CHAPTER 6

6 HOT-WIRE RESULTS

6.1 INTRODUCTION

It is generally accepted that the beneficial properties of additives are linked to their chemical reactivity with metals. The results of the hot-wire reactivity tests are presented in this chapter. As discussed in Chapter 4, a hot-wire rig has been developed using a new two-wire system and modern data logging equipment. This chapter will outline the test program and try to make some conclusions about the relative reactivities of the oil used in the fatigue tests.

The majority of the tests were carried out over a period of 10 minutes at temperatures between 300 °C and 450 °C. The 300 °C test denoted the lower temperature limit at which corrosion reactions could be detected by this method. Reaction films were found at lower temperatures as seen in EP immersion tests. The passivation of reactions due the build up of product films was found to be a major factor effecting corrosion.

The nature of the reaction products formed by the hot-wire tests were examined using SEM. In addition, the elemental content of these films was examined using EDAX. The corrosion of the wires was calculated by measuring changes in wire resistance. Some of the reactions were found to follow the parabolic law of reaction. In these cases the Arrhenius equation could be used to process the results. Using the Arrhenius equations the activation energies were calculated giving further information on the corrosion/diffusion mechanisms.

6.2 HOT-WIRE TESTING

The tests described below were undertaken to investigate the reactivities of additives on metal surfaces. Reaction films on bearing surfaces are difficult to analyse because the rolling and sliding actions can damage and remove them as they form. The hot-wire test is a static test where the film remains on the surface. One disadvantage with this is that the build up of the film can slow down the reaction. The temperature range of the reactions is lower than has been tested before. The maximum temperature used was 450 °C, which is close to the lowest temperature used by Barcroft and Sakurai.

6.2.1 Preliminary testing using the two wire rig

Initial tests were made to get a general feel for the scale of reactions over a wide range of temperatures. A test plan was devised to test reactivity of five oils at temperatures of 140 °C, 300 °C and 450 °C. Tests were carried out for a period of three hours using the stainless steel and iron wire. At 140 °C corrosion was not recorded, the temperature was found to be too low to cause corrosive reactions on the wire surface. Reaction films did form on some of the wire surfaces, and the results were backed up by what was found with the EP immersion tests. A description of the EP immersion tests is presented in Appendix (D).

Tests at 300 °C showed that corrosive surface reactions were starting to occur. Larger reaction films formed on the surfaces and small amounts of corrosion were recorded. 300 °C was found to be the lowest temperature at which the corrosion reactions could be detected. At 450 °C the lubricant reacted readily with the wires, especially on the iron wire which was seen to be aggressively attacked by the Volvo 97305 oil and Spirax AX 80W-90. Corrosion was severe in both cases and the iron wire was attacked locally causing the wire to break across the section of the wire. This caused the tests to be suspended prematurely. The results of the 450 °C tests are plotted in Figures 6.1 and 6.2, for iron wire and stainless steel respectively. As expected, the iron wire with 99.5% purity reacted more readily than the stainless steel.

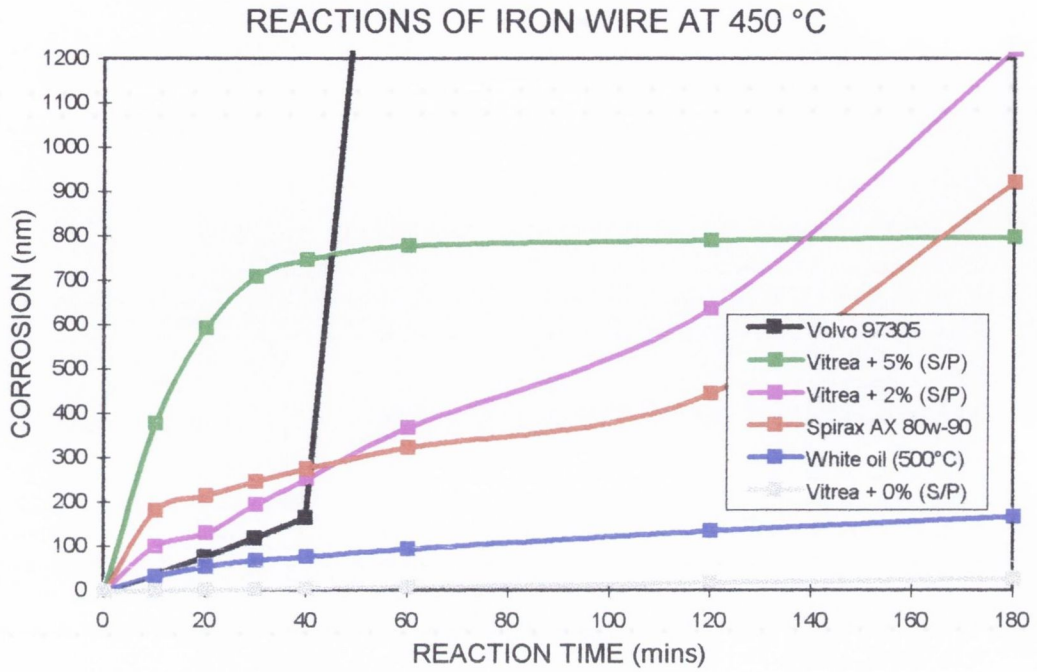

Figure 6.1 Three hour tests at 450 °C for iron wire

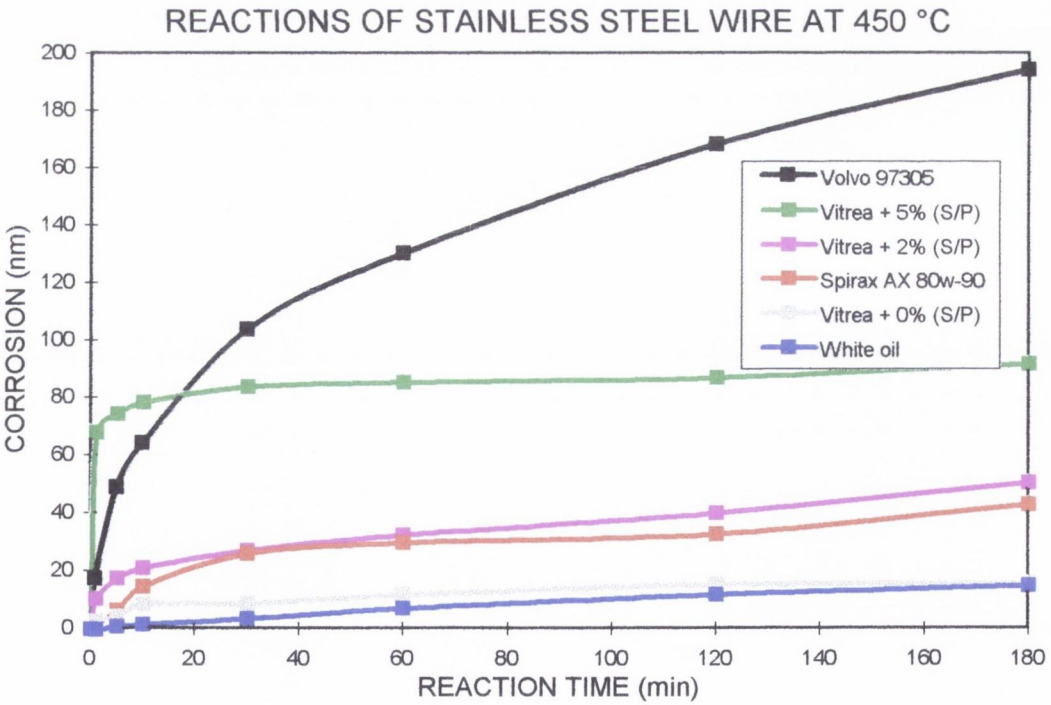

Figure 6.2 Three hour tests at 450 °C for stainless steel

6.2.2 Results of 3 hour tests at 450 °C

The iron wire was seen to react readily with the Vitrea + 5% (S/P) and the Volvo 97305 oil. In the case of the Volvo oil there was a localised attack on the wire. Caution must be shown when looking at such results because the second hot-wire test assumption is broken. The second assumption states that the corrosion must to be uniform over the entire length of the wire. Rapid increases in reactions may be caused by two things, (a) a grain boundary defect in the metal or (b) a kink in the wire. In both cases, corrosion is concentrated leading to high changes in resistance. The White Oil and Vitrea neat oils were found to be relatively unreactive as they do not contain additives to cause reactions. The Vitrea + 2% (S/P) and the Spirax reacted similarly over the 3 hours. For these oils, there was an increase in the rate of corrosion between hours 2 and 3, and rapid reactions started to occur.

Corrosion on the stainless steel wire for the 6 oils can be divided into three groups. The Volvo oil and the Vitrea + 5% (S/P) are very reactive, the Vitrea + 2% and the Spirax show a moderate corrosion and the White Oil and the Vitrea neat are fairly unreactive. None of the wires broke like in the tests with the iron wire. Reactions were split into the under 20 (nm), around 40-50 (nm) and over 80 (nm) ranges respectively.

6.2.3 Test plan for subsequent testing

After reviewing these results the decision was made to concentrate on reaction temperatures between 300 °C and 450 °C in 25 °C degree increments for periods of 10 minutes. Table 6.1 shows the series of tests carried out on the wires. This test program was repeated for annealed iron and stainless steels.

The 10 minute tests were divided into 6 reaction periods of 15, 15, 30, 60, 180 and 300 (sec). Short steps were taken over the initial part of the reaction as the reactions were seen to be higher at this time. The 6 subdivisions were needed to allow resistance measurements and corrosion calculations during the test. Test baths were allowed cool for 15 minutes between each reaction phase to allow the temperature of the oil to settle.

TEST OIL	REACTION TEMPERATURE (°C)						
Vitrea + 0% (S/P)	300	325	350	375	400	425	450
Vitrea + 2% (S/P)	300	325	350	375	400	425	450
Vitrea + 5% (S/P)	300	325	350	375	400	425	450
Spirax AX 80W-90	300	325	350	375	400	425	450
Volvo 97305	300	325	350	375	400	425	450

Table 6.1 The 10 minute test program for iron and stainless steel wires

6.3 RESULTS OF 10 MINUTE TESTS WITH IRON WIRE

Tests were carried out using iron wire for a period of 10 minutes at 25 °C increments between 300 °C and 450 °C. The temperatures presented in the following section are colour coded and shown in Table 6.2.

Red	Yellow	Green	Brown	Blue	Pink	Black
300 °C	325 °C	350 °C	375 °C	400 °C	425 °C	450 °C

Table 6.2 Colour code of temperatures used in hot-wire tests

The accuracy of the corrosion measurement is conservatively estimated to be about ±5 (nm). Figure 6.7 is an example of where measurement of small amounts of corrosion can cause the graph to jump above and under the zero corrosion line. In other graphs for reactions at 300 °C these small "negative" corrosion measurements have been rounded off to zero.

6.3.1 Vitrea M100 on iron wire

The first set of results, shown in Figure 6.3, is for Vitrea base oil on iron wire. Corrosion was found to increase steadily with temperature. The reactions follow a parabolic growth law. In this instance the Arrhenius equation can be applied to calculate activation energy of the reaction. The red line indicates that corrosion is not detectable at 300 °C. A thin reaction products film was seen at this temperature. The reactions between 325 °C and 375 °C are low, under 50 (nm). A maximum corrosion of 340 (nm) was found at 450 °C.

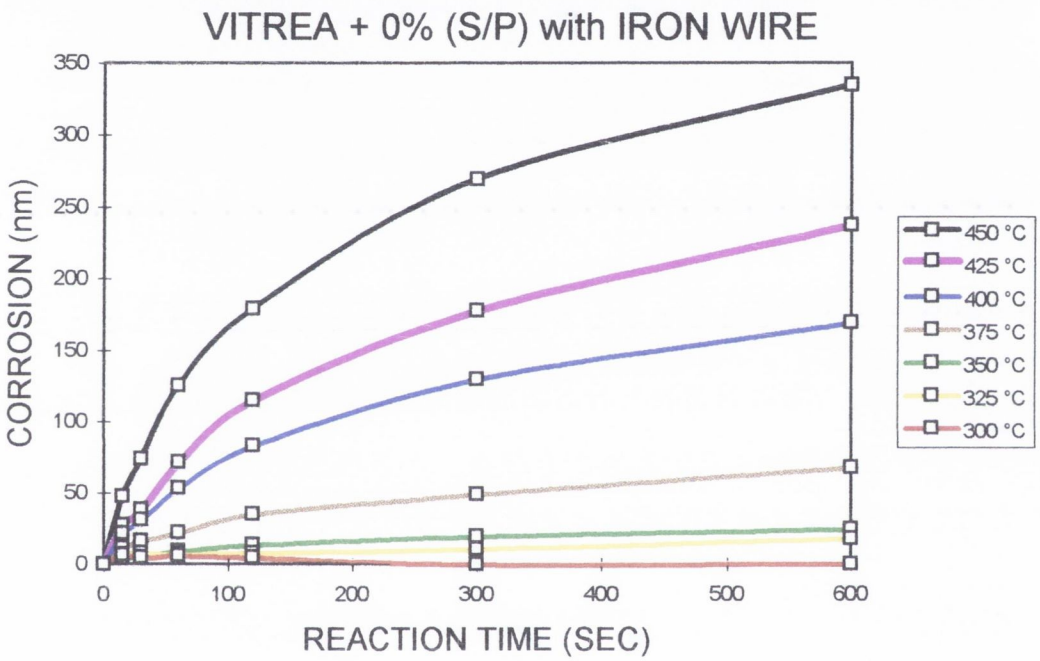

Figure 6.3 Corrosion of iron wire reacted with Vitrea + 0% S/P

Inspection of the reacted wire surfaces showed low film growth. The reaction was therefore not slowed down by this very small product film formation. This is characteristic of hot-wire reactions where additives are not present. The depth of corrosion is large compared to reactions with some additive concentrations. Passivation effects are not found when additives are not used. Relating this to dynamic testing at high temperatures, neat oil will produce less contamination compared to oils with additives under the same temperatures conditions.

6.3.2 Vitrea M100 + 2% (S/P) on iron wire

The second series of tests on iron wire used the oil combination Vitrea + 2% (S/P) additive package. Initial corrosion is high at temperatures of 400 °C, 425 °C and 450 °C. As the fast reactions occur films are formed which effectively protects the wire from further reactions. Therefore reactions at high temperatures slow down more rapidly. Conversely the reactions at lower temperatures initially start slowly and continue to react as the test proceeds. Reactions at 300 °C, 325 °C and 350 °C are all higher than when the base oil is used. After a slow start in the first two minutes, the reactions steadily get faster, with the final reaction rates increasing with increased temperature. It is clear that these reactions would continue if the test had been allowed to proceed..

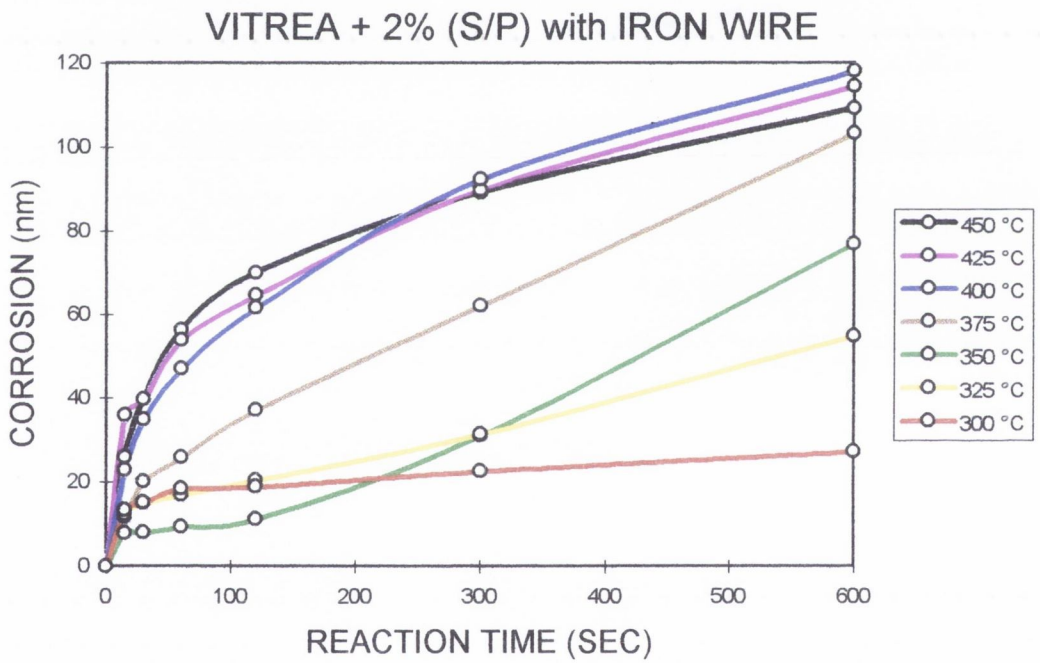

Figure 6.4 Corrosion of iron wire reacted with Vitrea + 2% S/P

The maximum corrosion thickness over the 10 minutes was 120 (nm) which is three times lower than with base oil. The temperature of maximum reaction is 400 °C. The reaction film thicknesses were seen to increase as a consequence of using additives in the oil. As the amount of products on the film increases, the ability of the oil to cause corrosion on the wire decreases. The reaction products produce a barrier through which reactions must occur.

6.3.3 Vitrea M100 + 5% (S/P) on iron wire

Figure 6.5 shows the corrosion that takes place on iron with Vitrea + 5% (S/P). With the increase in additive concentration, faster reactions occur than with Vitrea + 2% (S/P). There are two distinct reaction modes seen under these conditions. The lower temperatures 300-350 (°C) show a slow steady linear reaction that looks to be continuing after the 10 minutes. At the higher temperatures corrosion is initially fast over the first 120 seconds and then a passivation of the reaction occurs.

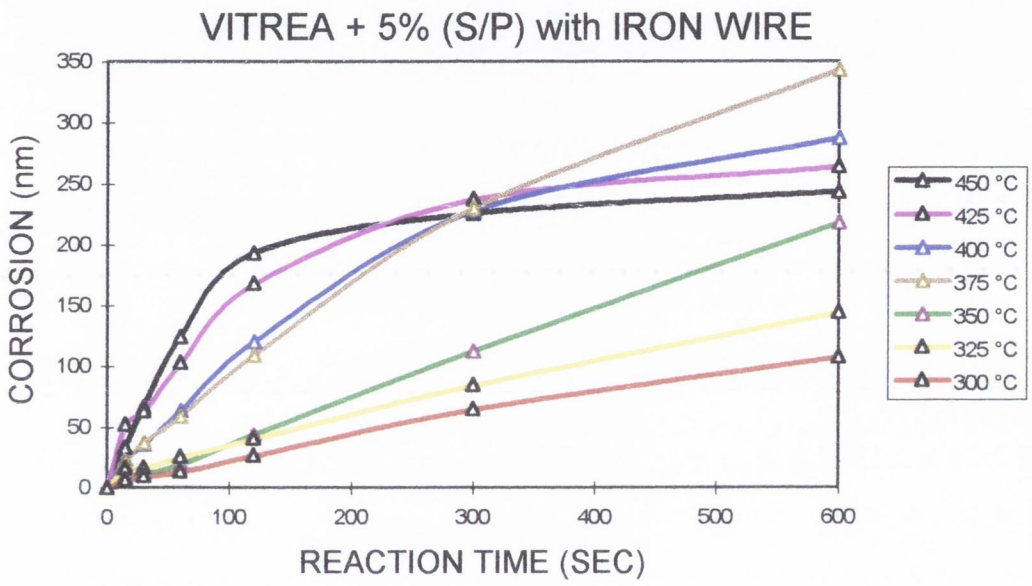

Figure 6.5 Corrosion of iron wire reacted with Vitrea + 5% S/P

The passivation is thought to be controlled by the formation of a thick (over 5 μm) reaction products film on the surface. The thickness of the film causing passivation could be much smaller. Maximum corrosion 350 (nm) occurs at 375 °C where there is a balance between the rate of corrosion and film formation. The maximum overall reactions are very similar to the tests with Vitrea neat oil. The lower temperature reactions are very different. For the four lower temperatures the reactions rates are about 7 times greater.

6.3.4 Spirax AX 80W/90 on iron wire

Figure 6.6 shows the corrosion plot for Spirax AX 80W-90. The Spirax oil was seen to react very rapidly with iron wire. Over 90% of the total reaction was completed in the first 60 seconds of the test. In the case of the highest temperatures the reaction was over even faster. A maximum corrosion of 260 (nm) was observed at temperatures of 425°C and 450°C. This value was slightly lower than that found in the Vitrea/Lubrizol mixtures but the rate of initial corrosion was much higher.

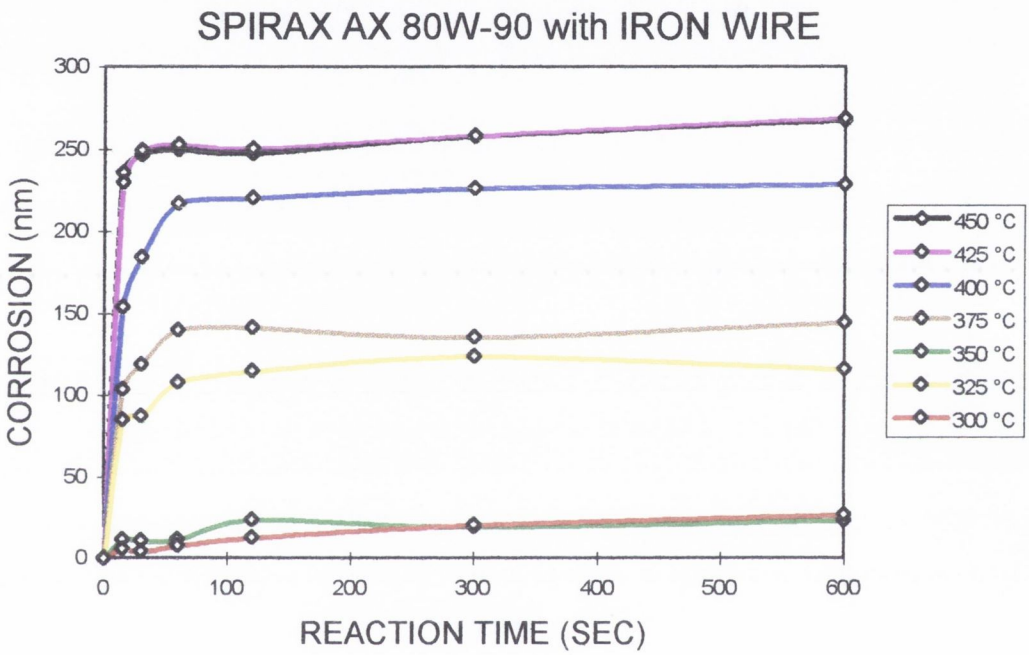

Figure 6.6 Corrosion of iron wire reacted with Spirax AX 80W-90

The reaction films were thicker in this case than for any other oil tested. The reason for a faster reaction at 325 °C than at 350 °C is not clear. The 325 °C wire may have undergone some type of localised attack or an initial temperature spike when the power was applied, giving a faster than expected reaction. The second explanation is unlikely as care was taken to limit the initial power surges avoiding such occurrences. The ability of Spirax to cause a fast initial reaction could be the key to it being a successful lubricant, as worn surfaces very quickly have films formed on them. On the other hand, if there are harsh rubbing conditions and the reaction film is being constantly removed, the metal surface faces a constant aggressive attack. This danger zone is possibly a breeding ground for premature failures.

6.3.5 Volvo 97305 on iron wire

The Volvo 97305 oil was the least reactive of the five oils tested with iron wire. The tests were repeated twice and the random scatter was seen again. Results with large scatter have been reported for various metal-oil combinations but trends can not usually be drawn from the results. This sort of trend was seen by Barcroft with EP additives, containing phosphorus as the only active element, were used. The reactions here are just 10% of that observed with Vitrea neat or Spirax on iron. Reactions at some temperatures hover around the zero reaction level, this can be seen in the way the yellow and pink lines goes above and below the x-axis.

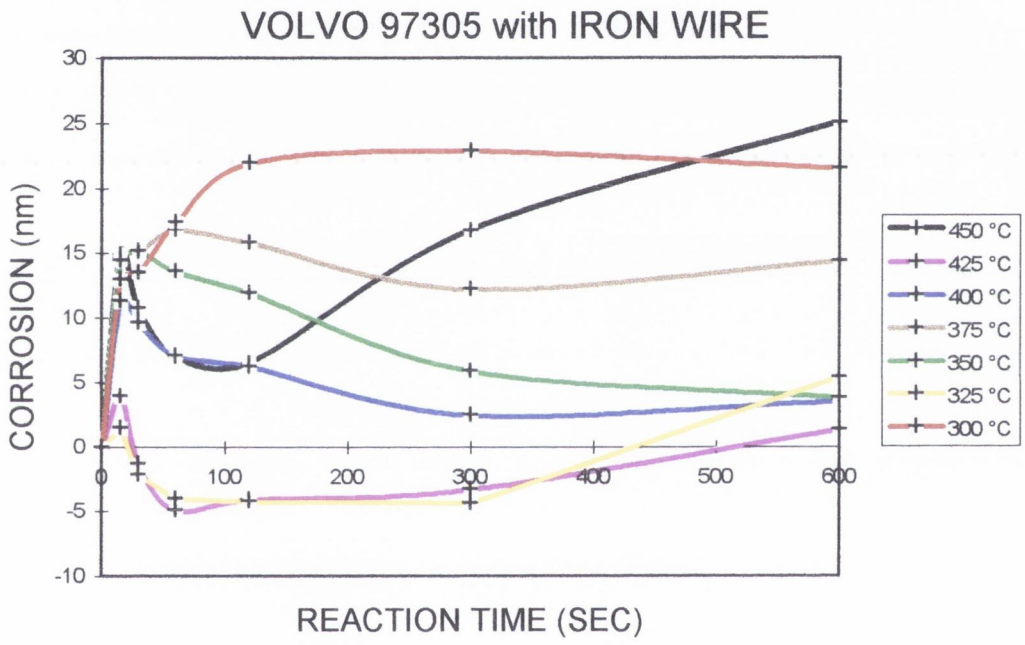

Figure 6.7 Corrosion of iron wire reacted with Volvo 97305

The reaction products on the surface were unique to the main test program. The reaction film was composed of two visibly different layers. The typical black layer was present coating the wire and over this there was a pale orange/brown as an outer coating. A number of tests where carried out using a Vitrea/Exxon Paranox 16 mixture. This ZDDP additive produced a deep red outer layer over the inner black layer. The potential for identifying unknown additive blends by examining their reaction films is discussed in Chapter 7.

6.4 RESULTS OF 10 MINUTE TESTS WITH STAINLESS STEEL

The series of tests, from Table 6.1, were repeated using the five oils on the stainless steel. Stainless steel has an electrical resistivity seven times greater than the iron wire. The typical initial resistance of the stainless steel wire is around 10 Ohms. Therefore changes in resistance per unit corrosion depth are seven times greater than in the iron wire. This makes the changes in diameter easier to measure as they are nearly an order of magnitude greater. Stainless steel, however by its nature is more resistant to surface attack. The overall effect is that the corrosion depth is generally smaller than in the iron wire but the measured resistance change is higher. The alloying elements of 302 stainless steel are shown in Table 6.3. The electrical properties of iron and stainless steel are given in Table 6.4.

Fe	Cr	Ni	Mn	C
71%	18%	8%	2%	trace

Table 6.3 Chemical composition of 302 Stainless Steel

	Resistivity (Ω.m) @ 20 °C	Temperature co-efficient (K^{-1})
Iron	10×10^{-8}	0.0065
Stainless steel	70×10^{-8}	0.0012

note: temperature co-efficient between 20-100 °C

Table 6.4 Electrical properties of iron and stainless steel

6.4.1 Vitrea M100 on stainless steel

Very small reactions were found with Vitrea + 0% (S/P), the average maximum corrosion was less that 3 (nm) which is close to the sensitivity limit of the instrumentation. With the exception of 450 °C test that showed the only sign of developing a reasonable corrosion depth, this oil/metal combination can be regarded is unreactive. The reaction of base oil on stainless steel does not cause significant corrosion.

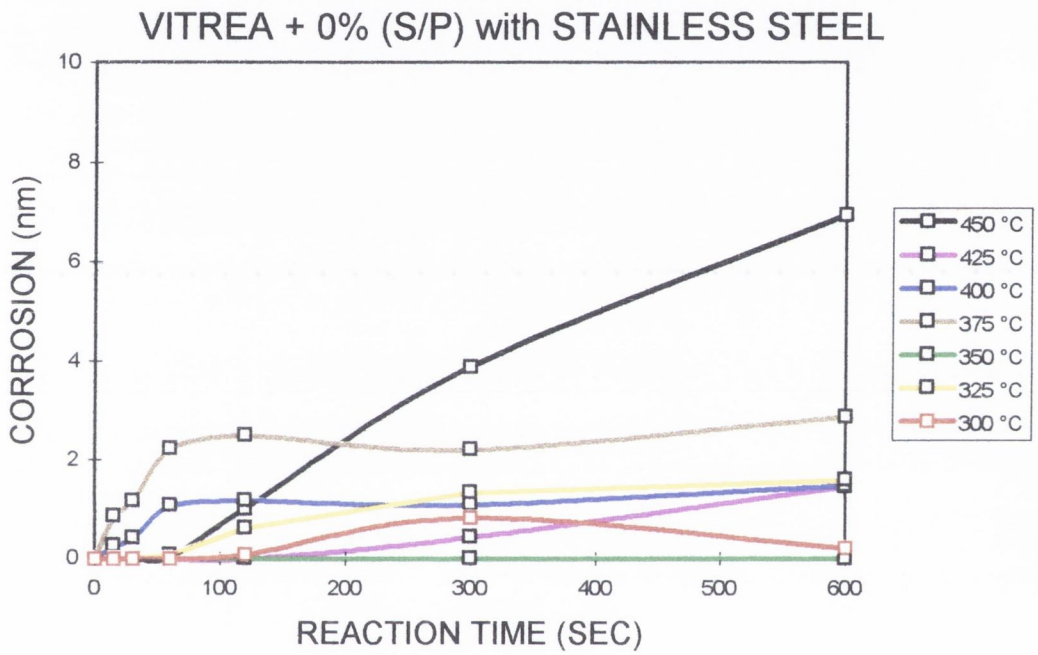

Figure 6.8 Corrosion of stainless steel wire reacted with Vitrea + 0 % (S/P)

The reactions on stainless steel contrast heavily with the reactions on iron wire. The ordered increases in reaction with temperature do not exist. This is another example of how oil/metal reactions can be unique to the combination of materials used. This set of results reinforces what happens when base oils are tested using the EP immersion tests. Film formation is low even at the higher temperatures.

6.4.2 Vitrea M100 + 2% (S/P) on stainless steel

Figure 6.9 shows the corrosion reactions of Vitrea + 2% (S/P) on stainless steel. The high temperatures produce a fast initial reaction, for lower temperatures the corrosion increased steadily. This time however the maximum corrosion occurred at 300 °C and 325 °C. After a very slow start corrosion is found to increase steadily with time. These tests were repeated and the trends were found to be the same. Maximum corrosion using this oil was 55 (nm). The average corrosion was about 20 (nm).

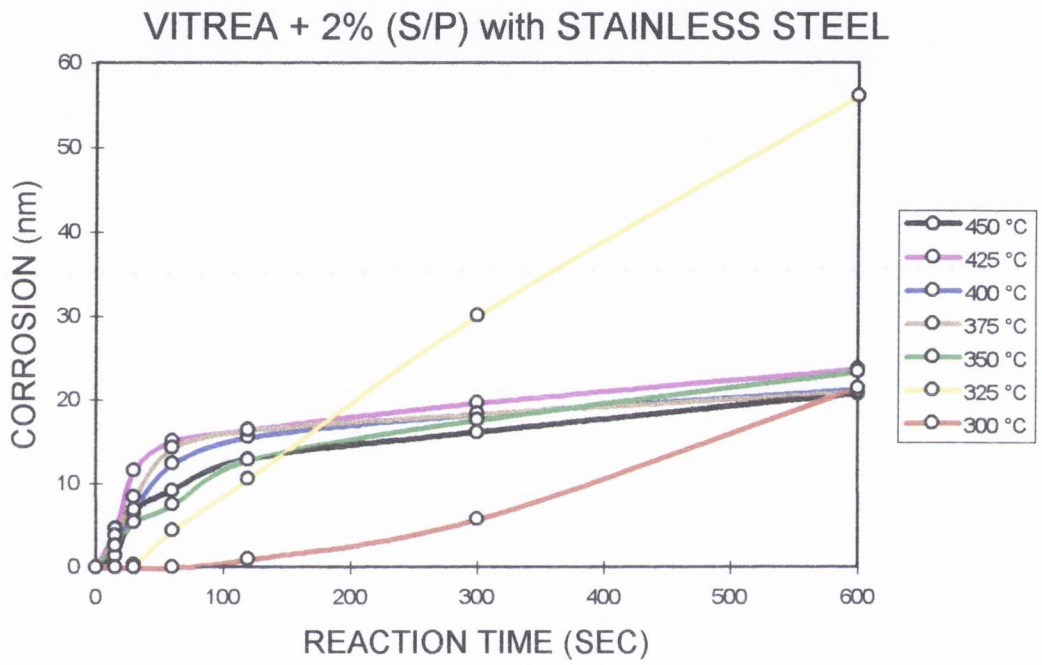

Figure 6.9 Corrosion of stainless steel wire reacted with Vitrea + 2% (S/P)

Close packing of all the corrosion results was seen in the temperature range 350 - 450 °C. The final corrosion in all cases was 20 (nm). In all cases there was a small but fast reaction followed by passivation.

6.4.3 Vitrea M100 + 5% (S/P) on stainless steel

For the case of Vitrea + 5% (S/P) the corrosion increases with temperature for the four lower temperatures and then became less and less for the remaining three highest temperature tests. The higher temperatures did have fast initial reactions but this was sort lived and the resultant overall reaction after 10 minutes was lower than for the lower temperatures. An explanation for this is that a thicker reaction-products layer forms on the surface at high temperatures and protects the wire from further corrosion. The 375 °C reaction caused most corrosion as low film growth and moderate corrosion prolonged the surface attack. The maximum corrosion was 140 (nm).

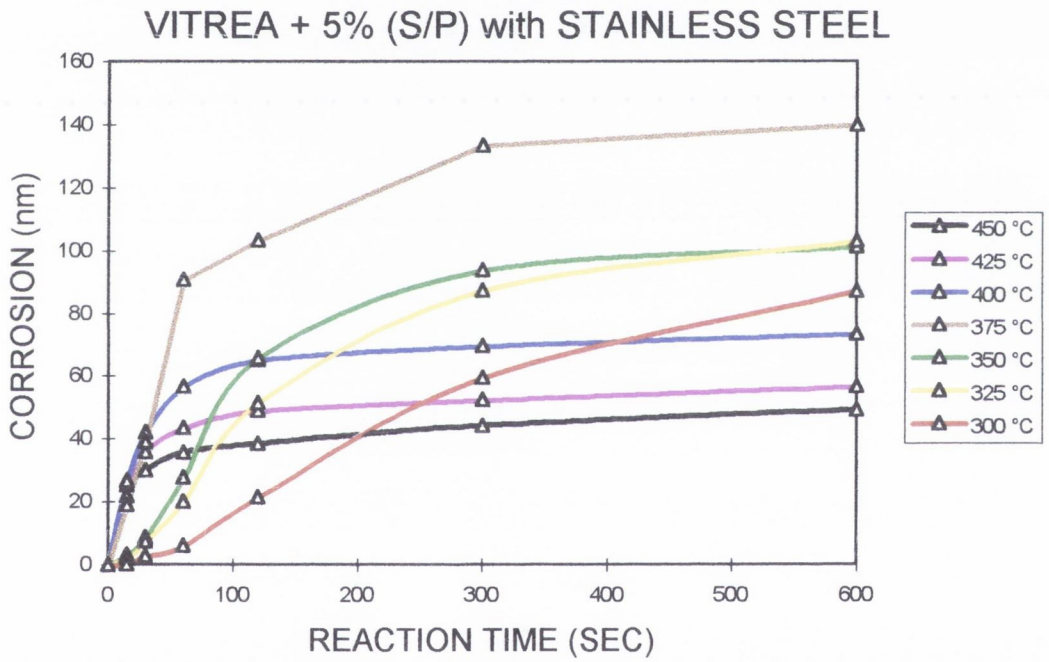

Figure 6.10 Corrosion of stainless steel wire reacted with Vitrea + 5% (S/P)

Comparing these results to those of the of the Vitrea alone and the Vitrea + 2% (S/P) on stainless steel the reactions with 5% are much greater. After five minutes of reacting it is noticeable that all reactions over 350 °C have almost stopped. The higher the temperature the shorter the corrosion lasts. Again this is due to the fast rate of reaction products building up on the surface.

6.4.4 Spirax AX 80W-90 on stainless steel

The fast initial reactions found on the iron wire was not seen on the stainless steel. Corrosion was very small with the average corrosion values of about 15 (nm). Trends similar to Vitrea + 2% (S/P) reactions were seen, the maximum corrosion is lower than 30 (nm). No reaction is found at 300 °C, slow initial reactions at 325 and 350 °C with a steady increase in reaction rate over the 10 minutes. At 375 °C the reaction curve changes from convex to concave. This change signifies a slowing down of the reaction.

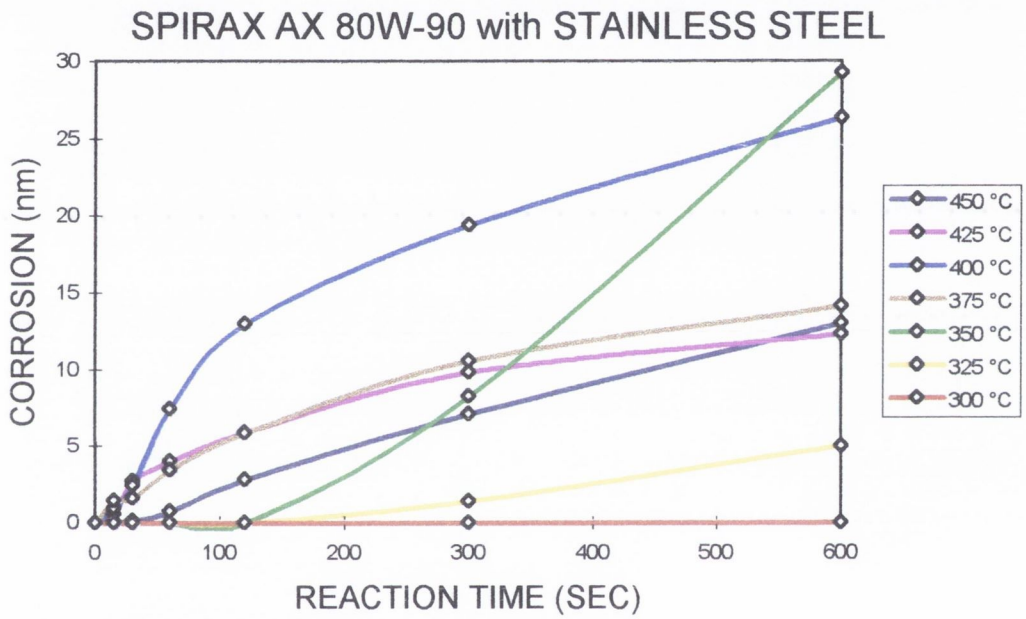

Figure 6.11 Corrosion of stainless steel wire reacted with Spirax AX 80W-90

There is a slow linear increase in corrosion with 450 °C, and the reaction reaches 15 (nm) after 15 minutes. Checking with the results of the first 10 minutes of the 3 hour test - 15 (nm) is repeatable. In this case a reaction film is thought to have built up very quickly preventing the quick initial reaction seen on the iron.

6.4.5 Volvo 97305 on stainless steel

Corrosion on stainless steel is seen for first time to increase steadily with temperature. Trends are the same as seen in literature, and were seen for the reactions between Vitrea and iron wire. Trends such as these again allow the use of the Arrhenius equations for analysis. The reaction film was similar to that seen when ZDDPs were tested using the hot-wire apparatus. A typical black layer was formed over the metal surface with an additional brittle brown/orange layer formed as an outer layer. The outer layer was tested and found to be electrically non-conducting. The conductivity of reaction films has been estimated in literature as being 1/10,000 of that of iron.

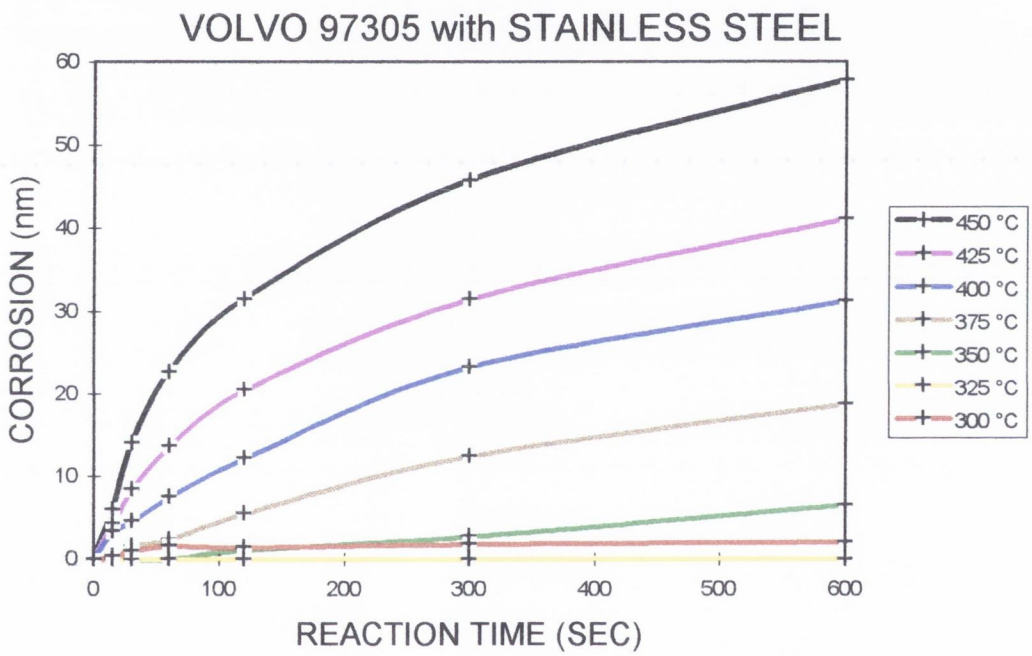

Figure 6.12 Corrosion of stainless steel wire reacted with Volvo 97305

The ordered increase in reaction is in contrast to the results of the reaction with iron wire. The maximum corrosion is 60 (nm) which reactions are also twice that seen with the iron wire. This highlights the complex nature of reactions for specific oil/metal combinations. The reaction rate follows the parabolic growth rate again and will be further examined later in the chapter.

Lubricant	Wire Material	Maximum Corrosion (nm)	Temp for max	Comment
Vitrea + 0%	Iron	330	450	Arrhenius
Vitrea + 2%	Iron	120	375	passivation
Vitrea + 5%	Iron	350	400	passivation
Spirax AX	Iron	260	425,450	fast start
Volvo 97305	Iron	25	450	random
Vitrea + 0%	Stainless	7	450	very low
Vitrea + 2%	Stainless	56	325	bunched
Vitrea + 5%	Stainless	140	375	passivation
Spirax AX	Stainless	30	350	passivation
Volvo 97305	Stainless	60	450	Arrhenius

Table 6.5 Summary of hot-wire test results

6.5 EXAMPLES OF PARABOLIC REACTIONS

It has been seen that the formation of reaction films can control the amount of corrosion on the wire surface. The corrosion is now determined by the diffusion of reactants though the reaction film.

Two examples were found from the 10 minute tests which obey the parabolic reaction rate. Vitrea without additive on iron wire and Volvo 97305 on stainless steel showed a steady increase in reaction with temperature. Figure 6.13 and 6.14 shows the two examples of where oil/metal reactions follow the Arrhenius rate equation. The corrosion has been squared (y-axis) and plotted against time (x-axis). The resulting graphs are then found to be approximately straight lines.

The parabolic law of reaction

$$(\Delta r)^2 = k.t \qquad 6.1$$

Sakurai and co-workers [63] using "elementary" sulphur solutions calculated the activation energy to be 20.6 kcal/mol. This value is equivalent 86.25 kJ/mol.

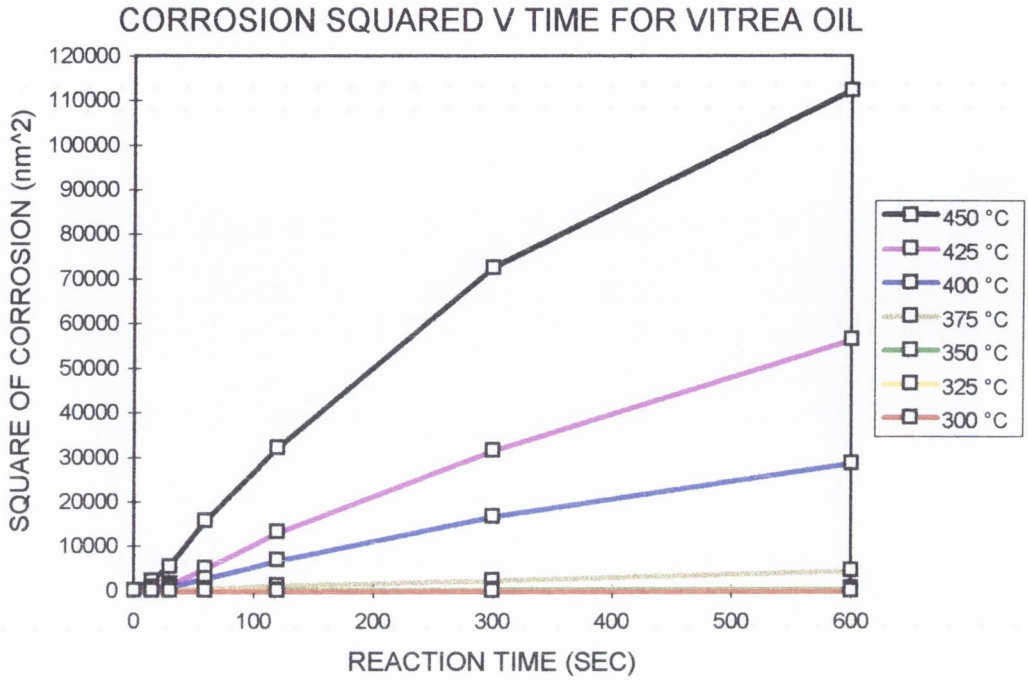

Figure 6.13 Square of corrosion verses time for Vitrea + 0% (S/P) on iron wire

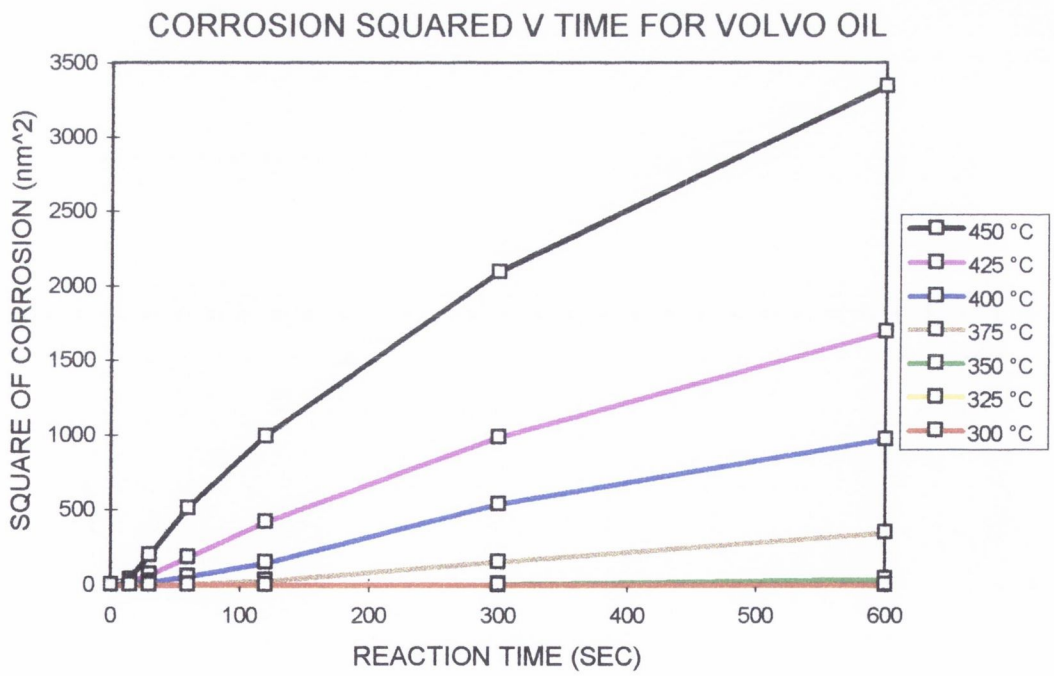

Figure 6.14 Square of corrosion verses time for Volvo on stainless

6.5.1 The Arrhenius Equation

A diffusive mechanism requires the diffusion of atoms through a material. For an atom to free itself from a solid it must acquire a certain energy. Arrhenius law states that the rate of corrosion increases exponentially with temperature. If the rate of any process that follows the Arrhenius law is plotted on a ln scale against 1/T, a straight line with a slope -Q/R is obtained.

6.5.2 Activation energy calculation

$$\frac{dh}{dt} = \frac{A}{h} e^{-\frac{Q}{RT}} \tag{6.2}$$

$$h.dh = \left(Ae^{-\frac{Q}{RT}} \right) dt \tag{6.3}$$

$$\frac{1}{2} h^2 = t\left(Ae^{-\frac{Q}{RT}} \right) \tag{6.4}$$

$$h^2 = 2t\left(Ae^{-\frac{Q}{RT}} \right) \tag{6.5}$$

Plot h^2 V t [Figure 6.13] and take slope:

$$2Ae^{-\frac{Q}{RT}} = 205 \tag{6.6}$$

(450 °C) $$\ln(2A) + \left(-\frac{Q}{R(450+273)} \right) = \ln(205) \tag{6.7}$$

(425 °C) $$\ln(2A) + \left(-\frac{Q}{R(425+273)} \right) = \ln(94.5) \tag{6.8}$$

(400 °C) $$\ln(2A) + \left(-\frac{Q}{R(400+273)} \right) = \ln(50) \tag{6.9}$$

Subtracting equation 6.8 from 6.7 and solve for Q, the activation energy:

$$\left(-\frac{Q}{8.31(425+273)}\right)+\left(-\frac{Q}{8.31(450+273)}\right)=\ln(205)+\ln(94.5) \qquad 6.10$$

Q = 130.5 kJ/mol

A = 2.8×10^{11} nm^2/s (diffusivity)

Subtracting equation 6.8 from 6.6 and solve for Q, the activation energy:

Q = 112.9 kJ/mol

A = 1.5×10^{10} nm^2/s (diffusivity)

Calculations were repeated using the reaction rates of the Volvo 97305 oil on stainless steel.

450 - 425	450 - 400
Q = 120 kJ/mol	Q = 107 kJ/mol
A = 1.48×10^9 nm^2/s	A = 1.65×10^8 nm^2/s

Table 6.6 Summary of results of Volvo on stainless reactions

6.6 ANALYSIS OF WIRE SECTION

A stainless steel wire was reacted at 450 °C for 30 minutes in a bath of Vitrea + 5% (S/P) oil. A thick reaction products film was formed for inspection. The wire was mounted in a resin and a section of the wire was polished for examination with SEM and EDAX.

6.6.1 Elemental analysis

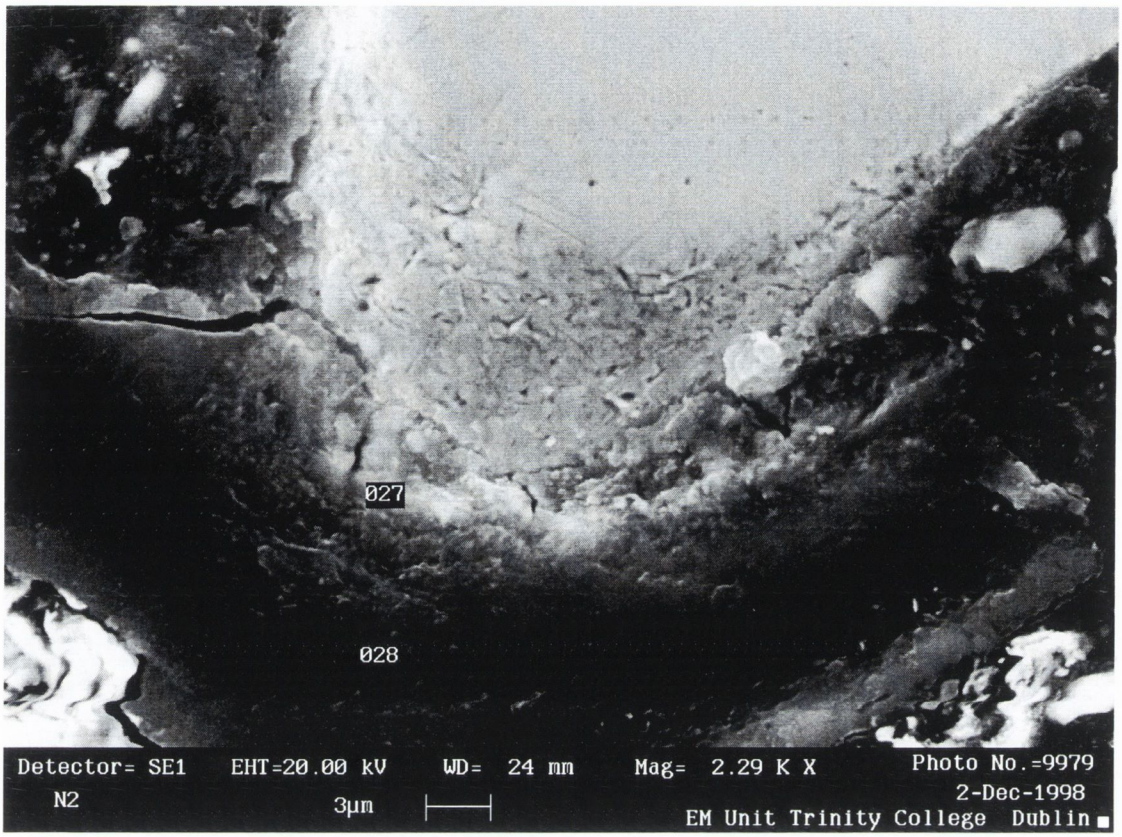

Figure 6.15 Photo of mounted wire section

Element	Atomic %	Atomic %	Atomic %	Atomic %
Ni	**8.94**	**0.86**	*0.04*	*0.1*
Fe	**70.9**	**6.74**	**0.6**	**0.44**
P	*0.38*	**7**	**3.49**	**4.35**
Cr	**19.7**	**2.39**	**0.27**	*0.18*
Mn	**0.74**	*0.1*	**0**	**0**
C	**0**	**82.16**	**94.42**	**93**
Cu	**0**	**0**	**0**	**0**
S	**0**	**0.4**	**1.14**	**1.84**
O	**0**	**0**	**0**	**0**
K	*0.14*	**0.35**	*0.04*	*0.09*
Distance into the film	Wire core	2 µm	10 µm	20 µm

note: figures in italics too small to be significant

Table 6.7 Composition of film at various distances into the film from the metal interface

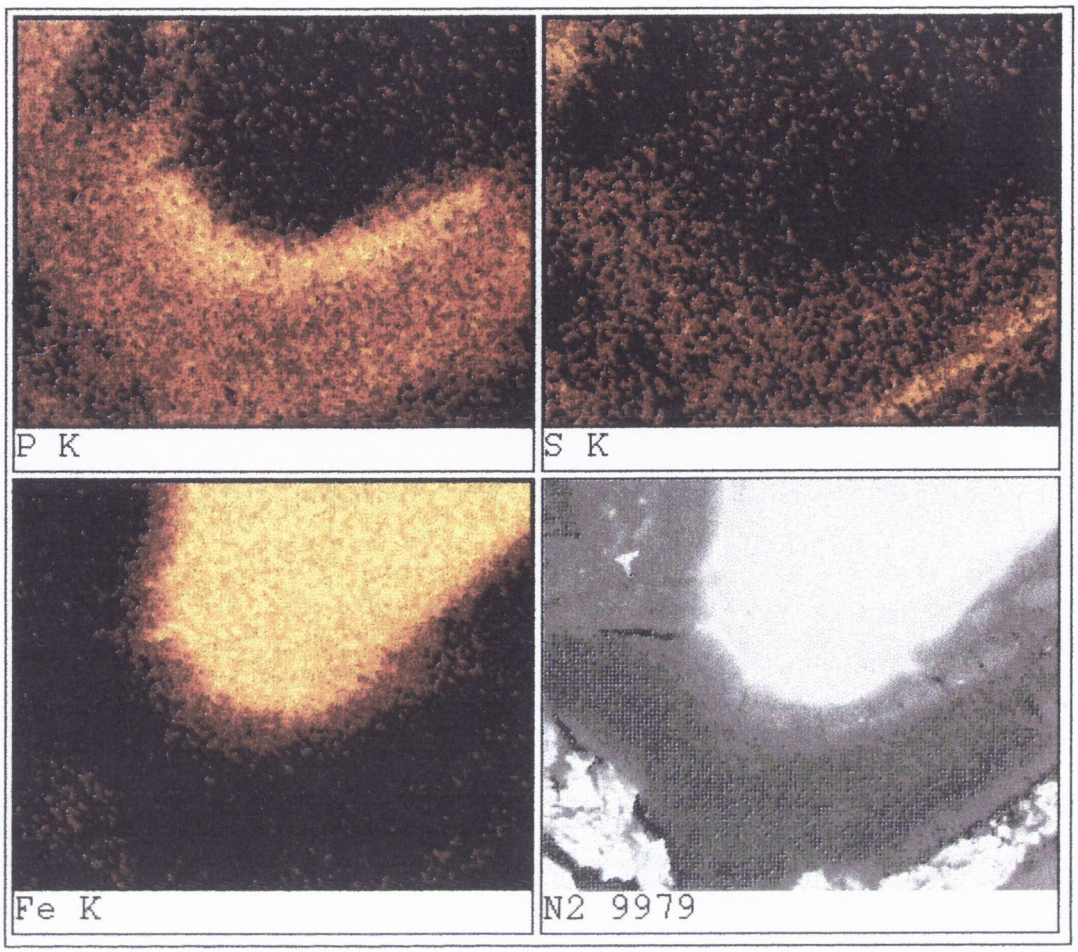

Figure 6.16 Elemental plots of phosphorus, sulphur and iron

6.6.2 Wire section discussion

A wire was mounted in resin and a polished section was examined in a scanning electron microscope. Elemental analysis was conducted on the reaction film using EDAX. Four points were taken and shown in Figure 6.15. From the outer radius of the wire one point was taken in the core of the wire, and three points were taken at distances of 2, 10 and 20 μm from wire surface into film.

An analysis of the wire core was taken first, this is shown in the first column of Table 6.6. The element iron, chromium and nickel are prominent as expected. The second column is taken at 2 μm from the wire surface, the noticeable change in element analysis is the 7% phosphorus and 82% carbon.

There was a visual difference in contrast between the film at 10 and 20 microns. Hence the composition differences may be significant. Figure 6.16 shows the distribution of

distribution of elements found across the wire section. The light areas in the top left hand side show the phosphorus concentration especially near to the wire surface. The top right photo shows the sulphur traces away on the outer fringes of the reaction layer. The bottom photos show the iron core and the original photo.

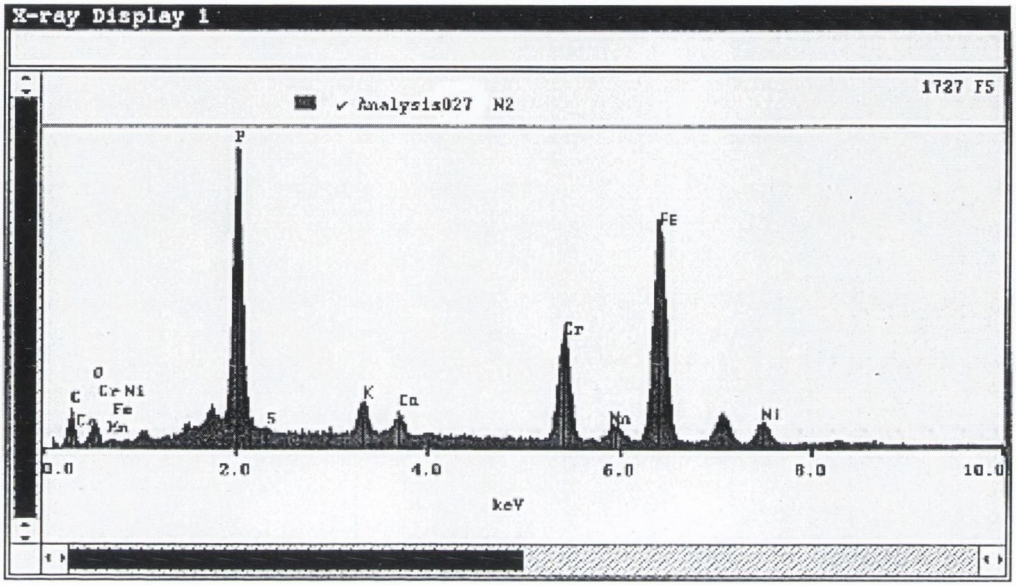

Figure 6.17 Example of EDAX profile plot showing phosphorus peak

The Figure 6.17 shows the analysis taken at point 27, the point analysis is at the 2 microns into the film from the surface. The high phosphorus peak (7%) is prominent, the stainless steel elements also visible.

6.7 REACTION FILMS ON WIRE SURFACE

The films that built up on the wire surfaces were examined using scanning electron microscopy. Most films were found to be black carbonaceous films of various thicknesses. Some of the films were found to contain two distinct films, a black layer close to the surface of the wire and a brown/red glassy outer layer. The layers seen by the Volvo oil were similar to the films formed when a solution of ZDDP was tested. If a database of reaction products from known additives was compiled, it could be possible to identify additive types simply by examining its hot-wire reaction film.

In some reactions under 300 °C corrosion was not recorded but a thin reaction product film was formed on the surface. This is similar to what happens in the EP immersion

tests, where surfaces are discoloured by heated oil. If we consider that contaminated oils are a cause of early failures, then the reaction products formed by the oils could be playing a significant role without ever causing corrosion.

In the presence of additives the temperature needed to produce corrosion and reaction product films was found to decrease. With low film growth, as seen in Figure 6.19, the reactive elements in the lubricant can travel though the thin film sustaining the reaction process. If the film is thick as in Figure 6.20, products layer is thought to passivate the reaction, as the build up of material separates the oil from the wire surface.

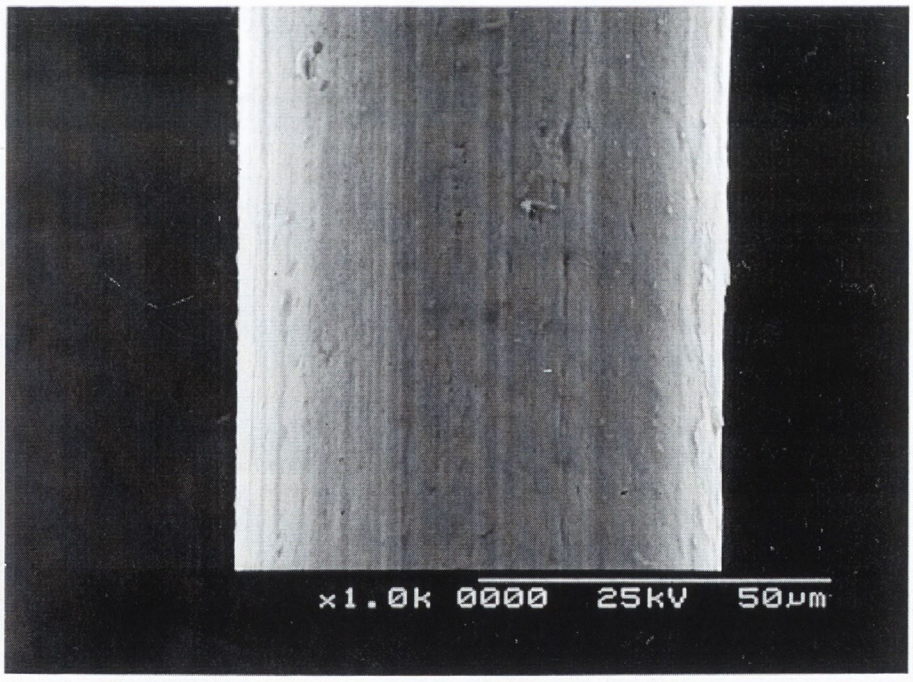

Figure 6.18 SEM photo of unreacted wire

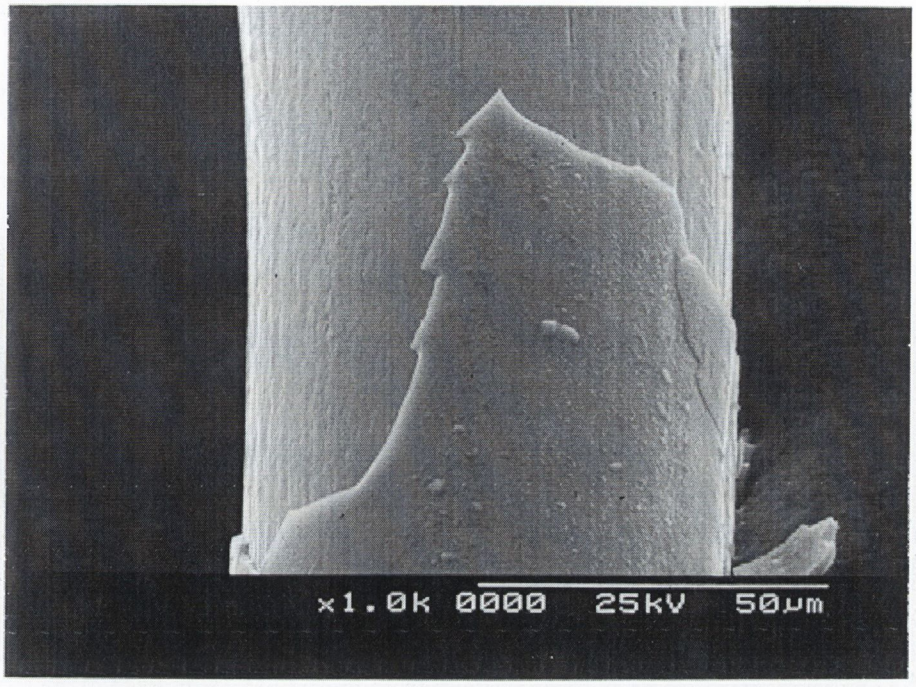

Figure 6.19 SEM photo of reacted wire with moderate corrosion < 5 µm

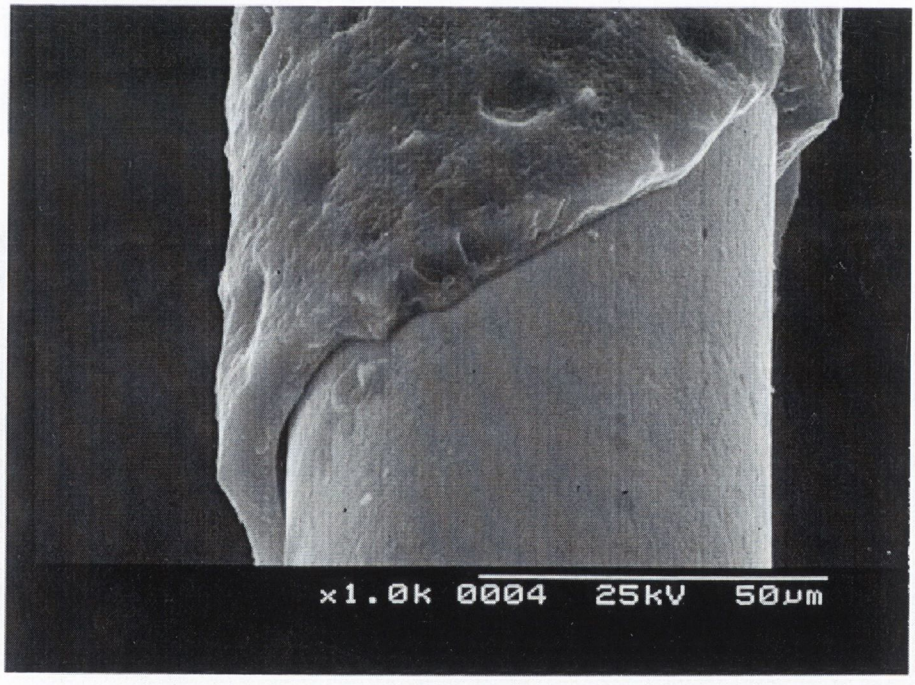

Figure 6.20 SEM photo of reacted wire with thick film > 5 µm

The films are normally hard and fracture readily when cut with a sharp scalpel, Figure 6.20 shows the edge of the broken products film.

6.7.1 Passivation caused by film formation

Figure 6.21 is a schematic diagram of additive attack in the hot-wire. The yellow layer represents the corroded layer that has been consumed in the reaction. As the reaction proceeds, reaction products (red layer) build up on the metal surface. This layer has been shown to be made up of mainly carbon. Two things happen that slow down the reaction. (A) the additive attack is slowed as the reactions must happen though this film and, (B) the temperature at the outer reaction layer is lower than at the surface of the wire. If the temperature is lowered at this ever changing interface, we can expect the decomposition reaction of the additive to slow down.

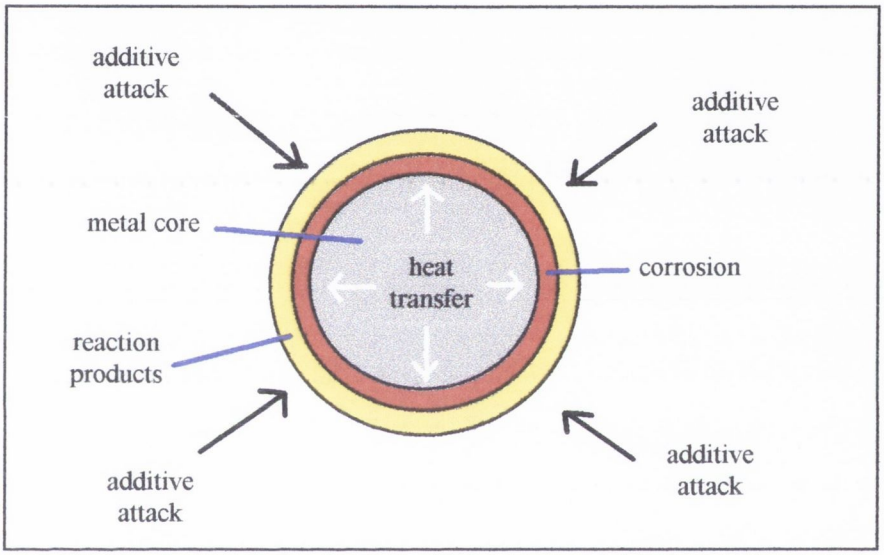

Figure 6.21 Schematic of hot-wire cross section showing film effects

When the reaction temperatures are high or when additives are present the reaction film grows quickly. This has the effect of protecting the wire from further attack. Under these static conditions the balance between the ability of the lubricant to corrode and the rate of reaction film formation decides the total corrosion. This presents a problem when trying to relate them to the results in rolling contact tests. Under the dynamic conditions thick films are difficult to build up as the rolling motion and the flow of lubricant can remove them from the surface, and as seen in Chapter 2 particles broken from the films may be recycled into the contact causing high localised stresses.

6.7.2 Links with bearing tests

The difference in the testing conditions between the hot-wire test and rolling contact fatigue tests make direct comparisons very difficult. The hot-wire rig shows in the reactivity products and the corrosion depths, making it more sophisticated than the EP immersion tests. The reactivity of certain lubricants with specific metals has been shown. Reaction products caused by thermal effects can be analysed as they are not worn away. Only small amounts of lubricants, (400ml), are needed for the hot-wire testing.

Bearing metals are subject to a gradual weakening caused by the accumulation of micro-stresses. The wires used in the hot-wire rig do not suffer the same effects. The maximum corrosion depth measured was about 350 (nm). The corrosion was found to be slowed down by the reaction film formation. In rolling contacts reaction products can be compacted on the surface, causing a film which can be removed by abrasion. The mechanism of additive reaction are not fully understood. Several complex mechanisms are likely to exist due to the number of lubricant combinations being used today.

When pitting occurs often the evidence of crack growth and metal fatigue are destroyed at the time of failure. The hot-wire can tell how fast the additive reacts with metal surfaces, Spirax was a good example of fast reacting additive. The amount of decomposition products that are produced at high temperatures can also be found. This can effect the contamination of the oil, directly influencing bearing life. So although the hot-wire technique cannot currently predict whether a lubricant will improve the life of a bearing, it can provide clues to how bearing might fail.

6.8 SUMMARY

The hot-wire technique is a quick method of assessing oil/metal reactivity. No corrosion was measurable at temperatures under 300 °C for the oils tested. Reaction products were formed in some cases at temperatures under 300 °C even when corrosion was not measured.

At low temperatures, the layer of reaction products was found to be thin, under 5μm. With neat oil even at temperatures of 450 °C the thickness remained small. The addition of additives in oil caused thick reaction product films to be formed, these films were over 5 μm in thickness. For tests with the Volvo oil, two distinct films were found on the wire surface, the normal inner black film and an outer brown glassy film. The glassy film was similar to that formed when a ZDDP solution was tested with the hot-wire method.

Spirax had a very fast initial reaction over the 60 seconds and the reaction quickly passivated. The reaction films were analysed using EDAX, the main constituents were carbon, iron and sulphur and phosphorus when additives were included. The films were found to adhere well to the wire, taking into account the fragility of the wire it proved difficult to remove this film.

Oil/Metal reactions are very sensitive to the combinations of materials used. Characteristic trends are not easily identifiable for series of metal and oils. With Vitrea neat oil alone considerable corrosion occurred on the iron wire. This is similar to what was seen when White Oil was used in the literature.

CHAPTER 7

7 FINAL DISCUSSION AND CONCLUSIONS

7.1 CONCLUDING DISCUSSION

Two different methods of testing have been used to study the influence of additives on bearing life. It has been found that for a lubricant containing sulphur/phosphorus, under different dynamic conditions, the fatigue life of a bearing can increase or decrease. The Spirax oil that showed this trend, was identified using the hot-wire test, to be one that caused fast reactions. Caution should be shown when using lubricants that corrode quickly. If the film formed cannot adhere properly to the surface, problems may occur. A fast reacting additive might not be beneficial in conditions of high temperature and pressure. It has been suggested earlier that the process of repeatedly uncovering fresh metal surfaces to aggressive attack could be the breeding ground for early failures.

The stresses used in the Bristol rig were similar to those found in normal bearing applications. The lambda ratio was lowered on purpose to an initial value of 0.4 to accelerate failure times. The resulting contact may be regarded as a bearing that has underdone a uniform degree of wear. The initial roughness of the inner ring decreases during the testing period. This polishing effect, as seen in section 5.6, was measured and was found to half the roughness value from approximately 0.5 (μm cla.) to 0.25 (μm cla.). A predicted L_{10} life of 35 hours for the these conditions, was low compared to the test results. The shortest L_{10} life of 105 hours with the Vitrea + 5% (S/P) tests, was 3 times greater than the predicted life. Spirax with a L_{10} life of 320 hours exceeded the life estimate by nearly a factor of 10.

The predicted L_{10} life for the bearings used in R2F rigs under radial loading was 29 hours. The L_{10} lives from the Volvo 97305 and Spirax tests, were found to be close to this at 36 hours and 72 hours respectively. The base oil and Volvo 97307 oil with L_{10} lives of 369 hours and 250 hours respectively, far outlived the predicted life. The L_{10} for the base oil was twelve times greater than the predicted life.

7.1.1 Hot-wire testing on used Spirax oil

A sample of used Spirax oil was taken from the sump of a Bristol rig. The oil had been circulating in the heated oil system for approximately 3,000 hours. There was a notable difference in appearance in the oil, it was darker in colour and appeared slightly more viscous. When the used Spirax was tested on stainless steel, using the hot-wire method, a sharp decrease in reactivity was noticed. In fact, the corrosion measured was up to ten times less than what was found with fresh oil. Initially this was regarded as an anomalous result, but in light of the oxidation studies using FTIR pointing to oxidation of the oils there could be another explanation.

If the effectiveness of a lubricant is related to its reactive properties, the oil should be kept in a condition that promotes beneficial effects to life. If through oxidation or thermal degradation the oil becomes unreactive it can loose its efficiency. The additive containing oil also degrades at lower temperatures compared to a base oil, causing contamination, which has a documented negative effect on life.

7.1.2 Reaction films with coloured outer layer

The hot-wire rig has the potential to be used as a aid to identify the constituents of an oil. Characteristic reaction films, especially double layered films, could be compared to known equivalents for identification. There seems to be individual trends of reactions and film appearance, for different combinations of material and oil additive. The ZDDP was an example of this, where the red outer surface in characteristic of reactions at temperature of 300-400 °C.

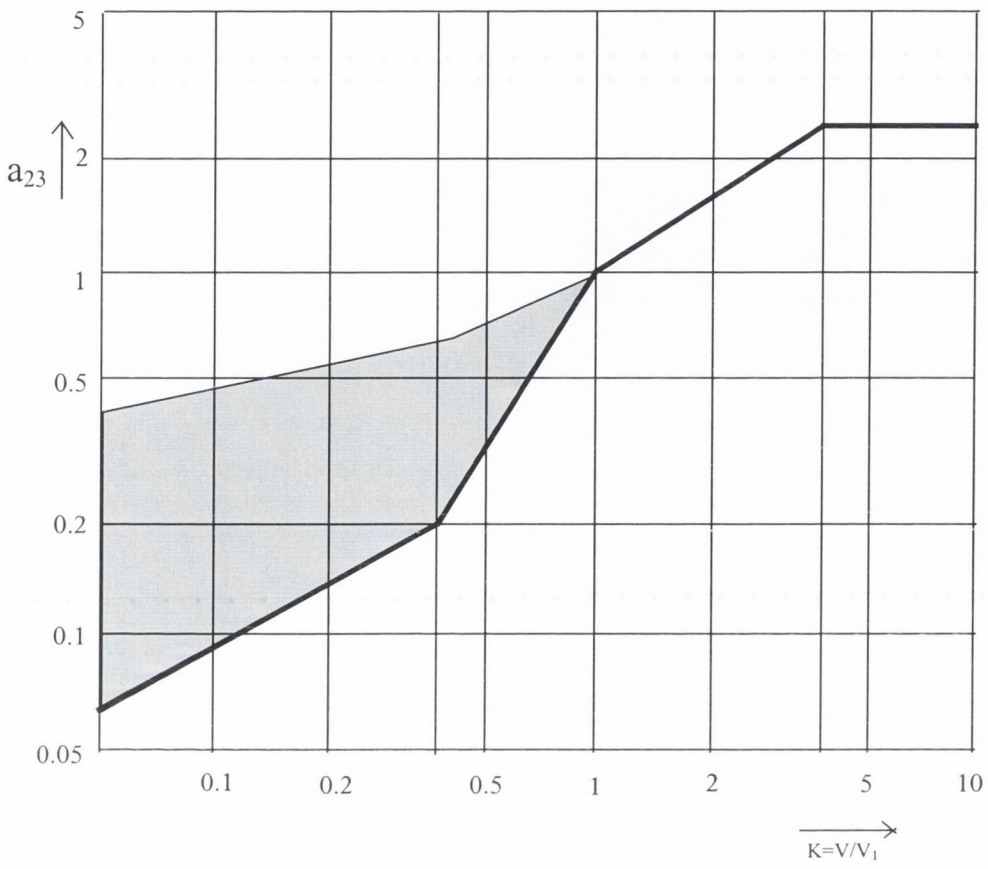

Figure 7.1 Kappa verses coefficient diagram

The effects of using sulphur additives on estimating life adjustment parameters is unsure. Figure 7.1 is a graph showing how, under clean conditions, the a_{23} combined life adjustment factor is obtained from the Kappa ratio value. The thick black line shows the coefficients expected when base oils are used, the grey area is an estimate of the improved life that is expected if additives (mainly lead) are used. The banning of lead for environmental reasons has added more question marks regarding the role of additives in bearings. The studies on early failures have suggested that there is a zone under this grey region where early failures can take place.

7.1.3 Limits of reactivity testing

Tests have shown that the corrosive reactions between oil and metals are fairly unique depending on what combinations are used. The response of Spirax oil on iron and stainless steel was seen to be significantly different. In the case of the Volvo oil, reactions with stainless steel increased with temperature, but reactions on iron showed no trends. The differences in reaction of these metals makes predicting the effects on bearing surfaces difficult. The best hot-wire results would be achieved if the wire used was made from bearing steel.

The biggest limitation of the hot-wire rig is the fragility of the wire, the 50 μm diameter does not allow rubbing during testing. The cross-section of the wire would be damaged and the contact at the terminals would be disturbed by small external forces. Attempts were made to remove the film by mounting the Pyrex bath in an ultrasonic cleaning device during testing. The adhering film was found to be unaffected this process. It was not clear if the oil viscosity damped out the ultrasonic vibrations.

The final limitation concerns the control of the reaction temperature when the power is applied to the wire. When reactions occur rapidly, the initial couple of seconds are of most interest. When the heating circuit is switched on care must be taken not to overshoot the desired reaction temperature. In practice this takes 2-3 seconds, as an overshoot into a higher temperature range would cause either excessive film growth or wire corrosion. For this reason the minimum reaction period used in this study was 15 seconds.

7.2 SUGGESTIONS FOR FUTURE WORK

The hot-wire reactions have been seen to produce unique results for each combination of metal and wire used. Future work allows the possibility of having some 52100 steel drawn into 50 micron wire. This will give the best indication of the reaction rates on bearing surfaces.

Characteristic reaction films were generated using the hot-wire test, especially the double layered films formed by the Volvo oil and the ZDDP containing oil. If a data base of reaction films of known additives was compiled it could be used to identify new or unknown lubricant mixtures. For example the ZDDP produced a red brittle outer layer for a certain temperature range. Apart from the appearance of the film, other factors such as corrosion rate, reaction film thickness and the passivation effects could be used for the purposes of comparison.

Hot-wire tests could be undertaken using the temperature and time conditions of the immersion tests. The immersion tests have shown that reactions can start between the 24 hour and 72 hour period. Reaction film formation and possible corrosion, at low temperature and over longer periods, could yield the most useful hot-wire results.

Several studies concerning additive effects on fatigue life have been published to date. The studies use a range of test rig and oil combinations. These results could be exploited by adding the reactivity dimension to the studies. Hot-wire tests could undertaken and compared to published fatigue results.

7.3 FINAL CONCLUSIONS

a) Under moderate loading conditions and low lambda ratio, seen in the Bristol tests, the Shell Spirax AX was seen to increase the life of the bearings. The high survival rate for the Spirax oil, seven of the twelve, makes it is difficult to say exactly how significant this improvement is. Under these conditions the bearing steel is elastically loaded and the reaction film can adhere to the surface allowing protection. With the Vitrea and Vitrea/additive combinations the lives were fairly similar, showing that in the presence of S/P additives early failures are not caused. A safe operating zone within the lambda range 0.4 - 0.8 at stresses of 2.2 GPa was identified.

b) At higher maximum Hertzian stresses of 4.2 (GPa) and with lambda conditions of around 4, the additive containing oils performed worse than the base oil. Rolling element failures were only found when additive containing oils were used. Unusual failure modes were noticed with the Volvo oils (of unknown additive concentration). Scuffing of the inner bore of the test bearing is very undesirable as the shaft of the rig can be damaged in the process. The Spirax oil gave a lower L_{10} than the base oil under these conditions. The fast reacting lubricant may have aggressively attacked the surface under conditions that a protective layer was unable to from. The amount of reaction product formed by Spirax in the hot-wire test and the EP immersion test was high. If the temperatures at metal contacts in the R2F rigs are high the oil risks becoming contaminated. Contamination can reduce bearing life drastically.

c) The various dynamic conditions experienced in rolling contacts, e.g. rubbing, friction and lubricant oxidation, makes the task of correlating fatigue results and hot-wire results difficult. The growth of the reaction film is seen to be an important factor effecting reactivity, passivation of the reaction is caused by thick film growth. The hot-wire test alone cannot, in its current state of development, be used to screen new oils for bearing applications. However, it can provide clues to how reactive the lubricant will be.

d) The hot-wire test can detect changes in reactivity of a particular oil which has been used for a period of time. This was found when the reactivity of some used Spirax oil from a Bristol fatigue rig was tested using the hot-wire test. A set of 10 minute tests were carried out, and the corrosion was found to be zero even at high temperatures. If the effectiveness of an additive is based on its ability to react, then this is a significant result. The technique could be used to let customers know that if attention is not paid to cleanliness, then the lubricant may not help keep their bearings running longer.

e) The relatively low temperature range investigated with the hot-wire rig gives this study some novelty value. To make the test even more representative of bearing operating conditions, two changes could be made. The reaction temperatures could be lowered again, and the tests run for longer reaction periods. The test would then be similar to the EP immersion tests. Lower temperatures could allow the use of thicker reaction wires, as the power requirements needed heat the material would be less. If the wire was more robust there would be a better possibility of being able to remove the reaction product film during testing, thus moving closer to the dynamic conditions found in bearing contacts.

7.4 CLOSURE

The hot-wire test has been found to give information on both metal corrosion and reaction product formation. The metal corrosion results have been seen to be strongly effected by a passivation effect. The technique was successful in identifying a fast additive attack as in the case of Shell Spirax. Looking back at the project, the importance of the reaction product film thickness was probably underestimated and overlooked. The thicknesses of the reacted films are relatively easy to measure with SEM, mounting is not even necessary when the films are large and break as shown in Chapter 6. In bearing contacts at high temperatures these films are compacted at the contact points and can cause effects such as polishing or contamination that effect life.

The fatigue results have highlighted how lubricants can increase or decrease bearing life depending on the operating conditions. This fatigue response has been observed before, as discussed in Chapter 2. In this cases of moderate stress and low lambda life was increased with Spirax, at higher stresses decreases in life were seen. It is also worth remembering that no significant benefit was attained by using the S/P package under the Bristol conditions. This is not, of course, to say that under different conditions it will behave in the same way. In bearing testing many tests have to be repeated under identical condition to produce one result for one condition.

With new lubricants appearing on the market each year, it is not surprising that their effects on bearing life are not always known. Bearing manufactures are not helped either by the secrecy surrounding the make up of lubricant/additive solutions. The job of trying to identify reaction products and mechanisms is made much more difficult if the additive is unknown. If additives are the "drugs" causing undesirable side effects, maybe a more holistic cure is needed. This could involve, lubricant manufactures being more open about their products, bearing manufactures using additives when necessary and bearing users paying more attention to lubricant selection and cleanliness.

REFERENCES

1. D. Summers-Smith, "The Unacceptable Face of Lubricating Oil Additives", Tribology International, Dec. 1978, pp.318-320.

2. A.A. Torrance, J.E. Morgan and G.T.Y. Wan, "An Additive Influence on the Pitting Failure and Wear of Bearing Steel", Wear, 192 (1996), pp. 66-73.

3. A.A. Torrance, "Chemical and Microstructural Changes Induced in Bearing Steel by Rolling Contact", Wear, 122 (1988), pp. 363-376.

4. G.T.Y. Wan, "The performance of one organic phosphonate additive in rolling-contact fatigue", Wear, 155 (1992) pp. 381-387.

5. F.T. Barcroft, " A Technique for Investigating Reactions Between E.P. Additives and Metal Surfaces at High Temperatures", Wear, 3 (1960), pp. 440-453.

6. T. Sakurai, K. Sato and K Ishido, "Reaction Between Sulphur Compounds and Metal Surfaces at High Temperatures", Bulletin of The Japan Petroleum Institute, Vol. 6, June 1964, pp. 40-49.

7. A.A. Manteuffel, K.P. Yeats, H.J. Bickford and G. Wolfram, "Radiotracers Reveal Activity of Extreme-Pressure Additives in Lubrication", ASLE Trans. 7, (1964) p 249.

8. X-A Han. And Q. Li, "Characteristics of Chemical Reactivity, Extreme-Pressure and Antiwear properties of Binary Systems", STLE, Tribology Trans., Vol. 36 (1993), 2, pp. 283-289.

9. T. E. Tallian, "Failure Atlas for Hertzian Contact Machine Elements" ASME Press, 1992.

10. SKF Catalogue 4000, "Life adjustment factor a_2", p 35, (1992)

11. I. M. Hutchings, "Foreward- New Directions in Tribology", 1st World Tribology Congress, IMechE., Sept (1997).

12. H. Czichos, "Current Aspects of Tribology", Wear, 77 (1982), pp.1-11.

13. SKF Catalogue 4000, "Basic Rating Life Equation", p 28, (1992)

14. G. Lundberg and A. Palmgren, "Dynanmic Capacity of Rolling Bearings", Acta Polytechnica, Mech. Engr. Series, Vol.1, No. 3 (1947).

15. G. Lundberg and A. Palmgren, "Dynanmic Capacity of Roller Bearings", Acta Polytechnica, Mech. Engr. Series, Vol. 1, No. 4 (1952).

16. R. Goss and E. Ioannides, "Performance Testing: Facilities and Opportunities", Ball Bearing Journal Special 1989, pp. 12-21.

17. P. Leenders, "Endurance Testing in Practice", Ball Bearing Journal, Vol. 217, pp. 24-31.

18. A. Cameron, "Lubricant Chemistry and Tribology Chemistry- Boundary and Extreme Pressure Lubrication", ", Proc. of the IMechE International Conference. (1987), pp.355-364.

19. Y. Wang, J.E. Fernandez and D.G. Cuervo, "Rolling-Contact Fatigue of Steel AISI 52100 Balls with Eight Mineral and Synthetic Lubricants", Wear, 196 (1996), pp. 110-119.

20. M.A. Plint and A.F. Alliston-Greiner, "Extreme Pressure and Anti-Wear Properties of Lubricants: A Critical Study of Current Test Methods and Suggestions for the Future", Tribology ASTM (1993) pp 60-79.

21. E. Kleinlein, "Mechano-Dynamics Testing of Lubricants in the Laboratory-Are the Results Applicable in the Field", FAG, Ball and Roller Bearing Engineering, 1983-2 / 1984-1, pp 40-45.

22. F.R. Morrison, T. Yonushonis and J. Zielinski, "Rolling Bearing Life Tests and Scanning Electron Microscopy", Rolling Contact Fatigue Testing of Bearing Steels,ASTM STP 771, J.J.C. Hoo, Ed., American Society for Testing and Materials, 1992, pp. 239-254.

23. T.E. Tallian, "Simplified Contact Fatigue Life Prediction Model- Part I: Review of Published Models", ASME Journal of Tribology, April 1992, Vol. 114, pp.207-213.

24. SKF Catalogue 4000, "Adjusted Rating Life Equation", p 35, (1992)

25. F. Hengerer, "The History of SKF 3", Ball Bearing Journal, Vol. 231(1), pp. 2-11.

26. E. Ioannides and T.A. Harris, "A New Fatigue life Model for Rolling Bearings", Journal of Tribology, Vol. 107, July 1985, pp.367-378.

27. J. Goodall Wuttkowski, and E. Ioannides, "The New Life Theory and its Practical Consequences", Ball Bearing Journal Special 1989, pp. 6-11.

28. H. Schlicht, E. Schreiber and O. Zwirlein, "Fatigue and Failure Mechanisms of Bearings", IMechE London, C285/86, (1986), pp. 85-90.

29. L.M. Keer, M.D. Bryant and G.K Haritos, "Subsurface and Surface Cracking Due to Hertian Contact", ASME Journal of Lubrication Technology, July 1982, Vol. 104, pp.347-351.

30. L.M. Keer and M.D. Bryant, "A Pitting Model for Rolling Contact Fatigue", ASME Journal of Lubrication Technology, April 1983, Vol. 105, pp.198-205.

31. M.T. Hanson and L.M. Keer, "An Analytical Life Prediction Model for the Crack Propagation Occurring in Contact Fatigue Failure", to be published in Tribology Transactions.

32. V. Bhargava, G.T. Hahn and C.A. Rubin, "Rolling Contact Deformation, Etching Effects and Failure of High Strength Steels", Metallurgical Trans., Vol. A 21A, (1990), pp.1921-1931.

33. J.W. Blake and H.S. Cheng, "A Surface Pitting Life Model for Spur Gears. Part1: Life Prediction", ASME Paper No. 90-Trib-59, (1990).

34. J.W. Blake and H.S. Cheng, "A Surface Pitting Life Model for Spur Gears. Part 2: Failure Probability Prediction", ASME Paper No. 90-Trib-60,(1990).

35. ASM Metals Handbook No. 13.

36. A. Kroon and H. Nutzel, "Bearing Steel Development", Ball Bearing Journal Special (1989), pp. 40-47.

37. H.-J. Christ, C. Sommer, H. Mughrabi, A.P. Voskamp, J.M. Beswick and F. Hengerer, "Fatigue Behaviour of Three Variants of the Roller Bearing Steel SAE 52100", Fatigue Fract. Engng. Mater. Struct. Vol. 15, No. 9, pp. 855-870, 1992.

38. J.E. Morgan, "Structural and Microstructural Changes in the Inner Races of Ball Bearings", Wear, 84 (1983), pp.53-64.

39. J.E. Morgan, "Cumulative Plastic Deformation Observed During Cyclic Testing in Rolling Ball-Cylinder and Static Ball-flat Plate Experiments", Wear, 92 (1983), pp. 25-30.

40. A.A. Torrance, "The Metallography of Worn Surfaces and Some Theories of Wear", Wear, 50(1978), pp. 169-182.

41. G. E. Hollox, A.P. Voskamp and E. Ioannides, "Failsafe Rating of Bearing Components", Ball Bearing Journal 231(1), pp. 20-27.

42. E.V. Zaretsky, R.J. Parker and W.J. Anderson, "Component Hardness Differences and Their Effect on Bearing Fatigue", ASME Trans. Journal of Lubrication Technology, Jan. 1967, pp. 47-62.

43. F. W. Lanchester, "Spur Gear Erosion", Engineering, June 7, (1921), p. 733.

44. S. Way, "Pitting Due To Rolling Contacts", Journal of Applied Mechanics, A49-A58, 1935.

45. W.E. Littmann and R.L. Widner, "Propagation of Contact Fatigue From Surface and Subsurface Origins", ASME Trans., Sept. (1966), pp. 624-636.

46. T.E. Tallian, "On Competing Failure Modes in Rolling Contact", ASLE Trans. 10, pp. 418-439, (1967).

47. T.E. Tallian, "Rolling Contact Fatigue Control through Lubrication", IMechE Conference on Lubrication and Wear, (1967), pp. 205-236.

48. J. A. Martin and A. D. Eberhardt, "Indentification of Potential Failure Nuclei in Rolling Contact Fatigue", ASME Trans., Dec. (1967), pp. 932-942

49. S Borgese, "An Electron Fractographic Study of Spalls Formed in Rolling Contact", Journal of Basic Engineering, Dec (1969), pp. 943-948.

50. D. Scott and J. Blackwell, "Study of the Effects of Elevated-Temperature Lubricants on Materials for Rolling Elements", Proceedings of the IMechE, Vol. 181, Part 30, (1966-67), pp. 101-107.

51. M. Ciftan and E. Saibel, "The Effect of The Zeta Potential on Pitting", Wear, 53 (1979), pp. 201-209.

52. R.S. Zhou, H.S. Cheng and T. Mura, "Micropitting in Rolling and Sliding Contact under Mixed Lubrication", ASME Journal of Tribology, Oct. 1989, Vol. 111, pp. 605-613.

53. C.J. Polk and C.N. Rowe, "Crack Growth Rate: Its Measurement and a Controlling Factor in Rolling Contact Fatigue", ASLE Trans., Vol. 19, 1, (1976), pp.23-32.

54. F.T. Barwell, "Advances in Friction and Wear Mechanisms", Tribology International, Dec. 1984, Vol. 17 no. 6, pp.299-307.

55. H.A. Spikes, A.V. Olver and P.B. Macpherson, "Wear in Rolling Contacts", Wear, 112 (1986), pp. 121-144.

56. N.P. Suh, "The Delamination Theory of Wear", Wear, 25 (1973) 111-124.

57. T.E. Tallian, "Prediction of Rolling Contact Fatigue Life in Contaminated Lubricant: Part I - Mathematical Model", ASME Trans., April 1976, pp.251-257.

58. T.E. Tallian, "Prediction of Rolling Contact Fatigue Life in Contaminated Lubricant: Part II - Experimental", ASME Trans., July 1976, pp.384-392.

59. F.J. Archard, "The Temperature of Rubbing Surfaces", Wear, 2 (1958/59), pp.438-455.

60. C.N. Rowe, "Some Aspects of the Heat of Adsorption in the Function of a Boundary Lubricant", ASLE Trans. Vol. 9 (1966), pp. 100-111.

61. H. Salehizadeh and N. Saka, "Crack Propagation in Rolling Line Contacts", ASME Journal of Tribology, Oct. 1992, Vol. 114, pp.690-697.

62. A.A. Torrance, "The Metallography of Worn Surfaces and Some Theories of Wear", Wear, 50(1978), pp. 169-182.

63. R. Osterlund and O. Vingsbo, "Phase Changes in Fatigued Ball-Bearings", Metallurgical Trans. A, Vol. 11A, May 1980, 701-707.

64. A Werker and A. Voskamp, "Characterization of Distressed Rolling Bearing Raceways by X-Ray Diffraction, SKF paper.

65. A.P. Voskamp, "Material Response to Rolling Contact Loading", Journal of Tribology, July 1985, Vol. 107, pp. 359-366.

66. A.P. Voskamp, "Crystallographic Preferred Orientation Induced by Cyclic RollingContact Loading", Eighth International Conference on Textures of Materials, The Metallurgical Society, 1988.

67. W.J. Bartz, "The Influence of Lubricants on Failings of Bearings and Gears", Tribology International, Oct. 1976, pp.213-224.

68. S. Dizdar and S. Andersson, "Friction Characterisation of Boundary Layers at very low sliding velocity", 7th Nordic Symposium on Tribology NORDTRIB 96, Bergen, Norway, 1996.

69. U. Olofsson and S. Dizdar, "Surface Analysis of Boundary-Lubricated Spherical Roller Thrust Bearings ", Paper B, Licentiate Thesis, Royal Institute of Technology, KTH, S-100 44 Stockholm (1997).

70. S. Dizdar and S. Andersson, "Influence of Pre-formed Boundary Layers on Wear Transition in Sliding Lubricated Contacts ", Paper C, Licentiate Thesis, Royal Institute of Technology, KTH, S-100 44 Stockholm (1997).

71. P. Schatzberg and I.M. Felsen, " Effects of Water and Oxygen during Rolling Contact Lubrication", Wear, 12, (1968), pp. 331-342.

72. J.A. Ciruna and H.J. Szieleit, "The Effects of Hydrogen on the Rolling Contact Fatigue Life of AISI 52100 and 440C Steel Balls", Wear, 24, (1973), pp. 107-118.

73. E. Ioannides and B. Jacobson, "Dirty Lubricants-Reduced Bearing Life", Ball Bearing Journal Special (1989), pp. 22-27.

74. G.T.Y. Wan, A.v.d. Kommer and H. Lankamp, "Fourier Transform Infrared (FTIR) Studies of Lubricant Oxidation and Water Content", 1st International Symposium on Tribology", China, October 18th-23rd, (1993).

75. E.S. Forbes, "Antiwear and Extreme Pressure Additives for Lubricants", Tribology Aug. 1970, pp.145-152.

76. A.R. Lansdown, "Lubricants", Proc. of the IMechE International Conference. (1987), pp.365-378.

77. P.L. Wong, R. Wang and S. Lingard, "Pressure and Temperature Dependance of the Density of Liquid Lubricants", Wear, 200 (1996), pp. 58-63.

78. F.G. Rounds, "Lubricant and Ball Steel Effects on Fatigue Life", ASME Trans. , Journal of Lubrication Technology, Vol. 93, 2, (1971), pp.236-245.

79. F.G. Rounds, "Influence of Steel Composition on Additive Performance", ASLE Trans. , Vol. 15, 1, pp.54-66.

80. A. Cameron, "Lubricant Chemistry and Tribology Chemistry- Boundary and Extreme Pressure Lubrication", ", Proc. of the IMechE International Conference. (1987), pp.355-364.

81. R.J. Parker and E.V. Zaretsky, "Rolling-Element Fatigue Lives of Through-Hardened Bearing Materials", ASME Trans. Journal of Lubrication Technology, April 1972, pp. 165-173.

82. R.J. Parker and E.V. Zaretsky, "Effect of Lubricant Extreme-Pressure Additives on Rolling-Element Fatigue Life", NASA TN D-7383, July 1973

83. R.I. Barber, "The Preparation of Some Phosphorus Compounds and their Comparison as Load-Carrying Additives by The Four-Ball Machine", ASLE Trans. 19, pp. 319-328.

84. I.N. Lacey, G.H. Kelsall, H.A. Spikes and P.B. MacPherson, "Thick Antiwear Films in Elastohydrodynamic Contacts. Part 1: Film Growth in Rolling/Sliding EHD Contacts", ASLE Trans. Vol. 29, 3, pp. 299-305.

85. I.N. Lacey, G.H. Kelsall, H.A. Spikes and P.B. MacPherson, "Thick Antiwear Films in Elastohydrodynamic Contacts. Part 2: Chemical Nature of the Deposited Films", ASLE Trans. Vol. 29, 3, pp. 306-311.

86. M.R. Phillips and T.F.J. Quinn, "The Effect of Surface Roughness and Lubricant Film Thickness on the Contact Fatigue Life of Steel Surfaces Lubricated with a Sulphur-Phosphorus Type of Extreme Pressure Additive", Wear, 51 (1978), pp. 11-24.

87. G.D. Galvin and H. Naylor, "Effect of Lubricants on the Fatigue of Steel and other Metals", Proc. Inst. Mech. Eng., Vol 179 part 3J, 1964-65, pp.56-77.

88. J.S. Sheasby, T.A. Caughlin and W.A. Mackwood, "A Comparison of the Boundary Lubrication of 52100 Steel, Zirconia and Silicon Nitride by S, P, S/P and Zinc Dialkyl Dithiophosphate Additives", Wear, 196 (1996), pp. 100-109.

89. H.A. Spikes and A. Cameron, "Additive Interference in Dibenzyl Disulfide Extreme Pressure Lubrication", ASLE Trans., Vol.17, 4, (1976), pp. 283-289.

90. J.M. Georges, J.M. Martin, T. Mathia, P.H. Kapsa, G. Meille and H. Montes, "Mechanisms of Boundary Lubrication with Zinc Dithiophosphate", Wear, 53 (1979), pp. 9-34.

91. B.A. Khorramian, G.R. Iyer, S. Kodali, P. Natarajan and R. Tupil, "Review of Antiwear Additives for Crankcase Oils", Wear, 169 (1993), pp. 87-95.

92. P. Cann, H.A. Spikes and A. Cameron, "Thick Film Formation by Zinc Dialkyl Dithiophosphates", ASLE Trans., Vol. 26, 1, pp. 48-52, (1983).

93. H. So and Y.C. Lin, "The Theory of Antiwear for ZDDP at Elevated Temperature in Boundary Lubrication Condition", Wear, 177 (1994), pp.105-115.

94. L. Rosado, "Evaluation of Fatigue and Wear Characteristics of M50 Steel using High Temperature Synthetic Turbine Engine Lubricants - Part II", Wear, 196 (1996), pp. 133-140.

95. A. Gauthier, H. Montes and J.M. Georges, "Boundary Lubrication with Tricresylphosphate (TCP). Importance of Corrosive Wear", ASLE Trans. Vol. 25, 4, pp. 445-455.

96. H.E. Bieber, E.E. Klaus and E.J. Tewksbury, "A Study of Tricresyl Phosphate as an Additive for Boundary Lubrication", ASLE Trans., 11, 1968, pp.155-161.

97. N.E. Gallopoulos and C.K. Murphy, "Interactions Between a Zinc Dialkylphos-phorodithioate and Lubricating Oil Dispersants", ASLE Trans. 14, pp. 1-7.

98. E.S. Forbes, "Antiwear and Extreme Pressure Additives for Lubricants", Tribology Aug. 1970, pp.145-152.

99. E.S. Forbes and J. Battersby, "The Effect of Chemical Structure on the Load-Carrying and Adsorption Properties of Dialkyl Phosphites", ASLE Trans. Vol. 17, 4, pp. 263-270.

100. K.G. Allum and E.S. Forbes, "The Load-Carrying Mechanism of Sulfur Compounds- Application of Electron Probe Microanalysis", ASLE Trans. 11, (1968), pp.162-175.

101. T.E. Tallian, "Rolling Contact Fatigue", Ball Bearing Journal, Vol. 217, pp. 5-13.

102. G. Lundberg and A Palmgren, "Dynanmic Capacity of Rolling Bearings", Journal of Applied Mechanics, June 1949, pp. 165-172.

103. R.E. Cantley, "Predicting the Effect of Lubricant Chemistry on Bearing Fatigue Life", ASLE Trans., Vol. 26, 1, pp. 80-86.

104. D. Scott, "Study of the Effect of Lubricant on Pitting Failure of Balls", Proc. Conference on Lubrication and Wear 1957, Paper 58, 463, IMechE.

105. D.M. Rowson and Y.L. Wu, "The Effect of the Additive Chemistry of Elemental Sulphur on the Contact Fatigue Life of Steel EN31 Discs", Wear, 70 (1981), pp. 373-381.

106. A. Begelinger and A.W.J.De Gee, "Thin Film Lubrication of Sliding Point Contacts of AISI 52100 Steel", Wear, 28 (1974), pp.103-114.

107. D. Godfrey, "The Lubrication Mechanism of Tricresyl Phosphate on Steel", ASLE Trans., 8, (1965), pp.1-11.

108. J.M. Hall, "Antiwear Additives in Neopentyl Ester Oils", ASLE Trans. Vol. 14, 4, pp. 292-300.

109. W. Davey, "Extreme Pressure Lubricants-Phosphorus Compounds as Additives", Industrial and Engineering Chemistry, Sept. 1950, pp. 1841-1847.

110. T.N. Mills and A. Cameron, "Basic Studies on Boundary, EP, and Piston-Ring Lubrication using a Special Apparatus", ASLE Trans., Vol. 25, 1, pp.117-124.

111. P.E. Fowles, A. Jackson and W.R. Murphy, "Lubricant Chemistry on Rolling Contact Fatigue- The Performance and Mechanism of one Antifatigue Additive", ASLE Trans., 24, 1, pp. 107-118.

112. T.P. Debies and W.G. Johnson, "Surface Chemistry of some Antiwear Additives as Determined by Electron Spectroscopy", ASLE Trans. Vol. 23, 3, (1980), pp. 456-464.

113. J. Dimnet and J.M. Georges, "Some Aspects of the Mechanical Behaviour of Films in Boundary Lubrication", ASLE Trans. Vol. 25, 4, pp. 456-464.

114. L. A. Hamilton and W.W. Woods, "Reaction of Iron with Organic Sulfur Compounds", Industrial and Engineering Chemistry", March 1950, pp. 513-519.

115. D. Godfrey, "Chemical Changes in Steel Surfaces during Extreme Pressures Lubrication", ASLE Trans., 5, (1962), pp.57-66.

116. P.E. Fowles, A. Jackson and W.R. Murphy, "Lubricant Chemistry on Rolling Contact Fatigue- The Performance and Mechanism of one Antifatigue Additive", ASLE Trans., 24, 1, pp. 107-118.

117. E.S. Forbes and N.T. Upsdell, "Phosphorus Load-Carrying Additives: Adsorption/Reaction Studies of Amine Phosphates and there Load-Carrying Mechanisms", Proceedings of the 1st European Tribology Conference (1973), pp. 277-286.

118. T. Sakurai and K. Sato, "Study of Corrosion and Correlation between Chemical Reactivity and Load-Carrying Capacity of Oils Containing Extreme Pressure Agents", ASLE Trans., 9 (1966) p. 77.

119. J.M. Georges, J.M. Martin, T. Mathia, P.H. Kapsa, G. Meille and H. Montes, "Mechanisms of Boundary Lubrication with Zinc Dithiophosphate", Wear, 53 (1979), pp. 9-34.

120. D. Godfrey, "Chemical Changes in Steel Surfaces during Extreme Pressures Lubrication", ASLE Trans., 5, (1962), pp.57-66.

121. T.E. Tallian, "Prediction of Rolling Contact Fatigue Life in Contaminated Lubricant: Part I - Mathematical Model", ASME Trans., April 1976, pp.251-257.

122. T.E. Tallian, "Prediction of Rolling Contact Fatigue Life in Contaminated Lubricant: Part II - Experimental", ASME Trans., July 1976, pp.384-392.

123. A. Sethuramiah, H. Okabe and T. Sakurai, "Critical Temperatures in EP Lubrication", Wear, 26 (1973), pp. 187-206.

124. G. Salomon, "Failure Criteria in Thin Film Lubrication- the IRG Program", Wear, Vol. 36, (1976), pp. 1-6.

125. F.J. Archard, "The Temperature of Rubbing Surfaces", Wear, 2 (1958/59), pp.438-455.

126. G.T.Y. Wan, H. Lankamp, A. de Vries and E. Ioannides, "The effect of extreme pressure (EP) lubricants on the life of rolling element bearings", Proc. Inst. Mech. Engrs., Vol. 208 (1994) pp. 247-252.

127. F.G. Rounds, "Influence of Steel Composition on Additive Performance", ASLE Trans. , Vol. 15, 1,(1972), pp.54-66.

128. F.G. Rounds, "Lubricant and Ball Steel Effects on Fatigue Life", ASME Trans. , Journal of Lubrication Technology, Vol. 93, 2, (1971), pp.236-245.

129. R.J. Stokes, J.S.C. Parry and A.A. Torrance, "A New Rolling Contact Fatigue Test Machine", An International Symposium - Performance and Testing of Gear Oils and Transmission Fluids", (1980), pp. 35-42.

130. F.G. Rounds, "Some Environmental Factors Affecting Surface Coating Formation with Lubricant Oil Additives", ASLE Trans., Vol. 9 (1966), pp. 88-100.

131. E.C. Levine and M.B. Peterson, N.A.C.A. Report TN 2460.

132. W. Davey, Journal of Inst. of Petroleum, 31, (1945), pp. 73-88.

133. F.T. Barcroft, R.J. Bird, J.F. Hutton and D. Park, " The Mechanism of Action of Zinc Thiophosphates as Extreme Pressure Agents", Wear, 77 (1982), pp. 355-384.

134. F.T. Barcroft and D. Park, "Interactions on Heated Metal Surfaces Between Zinc Dialkyldithiophosphates and Other Lubricating Oil Additives", Wear, 108, (1986), PP. 213-234.

135. T. Sakurai, H. Okabe and M. Tomaru," Effect of Stress-Induced Heterogeneity on Corrosion of Iron Surface at High Temperatures", Bulletin of The Japan Petroleum Institute, Vol. 14, No. 2, Nov. 1972, pp. 161-168.

136. T. Sakurai, "Role of Chemistry in the Lubrication of Concentrated Contacts", ASME Journal of Lubricated Contacts, Oct. 1981, Vol. 103, pp.473-485.

137. T. Sakamoto, H. Uetz, J. Fohl and M.A. Khosrawi, "The Reaction Layer Formed on Steel by Additives Based on Sulphur and Phosphorus Compounds under Conditions of Boundary Lubrication", Wear, 77 (1982), pp.139-157.

138. T. Sakurai and K. Sato, "Study of Corrosion and Correlation Between Chemical Reactivity and Load-Carrying Capacity of Oils Containing Extreme Pressure Agents", ASLE Trans. Vol. 9 (1966), pp. 77-87.

139. T. Sakurai and K. Sato, "Chemical Reactivity and Load Carrying Capacity of Lubricating Oils Containing Organic Phosphorus Compounds", ASLE Trans. Vol. 13, pp. 252-261.

APPENDIX A

HERTZIAN STRESS AND FILM-THICKNESS CALCULATIONS FOR BRISTOL TESTS

HERTZIAN STRESS CALCULATIONS

Principle radii of mating surfaces:

R_{11} = 5.556 mm

R_{12} = 5.556 mm

R_{21} = -5.87 mm

R_{22} = 15.75 mm

$$B = \frac{1}{4}\left(\frac{1}{R_{11}} + \frac{1}{R_{21}} + \frac{1}{R_{12}} + \frac{1}{R_{22}}\right) + \frac{1}{4}\sqrt{\left[\left[\left(\frac{1}{R_{11}} - \frac{1}{R_{12}}\right) + \left(\frac{1}{R_{21}} - \frac{1}{R_{22}}\right)\right]^2 - 4\left(\frac{1}{R_{11}} - \frac{1}{R_{12}}\right)\left(\frac{1}{R_{21}} - \frac{1}{R_{22}}\right)Sin^2\alpha\right]}$$

$$B = \frac{1}{4}\left(\frac{1}{5.556} + \frac{1}{-5.87} + \frac{1}{5.556} + \frac{1}{15.75}\right) + \frac{1}{4}\sqrt{\left[\left[\left(\frac{1}{5.556} - \frac{1}{5.556}\right) + \left(\frac{1}{-5.87} - \frac{1}{15.75}\right)\right]^2 - 4\left(\frac{1}{5.556} - \frac{1}{5.556}\right)\left(\frac{1}{-5.87} - \frac{1}{15.75}\right)Sin^2\alpha\right]}$$

B = 0.063276 + 0.058462

= 0.121738 mm^{-1}

$$A = \frac{1}{4}\left(\frac{1}{R_{11}} + \frac{1}{R_{21}} + \frac{1}{R_{12}} + \frac{1}{R_{22}}\right) - \frac{1}{4}\sqrt{\left[\left[\left(\frac{1}{R_{11}} - \frac{1}{R_{12}}\right) + \left(\frac{1}{R_{21}} - \frac{1}{R_{22}}\right)\right]^2 - 4\left(\frac{1}{R_{11}} - \frac{1}{R_{12}}\right)\left(\frac{1}{R_{21}} - \frac{1}{R_{22}}\right)Sin^2\alpha\right]}$$

$$A = \frac{1}{4}\left(\frac{1}{5.556} + \frac{1}{-5.87} + \frac{1}{5.556} + \frac{1}{15.75}\right) - \frac{1}{4}\sqrt{\left[\left[\left(\frac{1}{5.556} - \frac{1}{5.556}\right) + \left(\frac{1}{-5.87} - \frac{1}{15.75}\right)\right]^2 - 4\left(\frac{1}{5.556} - \frac{1}{5.556}\right)\left(\frac{1}{-5.87} - \frac{1}{15.75}\right)Sin^2\alpha\right]}$$

A = 0.063276 - 0.058462

$$= \quad 0.004814 \text{ mm}^{-1}$$

$$\Delta = \frac{2}{A+B}\left(\frac{1-\nu^2}{E_Y}\right)$$

$$\Delta = \frac{2}{(0.126552)}\left(\frac{1-(0.29)^2}{200\text{X}10^3}\right)$$

$$= \quad 72.373 \text{ X } 10^{-6} \text{ mm}^3/\text{N}$$

$$\frac{B}{A} = \frac{0.12174}{0.00481} = 25.310$$

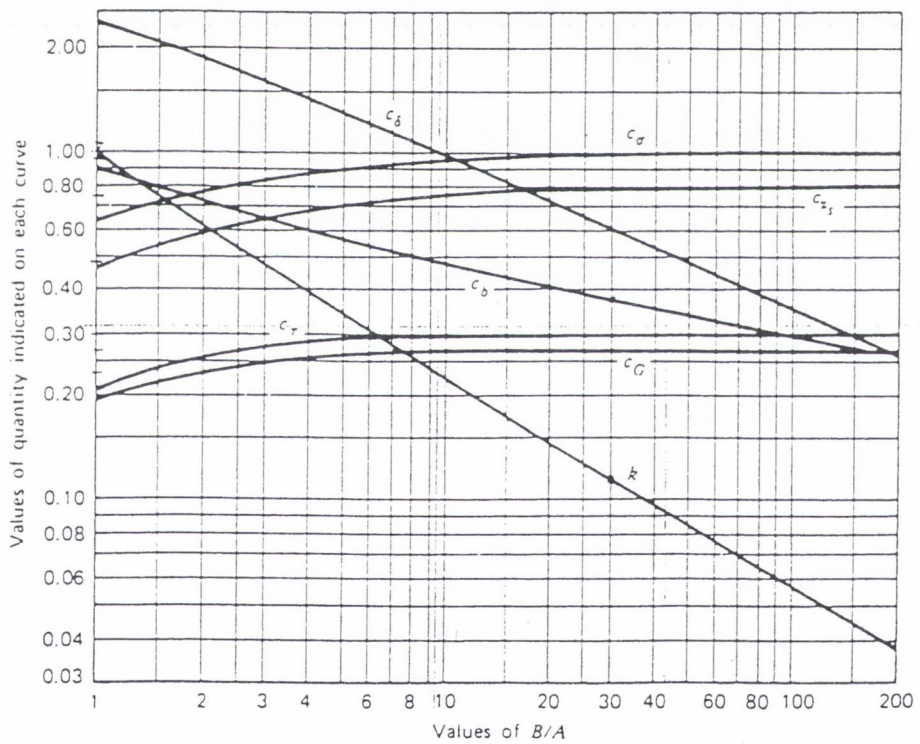

Figure A1 Stress and deflection coefficients for two bodies in contact at a point

From graph:

Cb	=	0.38	K	=	0.13
Cσ	=	1.00	Cτ	=	0.30
Cg	=	0.27	Czs	=	0.80

$$P = 100 \text{ (Bar)}$$

$$= 100(101300) \text{ (Pa)}$$

$$= 10.13 \text{ (N/mm}^2\text{)}$$

$$A = \pi r^2$$

$$= \pi(5.556)^2$$

$$= 96.98 \text{ (mm}^2\text{)}$$

$$F = 982.40 \text{ (N)}$$

$$b = 0.38\left[(982.4)(72.373 \times 10^{-6})\right]^{-0.33}$$

$$= 0.1574 \text{ mm (semi-minor axis)}$$

$$a = \frac{b}{k}$$

$$= 0.1574/0.13$$

$$= 1.211 \text{ mm (semi-major axis)}$$

$$\frac{b}{\Delta} = \frac{0.1574}{72.373 \times 10^{-6}}$$

$$= 2174.8 \text{ (MPa)}$$

$\sigma_{max} = -C\sigma(b/\Delta) = -1.00(2175) = -2175$ (MPa)

$\tau_{max} = C\tau(b/\Delta) = 0.30(2175) = 652.5$ (MPa)

$\tau_{oct} = Cg(b/\Delta) = 0.27(2175) = 587.3$ (MPa)

σ_{max} = Max. Hertzian stress = 2.175 (GPa) compressive

FILM THICKNESS CALCULATIONS

Hamrock and Dowson Equations

Central-film-thickness equation:

$$H_c = \left[2.69(U)^{0.67}(\alpha E')^{0.53}(W)^{-0.067}\left(1-0.61e^{-0.73k}\right)\right]$$

Minimum-film-thickness equation:

$$H_0 = \left[3.63(U)^{0.68}(\alpha E')^{0.49}(W)^{-0.073}\left(1-e^{-0.68k}\right)\right]$$

Dimensionless film thickness

$$H_c = \frac{h_c}{R_x} \qquad H_o = \frac{h_0}{R_x}$$

where

$$\frac{1}{R_x} = \frac{1}{r_{11}} + \frac{1}{r_{21}}$$

$$= \frac{1}{5.556\times10^{-3}} + \frac{1}{15.75\times10^{-3}}$$

$$= 179.98 + 63.49$$

$$= 243.47$$

$$R_x = 0.004107$$

Dimensionless speed parameter

$$U = \frac{\eta_0 u}{E' R_x}$$

$$= \frac{\left(2.47\times10^{-2}\right)(1.65)}{\left(2.27\times10^{11}\right)(0.00411)}$$

$$= 4.3622 \text{ x } 10^{-11}$$

where

$$u = \frac{u_a + u_b}{2}$$

$$= \frac{1.65 + 1.65}{2}$$

$$= \quad 1.65$$

$$k = 1.03\left(\frac{R_y}{R_x}\right)^{0.64}$$

$$= 1.03\left(\frac{0.104}{0.00411}\right)^{0.64}$$

$$= 8.142$$

where $$\frac{1}{R_y} = \frac{1}{r_{12}} + \frac{1}{r_{22}}$$

$$= \frac{1}{5.556\times10^{-3}} + \frac{1}{-5.87\times10^{-3}}$$

$$= 179.98 - 170.36$$

$$= 9.62$$

$$R_y = 0.104$$

Dimensionless load parameter

$$W = \frac{F}{E' R_x^2}$$

$$W = \frac{982.4}{\left(2.27\times10^{11}\right)\left(.00411\right)^2}$$

$$= 2.562 \text{ x } 10^{-4}$$

where $$E' = \frac{2}{\frac{1-\nu_1^2}{E_1} + \frac{1-\nu_2^2}{E_2}}$$

$$= \frac{2}{\frac{1-0.3^2}{2.07\times10^{11}} + \frac{1-0.3^2}{2.07\times10^{11}}}$$

$$= 2.27 \text{ x } 10^{11}$$

R_{11}	=	ball radius x-direction	R_{12}	=	ball radius y-direction
R_{21}	=	race radius x-direction	R_{22}	=	race radius y-direction

u	=	surface velocity in x direction	=	1.65 (m/s)
F	=	total normal load	=	982.4 (N)
$E1,E2$	=	Young's moduli of ball , race	=	2.07×10^{11} (N/m^2)
E'	=	reduced Young's Modulus	=	2.27×10^{11} (N/m^2)
ν_1 , ν_2	=	Poisson's ratios of ball , race	=	0.3
R_x	=	reduced radius	=	0.004107 (m)
R_y	=	reduced radius	=	0.103865 (m)
η_o	=	dynamic viscosity	=	2.47×10^{-2} (Pa s)
α	=	pressure-viscosity coefficient	=	2.5×10^{-8} (m^2/N)
h_c	=	central film thickness (m)	=	2.147×10^{-7} (m)
h_o	=	minimum film thickness (m)	=	1.694×10^{-7} (m)

LAMBDA RATIO EQUATION

$$\Lambda = \frac{h_o}{\sqrt{\left(R_{q1}^{\ 2} + R_{q2}^{\ 2}\right)}}$$

$$= \frac{0.17}{\sqrt{\left(0.5^2 + 0.03^2\right)}}$$

$$= 0.4$$

Where:

h_o = minimum EHD film thickness

$R_{q1}^{\ 2}$ = RMS roughness of the raceway

$R_{q2}^{\ 2}$ = RMS roughness of the ball

APPENDIX B

HERTZIAN STRESS AND FILM-THICKNESS CALCULATIONS FOR R2F TESTS

HERTZIAN STRESS CALCULATIONS

Principle radii of mating surfaces:

R_{11} = 5.556 mm

R_{12} = 5.556 mm

R_{21} = -5.73 mm

R_{22} = 17.5 mm

$$B = \frac{1}{4}\left(\frac{1}{R_{11}} + \frac{1}{R_{21}} + \frac{1}{R_{12}} + \frac{1}{R_{22}}\right) + \frac{1}{4}\sqrt{\left[\left[\left(\frac{1}{R_{11}} - \frac{1}{R_{12}}\right) + \left(\frac{1}{R_{21}} - \frac{1}{R_{22}}\right)\right]^2 - 4\left(\frac{1}{R_{11}} - \frac{1}{R_{12}}\right)\left(\frac{1}{R_{21}} - \frac{1}{R_{22}}\right)Sin^2\alpha\right]}$$

$$B = \frac{1}{4}\left(\frac{1}{5.556} + \frac{1}{-5.73} + \frac{1}{5.556} + \frac{1}{17.5}\right) + \frac{1}{4}\sqrt{\left[\left[\left(\frac{1}{5.556} - \frac{1}{5.556}\right) + \left(\frac{1}{-5.73} - \frac{1}{17.5}\right)\right]^2 - 4\left(\frac{1}{5.556} - \frac{1}{5.556}\right)\left(\frac{1}{-5.73} - \frac{1}{17.5}\right)Sin^2\alpha\right]}$$

B = 0.060625 + 0.0579

= 0.1185 mm^{-1}

$$A = \frac{1}{4}\left(\frac{1}{R_{11}} + \frac{1}{R_{21}} + \frac{1}{R_{12}} + \frac{1}{R_{22}}\right) - \frac{1}{4}\sqrt{\left[\left[\left(\frac{1}{R_{11}} - \frac{1}{R_{12}}\right) + \left(\frac{1}{R_{21}} - \frac{1}{R_{22}}\right)\right]^2 - 4\left(\frac{1}{R_{11}} - \frac{1}{R_{12}}\right)\left(\frac{1}{R_{21}} - \frac{1}{R_{22}}\right)Sin^2\alpha\right]}$$

$$A = \frac{1}{4}\left(\frac{1}{5.556} + \frac{1}{-5.73} + \frac{1}{5.556} + \frac{1}{17.5}\right) - \frac{1}{4}\sqrt{\left[\left[\left(\frac{1}{5.556} - \frac{1}{5.556}\right) + \left(\frac{1}{-5.73} - \frac{1}{17.5}\right)\right]^2 - 4\left(\frac{1}{5.556} - \frac{1}{5.556}\right)\left(\frac{1}{-5.73} - \frac{1}{17.5}\right)Sin^2\alpha\right]}$$

A = 0.060625 - 0.0579

= 0.00273 mm^{-1}

$$\Delta = \frac{2}{A+B}\left(\frac{1-\nu^2}{E}\right)$$

$$\Delta = \frac{2}{(0.12123)}\left(\frac{1-(0.29)^2}{200X10^3}\right)$$

$$= 75 \text{ X } 10^{-6} \text{ mm}^3/\text{N}$$

$$\frac{B}{A} = \frac{0.1185}{0.00273} = 43.4$$

From Figure A1:

Cb	=	0.35	K	=	0.092
Cσ	=	1.00	Cτ	=	0.30
Cg	=	0.27	Czs	=	0.80

$$P = \frac{4P_0}{n}$$

P_0 = dynamic load rating

n = No. of balls

F = 9.75 (kN)

$$b = 0.35\left[(9750)(75\times10^{-6})\right]^{-0.33}$$

= 0.315 mm (semi-minor axis)

$$a = \frac{b}{k}$$

= 0.315/0.092

= 3.427 mm (semi-major axis)

$$\frac{b}{\Delta} = \frac{0.315}{75\times10^{-6}}$$

= 4200 (MPa)

σ_{max}	=	$-C\sigma(b/\Delta)$	=	-1.00(4200)	= -4200	(MPa)
τ_{max}	=	$C\tau\ (b/\Delta)$	=	0.30(4200)	= 1260	(MPa)
τ_{oct}	=	$Cg(b/\Delta)$	=	0.27(4200)	= 1134	(MPa)

σ_{max} = Max. Hertzian stress = 4.2 (GPa) compressive

FILM THICKNESS CALCULATIONS

Hamrock and Dowson Equations

Central-film-thickness equation:

$$H_c = \left[2.69(U)^{0.67}(\alpha E')^{0.53}(W)^{-0.067}\left(1-0.61e^{-0.73k}\right)\right]$$

Minimum-film-thickness equation:

$$H_0 = \left[3.63(U)^{0.68}(\alpha E')^{0.49}(W)^{-0.073}\left(1-e^{-0.68k}\right)\right]$$

Dimensionless film thickness

$$H_c = \frac{h_c}{R_x} \qquad H_o = \frac{h_0}{R_x}$$

where

$$\frac{1}{R_x} = \frac{1}{r_{11}} + \frac{1}{r_{21}}$$

$$= \frac{1}{5.556\times10^{-3}} + \frac{1}{17.5\times10^{-3}}$$

$$= 179.98 + 57.14$$

$$= 237.12$$

$$R_x = 0.004217$$

Dimensionless speed parameter

$$U = \frac{\eta_0 u}{E' R_x}$$

$$= \frac{\left(1.28\times10^{-2}\right)(4.581)}{\left(2.27\times10^{11}\right)(0.004217)}$$

$$= 0.613 \text{ x } 10^{-10}$$

where

$$u = \frac{u_a + u_b}{2}$$

$$= \frac{4.581+4.581}{2}$$

$$= \quad 4.581$$

$$k = 1.03\left(\frac{R_y}{R_x}\right)^{0.64}$$

$$= 1.03\left(\frac{0.1831}{0.004217}\right)^{0.64}$$

$$= 11.509$$

where $$\frac{1}{R_y} = \frac{1}{r_{12}} + \frac{1}{r_{22}}$$

$$= \frac{1}{5.556\times10^{-3}} + \frac{1}{-5.73\times10^{-3}}$$

$$= 179.98 - 174.52$$

$$= 5.45$$

$$R_y = 0.1831$$

Dimensionless load parameter

$$W = \frac{F}{E' R_x^2}$$

$$W = \frac{9750}{\left(2.27\times10^{11}\right)(.004217)^2}$$

$$= 2.415 \text{ x } 10^{-3}$$

where $$E' = \frac{2}{\frac{1-\nu_1^2}{E_1} + \frac{1-\nu_2^2}{E_2}}$$

$$= \frac{2}{\frac{1-0.3^2}{2.07\times10^{11}} + \frac{1-0.3^2}{2.07\times10^{11}}}$$

$$= 2.27 \text{ x } 10^{11}$$

R_{11}	=	ball radius x-direction	R_{12}	=	ball radius y-direction
R_{21}	=	race radius x-direction	R_{22}	=	race radius y-direction

u	=	surface velocity in x direction	=	4.581 (m/s)
F	=	total normal load	=	9750 (N)
$E1,E2$	=	Young's moduli of ball , race	=	2.07×10^{11} (N/m^2)
E'	=	reduced Young's Modulus	=	2.27×10^{11} (N/m^2)
ν_1, ν_2	=	Poisson's ratios of ball , race	=	0.3
R_x	=	reduced radius	=	0.004217 (m)
R_y	=	reduced radius	=	0.1831 (m)

For TT 68 @ 80 °C

η_o	=	dynamic viscosity	=	1.28×10^{-2} (Pa s)
α	=	pressure-viscosity coefficient	=	2.5×10^{-8} (m^2/N)
h_c	=	central film thickness (m)	=	2.38×10^{-7} (m)
h_o	=	minimum film thickness (m)	=	0.17×10^{-7} (m)

LAMBDA RATIO EQUATION

$$\Lambda = \frac{h_o}{\sqrt{\left(R_{q1}^{\ 2} + R_{q2}^{\ 2}\right)}}$$

$$= \frac{0.17}{\sqrt{\left(0.03^2 + 0.03^2\right)}}$$

$$= 4$$

Where:

h_o = minimum EHD film thickness

$R_{q1}^{\ 2}$ = RMS roughness of the raceway

$R_{q2}^{\ 2}$ = RMS roughness of the ball

APPENDIX C

WEIBULL ANALYSES OF ROLLING CONTACT FATIGUE RESULTS.

Distribution Function Analysis
Weibull Dist. Parameter Estimates (ML)

	Life		F %
SUBGROUP 1:	156.4 Hrs	FAILED	5.6
SUBGROUP 2:	159.0 Hrs	FAILED	13.7
SUBGROUP 3:	185.8 Hrs	FAILED	21.8
SUBGROUP 4:	193.2 Hrs	FAILED	29.8
SUBGROUP 5:	237.0 Hrs	FAILED	37.9
SUBGROUP 6:	247.6 Hrs	FAILED	46.0
SUBGROUP 7:	286.9 Hrs	FAILED	54.0
SUBGROUP 8:	340.4 Hrs	FAILED	62.1
SUBGROUP 9:	364.3 Hrs	FAILED	70.2
SUBGROUP 10:	382.3 Hrs	FAILED	78.2
SUBGROUP 11:	469.0 Hrs	FAILED	86.4
SUBGROUP 12:	671.6 Hrs	SUSPENDED	94.3

12 Subgroup(s), 11 Failed, Subgroup Size = 1

Shape: 2.27262
Scale: 349.042

Percentile Estimates

Percent	Percentile	90% CI Approximate Lower Limit	90% CI Approximate Upper Limit
1	46.110	17.708	120.068
2	62.694	27.192	144.547
3	75.107	34.965	161.334
4	85.436	41.815	174.565
5	94.466	48.058	185.692
6	102.594	53.863	195.410
7	110.050	59.334	204.113
8	116.984	64.539	212.046
9	123.499	69.525	219.375
10	129.669	74.328	226.214
20	180.402	116.306	279.821
30	221.752	152.863	321.687
40	259.724	187.374	360.009
50	297.055	221.448	398.477
60	335.870	256.323	440.104
70	378.748	293.465	488.815
80	430.347	335.497	552.012
90	503.802	389.797	651.150
91	513.819	396.721	665.480
92	524.730	404.141	681.301
93	536.761	412.181	698.994
94	550.237	421.017	719.116
95	565.651	430.915	742.515
96	583.819	442.310	770.600
97	606.229	455.988	805.970
98	636.131	473.647	854.354
99	683.470	500.380	933.553

Table C1 Bristol tests with Vitrea M100 + 0% (S/P)

Weibull Dist. Parameter Estimates (ML)

	Life		F %
SUBGROUP 1:	78.3 Hrs	FAILED	5.6
SUBGROUP 2:	239.0 Hrs	FAILED	13.7
SUBGROUP 3:	253.5 Hrs	FAILED	21.8
SUBGROUP 4:	279.3 Hrs	FAILED	29.8
SUBGROUP 5:	312.7 Hrs	FAILED	37.9
SUBGROUP 6:	327.1 Hrs	FAILED	46.0
SUBGROUP 7:	399.6 Hrs	FAILED	54.0
SUBGROUP 8:	429.3 Hrs	FAILED	62.1
SUBGROUP 9:	580.7 Hrs	FAILED	70.2
SUBGROUP 10:	610.7 Hrs	FAILED	78.2
SUBGROUP 11:	671.4 Hrs	SUSPENDED	86.4
SUBGROUP 12:	719.4 Hrs	SUSPENDED	94.3

Shape: 2.29372
Scale: 460.884

Percentile Estimates

Percent	Percentile	90% CI Approximate ower Limit	90% CI Approximate Upper Limit
1	62.029	22.232	173.07
2	84.100	34.477	205.14
3	100.585	44.593	226.88
4	114.282	53.550	243.89
5	126.245	61.746	258.12
6	137.002	69.390	270.49
7	146.864	76.612	281.53
8	156.030	83.496	291.57
9	164.637	90.104	300.82
10	172.785	96.480	309.44
20	239.658	152.547	376.51
30	294.032	201.693	428.65
40	343.879	248.160	476.52
50	392.822	293.905	525.03
60	443.648	340.339	578.32
70	499.733	389.061	641.89
80	567.147	442.963	726.15
90	662.991	510.494	861.04
91	676.050	518.948	880.71
92	690.273	527.974	902.46
93	705.953	537.714	926.83
94	723.511	548.375	954.58
95	743.591	560.267	986.90
96	767.250	573.895	1025.75
97	796.425	590.177	1074.75
98	835.338	611.082	1141.89
99	896.909	642.523	1252.01

Table C2 Bristol tests with Vitrea M100 + 2% (S/P)

Weibull Dist. Parameter Estimates (ML)

	Life		F %
SUBGROUP 1:	105.5 Hrs	FAILED	5.6
SUBGROUP 2:	168.1 Hrs	FAILED	13.7
SUBGROUP 3:	168.7 Hrs	FAILED	21.8
SUBGROUP 4:	192.5 Hrs	FAILED	29.8
SUBGROUP 5:	197.0 Hrs	FAILED	37.9
SUBGROUP 6:	239.6 Hrs	FAILED	46.0
SUBGROUP 7:	274.1 Hrs	FAILED	54.0
SUBGROUP 8:	281.1 Hrs	FAILED	62.1
SUBGROUP 9:	343.3 Hrs	FAILED	70.2
SUBGROUP 10:	422.5 Hrs	FAILED	78.2
SUBGROUP 11:	475.3 Hrs	FAILED	86.4
SUBGROUP 12:	749.9 Hrs	SUSPENDED	94.3

Shape: 1.91041
Scale: 342.226

Percentile Estimates

Percent	Percentile	90% CI Approximate Lower Limit	90% CI Approximate Upper Limit
1	30.800	9.912	95.71
2	44.390	16.497	119.44
3	55.032	22.239	136.18
4	64.149	27.504	149.62
5	72.293	32.448	161.07
6	79.751	37.155	171.18
7	86.692	41.679	180.32
8	93.229	46.057	188.71
9	99.437	50.313	196.52
10	105.375	54.468	203.86
20	156.074	92.705	262.76
30	199.504	128.261	310.32
40	240.774	163.347	354.90
50	282.484	199.216	400.56
60	326.919	237.034	450.89
70	377.148	278.414	510.90
80	439.033	326.484	590.38
90	529.560	390.358	718.40
91	542.108	398.636	737.22
92	555.830	407.539	758.08
93	571.024	417.224	781.52
94	607.769	439.933	839.63
96	631.060	453.842	877.48
97	659.980	470.633	925.51
98	698.884	492.457	991.84
99	761.182	525.801	1101.93

Table C3 Bristol tests with Vitrea M100 + 5% (S/P)

Weibull Dist. Parameter Estimates (ML)

	Life		F %
SUBGROUP 1:	134.3 Hrs	FAILED	5.6
SUBGROUP 2:	342.3 Hrs	FAILED	13.7
SUBGROUP 3:	378.9 Hrs	FAILED	21.8
SUBGROUP 4:	398.9 Hrs	FAILED	29.8
SUBGROUP 5:	462.9 Hrs	FAILED	37.9
SUBGROUP 6:	623.2 Hrs	SUSPENDED	46.0
SUBGROUP 7:	654.8 Hrs	SUSPENDED	54.0
SUBGROUP 8:	659.7 Hrs	SUSPENDED	62.1
SUBGROUP 9:	671.3 Hrs	SUSPENDED	70.2
SUBGROUP 10:	671.8 Hrs	SUSPENDED	78.3
SUBGROUP 11:	671.9 Hrs	SUSPENDED	86.4
SUBGROUP 12:	681.7 Hrs	SUSPENDED	94.3

Shape: 3.71524
Scale: 586.642

Percentile Estimates

Percent	Percentile	90% CI Approximate Lower Limit	90% CI Approximate Upper Limit
1	170.073	86.116	335.88
2	205.236	113.884	369.87
3	229.218	134.165	391.61
4	248.015	150.760	408.01
5	263.737	165.078	421.36
6	277.393	177.823	432.72
7	289.557	189.402	442.67
8	300.584	200.078	451.58
9	310.716	210.027	459.68
10	320.122	219.380	467.13
20	391.775	293.728	522.55
30	444.490	350.825	563.16
40	489.611	400.087	599.17
50	531.532	445.040	634.83
60	572.999	487.560	673.41
70	616.697	529.094	718.81
80	666.810	571.676	777.77
90	734.290	620.770	868.57
91	743.186	626.637	881.41
92	752.801	632.841	895.50
93	763.313	639.471	911.14
94	774.978	646.652	928.77
95	788.187	654.576	949.07
96	803.577	663.549	973.16
97	846.886	687.507	1043.21
99	884.899	707.226	1107.21

Table C4 Bristol tests with Shell Spirax AX 80W-90

Distribution Function Analysis
Weibull Dist. Parameter Estimates (ML)

	Life		F %
SUBGROUP 1:	390 Hrs	SUSPENDED	9.4
SUBGROUP 2:	394 Hrs	FAILED	22.8
SUBGROUP 3:	574 Hrs	FAILED	36.4
SUBGROUP 4:	790 Hrs	SUSPENDED	50.0
SUBGROUP 5:	938 Hrs	FAILED	63.5
SUBGROUP 6:	1300 Hrs	FAILED	77.1
SUBGROUP 7:	1342 Hrs	FAILED	90.5

Shape: 2.44077
Scale: 927.592

Percentile Estimates

Percent	Percentile	90% CI Approximate Lower Limit	90% CI Approximate Upper Limit
1	140.88	39.94	496.87
2	187.53	62.66	561.29
3	221.88	81.57	603.54
4	250.17	98.41	635.95
5	274.70	113.87	662.69
6	296.64	128.33	685.70
7	316.67	142.02	706.07
8	335.21	155.10	724.47
9	352.56	167.67	741.33
10	368.93	179.81	756.95
20	501.73	287.02	877.04
30	608.02	381.23	969.74
40	704.42	470.11	1055.52
50	798.26	557.11	1143.77
60	894.96	644.53	1242.69
70	1000.89	734.75	1363.43
80	1127.28	831.99	1527.39
90	1305.45	948.60	1796.54
91	1329.60	962.72	1836.28
92	1355.87	977.68	1880.34
93	1384.79	993.68	1929.83
94	1417.13	1011.03	1986.36
95	1454.06	1030.17	2052.38
96	1497.50	1051.84	2131.99
97	1550.95	1077.36	2232.74
98	1622.06	1109.55	2371.30
99	1734.18	1156.83	2599.66

Table C5 SKF R2F tests with TT68

Weibull Dist. Parameter Estimates (ML)

	Life		F %
SUBGROUP 1:	39 Hrs	SUSPENDED	8.3
SUBGROUP 2:	39 Hrs	FAILED	20.1
SUBGROUP 3:	101 Hrs	FAILED	32.0
SUBGROUP 4:	191 Hrs	FAILED	44.4
SUBGROUP 5:	416 Hrs	FAILED	55.9
SUBGROUP 6:	902 Hrs	FAILED	67.9
SUBGROUP 7:	1004 Hrs	FAILED	79.8
SUBGROUP 8:	1700 Hrs	FAILED	91.7

Shape: 0.849391
Scale: 505.097

Percentile Estimates

Percent	Percentile	90% CI Approximate Lower Limit	90% CI Approximate Upper Limit
1	2.25	0.08	66.63
2	5.11	0.27	97.46
3	8.28	0.56	122.18
4	11.69	0.95	143.76
5	15.30	1.43	163.38
6	19.08	2.00	181.63
7	23.02	2.66	198.88
8	27.11	3.41	215.36
9	31.34	4.25	231.23
10	35.71	5.17	246.62
20	86.39	19.25	387.70
30	150.06	42.79	526.22
40	229.04	77.26	679.07
50	328.08	124.81	862.40
60	455.70	188.62	1100.92
70	628.47	273.85	1442.32
80	884.50	390.92	2001.25
90	1348.39	571.32	3182.40
91	1421.32	596.47	3386.86
92	1503.52	623.94	3623.08
93	1597.54	654.29	3900.61
94	1707.12	688.35	4233.71
95	1838.10	727.35	4645.10
96	2000.33	773.35	5174.00
97	2212.44	830.13	5896.50
98	2516.62	905.91	6991.17
99	3049.46	1025.91	9064.39

Table C6 SKF R2F tests with Volvo 97305

Weibull Dist. Parameter Estimates (ML)

	Life		F %
SUBGROUP 1:	99 Hrs	FAILED	9.4
SUBGROUP 2:	382 Hrs	FAILED	22.8
SUBGROUP 3:	575 Hrs	FAILED	36.4
SUBGROUP 4:	1513 Hrs	FAILED	50.0
SUBGROUP 5:	1696 Hrs	FAILED	63.5
SUBGROUP 6:	1696 Hrs	SUSPENDED	77.1
SUBGROUP 7:	2387 Hrs	FAILED	90.5

Shape: 1.36898
Scale: 1293.28

Percentile Estimates

Percent	Percentile	90% CI Approximate Lower Limit	90% CI Approximate Upper Limit
1	44.91	4.21	478.68
2	74.79	9.61	582.04
3	100.95	15.58	653.98
4	125.02	21.97	711.36
5	147.72	28.71	760.11
6	169.41	35.74	803.09
7	190.33	43.03	841.92
8	210.65	50.56	877.61
9	230.48	58.32	910.85
10	249.91	66.29	942.13
20	432.37	156.13	1197.34
30	609.03	262.42	1413.46
40	791.76	384.60	1629.97
50	989.51	523.29	1871.11
60	1213.28	679.86	2165.23
70	1481.09	857.12	2559.31
80	1830.90	1062.75	3154.25
90	2378.39	1325.30	4268.26
91	2457.40	1358.15	4446.35
92	2544.64	1393.19	4647.75
93	2642.22	1430.94	4878.87
94	2753.25	1472.17	5149.12
95	2882.48	1518.07	5473.19
96	3037.79	1570.52	5875.88
97	3233.81	1632.97	6403.99
98	3502.89	1712.83	7163.72
99	3946.17	1832.30	8498.78

Table C7 SKF R2F tests with Volvo 97307

Weibull Dist. Parameter Estimates (ML)

	Life		F %
SUBGROUP 1:	51 Hrs	FAILED	5.1
SUBGROUP 2:	111 Hrs	FAILED	12.5
SUBGROUP 3:	137 Hrs	FAILED	20.0
SUBGROUP 4:	141 Hrs	FAILED	27.5
SUBGROUP 5:	182 Hrs	FAILED	35.0
SUBGROUP 6:	209 Hrs	FAILED	42.5
SUBGROUP 7:	240 Hrs	SUSPENDED	50.0
SUBGROUP 8:	319 Hrs	SUSPENDED	57.4
SUBGROUP 9:	713 Hrs	FAILED	64.9
SUBGROUP 10:	735 Hrs	FAILED	72.4
SUBGROUP 11:	780 Hrs	FAILED	79.9
SUBGROUP 12:	1132 Hrs	SUSPENDED	87.4
SUBGROUP 13:	1233 Hrs	FAILED	94.8

Shape: 1.17289
Scale: 487.706

Percentile Estimates

Percent	Percentile	90% CI Approximate Lower Limit	90% CI Approximate Upper Limit
1	9.66	1.454	64.14
2	17.51	3.370	91.02
3	24.85	5.517	111.97
4	31.90	7.834	129.91
5	38.76	10.292	145.96
6	45.48	12.872	160.69
7	52.10	15.561	174.44
8	58.65	18.352	187.44
9	65.14	21.236	199.84
10	71.60	24.210	211.74
20	135.76	58.294	316.16
30	202.50	99.681	411.38
40	275.06	148.593	509.18
50	356.82	206.067	617.85
60	452.68	274.032	747.78
70	571.34	356.101	916.66
80	731.76	460.272	1163.38
90	993.07	611.452	1612.87
91	1031.69	632.031	1684.05
92	1074.56	654.412	1764.45
93	1122.81	679.041	1856.59
94	1178.07	706.561	1964.23
95	1242.86	737.956	2093.21
96	1321.37	774.840	2253.38
97	1421.41	820.171	2463.40
98	1560.40	880.400	2765.61
99	1793.23	975.262	3297.25

Table C8 SKF R2F tests with Shell Spirax AX 80W-90

APPENDIX D

RESULTS OF SKF EP IMMERSION TESTS

SKF EP IMMERSION TESTS

Test method

The SKF EP reaction test is a simple method of testing the reactivity of oils and greases. Standard 4-ball 52100 balls were immersed in EP oils for time periods of 24 and 72 hours and heated in ovens at temperatures of 120 °C, 140 °C and 160 °C.

Preparation

100ml glass beakers were filled with 40ml samples of the test oil. The balls used in testing are cleaned in three stages with distilled petroleum ether. After drying, three balls were added to each of the beakers. The beakers were then put in pre-heated ovens, and left to react for the reaction period. After testing the balls were removed from the beaker and placed on paper to allow access oil to drain off. Balls were rated surfaces by visual inspection. The reacted balls have been ranked according to discolouration. The rating guidelines are given in Table D1

0	no colour change
1	yellow colour
2	shiny black colour on 50% of surface
3	shiny black colour on 80% of surface
4	shiny black colour on 100% of surface
5	matt black surface

Table D1 Discolouration ratings for EP immersion tests

Note: EP reactivity tests on two oils have been reported before in SKF report (AT98C343) and will act as a reference for measuring discolouration.

Results of immersion tests

	Lubricant	**120°C**	**140°C**	**160°C**
(1)	Spirax AX	0	0	3-4
(2)	Volvo 97305	0	0	3-4
(3)	Volvo 97307	0	0	0
(4)	Cat Toto 50	0	0	3-4
(5)	Mobil XRP 978E	0	0	0
(6)	Vitrea	0	0	1
(7)	Vitrea + 2%	0	1	3
(8)	Vitrea + 5%	0	1	3-4

Table D2 Results of EP immersion tests over 24 hour tests

	Lubricant	**120°C**	**140°C**	**160°C**
(1)	Spirax AX	0	3	3-4
(2)	Volvo 97305	0	3	3-4
(3)	Volvo 97307	0	0	0
(4)	Cat Toto 50	0	3	3-4
(5)	Mobil XRP 978E	0	0	0
(6)	Vitrea	0	0	1
(7)	Vitrea + 2%	0	2	3
(8)	Vitrea + 5%	0	2-3	4

Table D3 Results of EP immersion tests over 72 hour tests

Note: No reactions were seen for any oils at 120 °C. The reactions begin in some cases between 24 hours and 72 hours. With the Cat Toto 50 oil at 140 °C there is no reaction after 24 hours but there is a reaction rated (3) after 72 hours. Similar effects are seen at 140 °C for Spirax and Volvo 97305 oils. At 160 °C most of the reactions were completed by within the first 24 hours the exceptions being Vitrea + 2% and Vitrea + 5%, where reactions continued over the 72 hours.

Examples of EP immersion tests using Vitrea with/ without additive

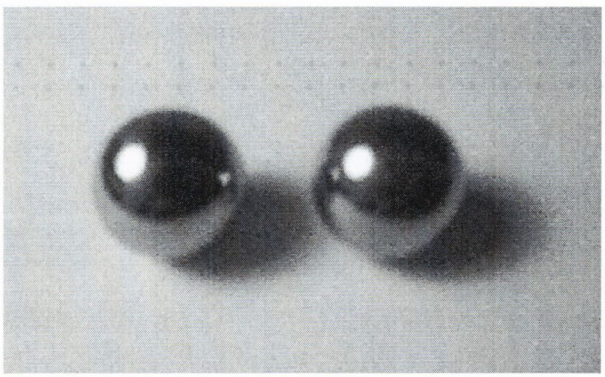

Figure D1 is a photo of the standard balls used in the EP immersion tests by SKF. The balls are the same type that are used in the 4-ball test machines. The surfaces are cleaned before use with petroleum ether.

Figure D1 Photo of standard ½ inch balls used EP immersion tests

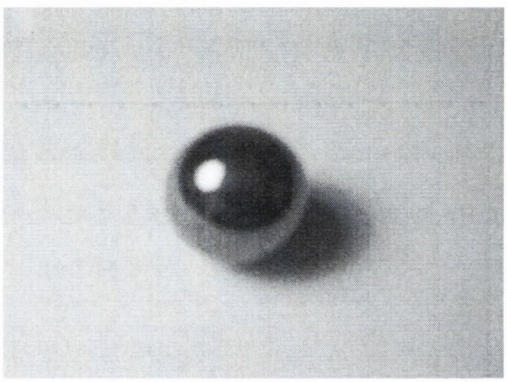

Figure D2 shows a ball reacted at 160 °C for 72 hours with the neat oil. The surface was a slightly yellow colour. This means that result of the test is a ranking of 1. This result demonstrates the relative unreactive nature of base oil without additives.

Figure D2 Photo of EP immersion tests with Vitrea M100

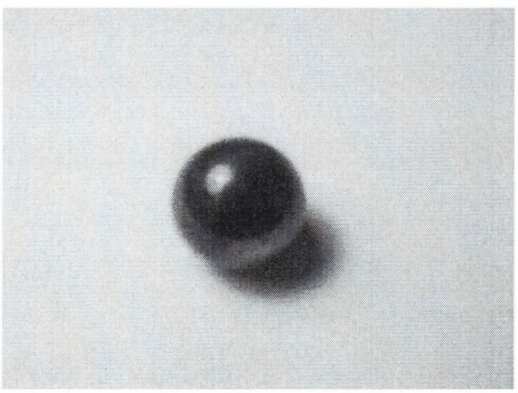

Figure D3 show the reaction with Vitrea + 2% (S/P). 80% of the surface is a shiny black colour giving it a 3 rating. The increased reaction is a consequence of the presence of additive.

Figure D3 Photo of EP immersion tests with Vitrea M100 + 2% (S/P)

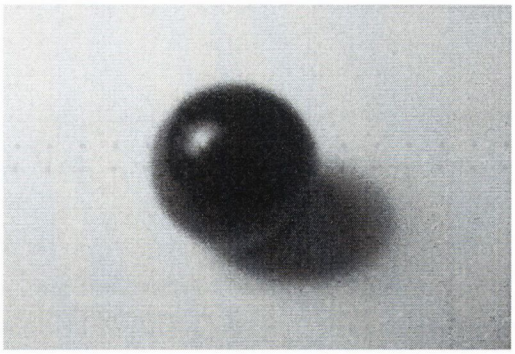

Figure D4 shows the black surface produced when 5% (S/P) additive is reacted over 72 hours. This ranks as a 4 rating as the entire surface is covered with a shiny black surface. This is the same as is seen for other oil with additives such as Spirax and Volvo 97305.

Figure D4 Photo of EP immersion tests with Vitrea M100 + 5% (S/P)

Immersion test conclusions

a) Reactivity in the form of surface films is seen with increased temperature and additive content.
b) Reactions can start in the period between 24 hrs and 72 hrs.
c) Thick film formation starts to occur under these static conditions between 140°C and 160°C.